THE EFFECTS OF COMPOSITION ON WELD SOLIDIFICATION

CRACKING IN LOW ALLOY HIGH TENSILE STEELS

By

Chao Ming Cho, Dipl-Ing

A thesis submitted for the degree of Doctor of

Philosophy of the University of Aston in Birmingham

June 1979

THE EFFECTS OF COMPOSITION ON WELD SOLIDIFICATION

CRACKING IN LOW ALLOY HIGH TENSILE STEELS

Chao Ming Cho

A thesis submitted for the degree of PhD of the
University of Aston in Birmingham   June 1979

SUMMARY

A study was made of the effects of material composition on weld solidification cracking in the TIG arc welding of thin alloy steel sheet. The main points of this study included the effects of oxygen, manganese, Mn/S and O/S ratios on the sulphur induced cracking, and the possibility of predicting crack susceptibility based on the material composition.

Materials for this study included a series of Fe-Mn-S-O alloys and a series of SAE4130 experimental steels (both having a 2^3 factorial design with Mn, S and O each at high and low levels), and a number of commercial high tensile steels. The Huxley cracking test was employed for assessing the crack susceptibility of these steels. Oxygen analysis of weld and parent metals was made in order to determine the oxygen pick-up during welding. In addition examination of weld microstructure and detailed investigation of fresh weld crack surfaces were made in order to study the weld crack morphology.

The results of this study showed that Mn, O, Mn/S and O/S have no significant effects on solidification cracking, but it was confirmed that sulphur, phosphorus and carbon have a harmful effect on solidification cracking. Main alloying elements in alloy steels such as Si, Ni, Cr, Mo have no obvious beneficial or harmful effect on weld solidification cracking according to the statistical analysis. Based on the cracking test data collected, it was not possible to derive a regression equation for the prediction of weld crack susceptibility for all types of steels, but it was possible to produce a regression equation for the prediction of crack susceptibility of a particular type of steel.

Examination of fresh weld crack surfaces by using a scanning electron microscope revealed many features of solidification cracking, and based on these findings the existing theories on solidification cracking are discussed and comments given.

Key Words:

Weld
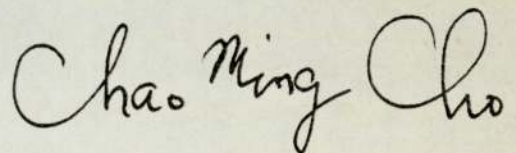Solidification
Cracking
Steel
Composition

THE EFFECTS OF COMPOSITION ON WELD SOLIDIFICATION
CRACKING IN LOW ALLOY HIGH TENSILE STEELS

Chao Ming Cho

A thesis submitted for the degree of PhD of the
University of Aston in Birmingham.   June 1979

DECLARATION

I, the undersigned, hereby declare that no part of the work described in this thesis was done in collaboration, and that the work has not been submitted for any other award.

Chao Ming Cho

Chao Ming Cho

THE EFFECTS OF COMPOSITION ON WELD SOLIDIFICATION

CRACKING IN LOW ALLOY HIGH TENSILE STEELS

1. INTRODUCTION

Cracking of welds is a problem in fabrications where high integrity welds are mandatory, as in the aerospace industry. The presence of large cracks prevents structures being put into service, while the presence of smaller cracks, if undetected, may cause even more troublesome failures such as fatigue, brittle fracture and stress corrosion.

Two types of weld cracks might occur in the welding of ferritic steels: cold cracks and high temperature cracks. Cold cracking occurs in the weld metal and the heat affected zone immediately adjacent to the fusion boundary when cooling rates are fast enough to produce martensitic microstructures. It is the result of the combined action of stress, hydrogen and a crack susceptible microstructure. High temperature cracking might occur in the weld metal as solidification cracking, and in the heat affected zone as liquation cracking. Solidification cracking occurs in several forms: it may appear as continuous centreline cracking, transverse cracking, root cracking or crater cracking.

For the aerospace industry, the welding of high tensile steels in sheet form is a very difficult task, because the production of crack free welds is mandatory, and this can be achieved only by a careful selection of materials and correct selection of welding parameters. High tensile steels have been recognized for a long time as materials susceptible to weld solidification cracking. The relationship between steel composition and weld crack susceptibility has been discussed at length by many investigators, but no final agreed conclusions appear to have been drawn. An exception is the harmful effects of carbon, sulphur and phosphorus on the crack susceptibility which are

generally accepted by all workers in the field.

The detailed relationship between composition and solidification cracking in the high tensile steels is far from being clearly understood. This research is going to deal with the following questions which do not appear to have been settled:

1) What amounts of sulphur and phosphorus are tolerable in various types of steels if cracking is to be avoided?

2) Can the presence of oxygen reduce sulphur-induced solidification crack susceptibility? What is the necessary level of oxygen to counteract the harmful effect of sulphur?

3) Is the effect of manganese or Mn/S on solidification cracking significant? If so, what level of manganese or Mn/S is required for the avoidance of cracking?

4) Can it be assumed that the effect of each alloying element is linear and additive on weld crack susceptibility, so that a linear regression equation is applicable for the prediction of crack susceptibility?

To answer the above questions, two approaches have been adapted. One approach is experimental and involves crack testing and concurrent metallurgical investigation of a range of steels with designed variations of composition. The second approach involves collection and statistical analysis of all the cracking/composition data available in this research and the published literature.

Materials available for this study were 12 casts of specially designed Fe-Mn-S-O alloys, 10 SAE4130 experimental steels with planned variations of sulphur, manganese and oxygen contents, 6 SAE4130 steels with varying carbon contents and 19 other commercial steels of various alloying contents. The weld solidification crack susceptibility of these steels was assessed by using the Huxley cracking test, and by a compa-

rison of the testing results, the effects of manganese, oxygen and
sulphur as well as their combined effects were assessed. In addition
investigations of the weld crack surfaces by using a scanning electron
microscope, weld and parent metal oxygen analysis and metallographic
examinations of the weld solidification microstructures were carried
out. This was done in order to see what particular characteristics
were connected with the weld crack susceptibility and how the composi-
tion of the weld affected the weld microstructure and cracking tendency.
The information obtained from the investigations of fresh solidification
surfaces was furthermore used for the construction of a possible me-
chanism of crack morphology, and for a comparison with other existing
theories of solidification cracking.

There is a considerable amount of cracking test data for fer-
ritic steels available in the relevant literature and it is the aim
of this investigation to use as much of it as possible. The data was
analysed by regression, using a computer programme, in order to see the
cracking and composition relationship and find out what kind of regres-
sion equation could be used for the prediction of crack susceptibility.

It is hoped that the efforts of this research will show more
clearly the cracking and composition relationships and establish a
reliable quide for the production and selection of steels which are
not susceptible to solidification cracking.

2. LITERATURE SURVEY

Solidification cracks, sometimes also termed hot cracks, are intergranular failures occurring during or immediately after the weld metal is solidified. They differ from cold cracks or mechanical fracture in several ways. First of all, they form when weld metal solidification occurs under thermally or mechanically restrained conditions. Secondly, they are predominately of an intergranular nature, apparently grain boundary phases in liquid or solid state play a great role in their formation. Thirdly, the crack surfaces caused by the solidification process are exposed to the atmosphere at very high temperatures and are oxidized.

There are many types of solidification cracks, but in the tungsten inert gas arc welding of crack susceptible steel sheet, the cracks normally run along the weld centreline. Transverse cracks may also occur when steels to be welded are very susceptible to cracking or extra stresses are introduced.

In this literature survey, the technological factors known or believed to affect weld crack formation are reviewed, and the concepts which explain the causes and extent of solidification crack susceptibility are studied. The iron-based phase diagrams of the Fe-S, Fe-O-S, Fe-Mn-S and Fe-Mn-S-O systems are introduced in order to explain the conditions for the formation of low melting sulphide inclusions, and hence to relate the possible effects of composition on weld crack susceptibility. Because solidification cracking is directly related to the solidification process of the weld metal, the basic principles of metal solidification and the characteristics of weld pool solidification are also reviewed in detail.

After considering the theories, the experimental approaches

for the assessment of crack susceptibility, especially the methods for
thin sheet, are introduced and compared. Following this, the equations
or parameters claimed to be able to predict or describe the amount of
cracking are reviewed and any contradictions pointed out. Finally, a
summary of the main conclusions of the literature survey is made and
an indication given of the problems still remaining to be solved.

2.1 Technical Factors

2.1.1 Stresses

The direct causes for the occurrence of cracks are stresses
within the welded components, which can be subdivided in three groups:

1) Internal stresses: which are present before welding as a
result of cold working, sudden and non-uniform cooling after hot rolling
or heat treatment. They can also be produced by the neighbouring weld
runs.

2) External stresses: They are caused by an unsuitable weld
construction. Examples are restrained contraction as a result of rigid
clamping, or the stresses produced by an inappropriate welding procedure.

3) Weld bead stresses: They are caused by the expansion of
material as a result of heating and by contraction during cooling after
welding.

According to F Bollenrath and H Cornelius[1] the lower the
yield strength of the material to be welded, the easier the stresses
can be accommodated by a plastic deformation. It would be expected
therefore, that the higher the material strength, the more difficult
will be the stress release without crack formation.

2.1.2 Welding process parameters

According to JC Borland[2] and various sources the following process parameters are considered to affect weld metal crack susceptibility:

1) Electrode quality, diameter and sharpness.

2) Heat input and its associated arc current and voltage.

3) Shielding gas composition.

4) Shielding gas flow rate.

5) Ambient atmosphere and temperature.

6) Clamping device.

7) Backing material and its geometry.

8) Welding speed.

9) Arc gap.

10) Direction of welding (toward or away from the edge).

Though there are so many welding parameters which may affect weld cracking, most of them have standardized values for a desirable performance and afford less margin for modification. The two realistic parameters which can be varied are the heat input and the welding speed. However, for a full penetration of the weld bead a defined welding speed is associated with a constant heat input, and the required current and voltage are not freely adjustable. Welding with a higher welding speed tends to form a tear-shaped weld pool and leave a longer crack suscep- tible zone behind it, and the tensile forces on this zone are lower. The balance of these effects determines the cracking behaviour of the weld. EJ Morgan-Warren[3] demonstrated that the effect of welding speed on cracking in a thin steel sheet is complex and the general effect of an increase in speed is to first increase, than decrease, the weld crack susceptibility.

2.1.3 Steelmaking process

According to KL Zeyen[4] steelmaking processes also play a role in the modification of solidification crack susceptibility of steel. He discovered that the 1% chromium and 0.2% molybdenum high tensile steels made by the open hearth steelmaking process were more susceptible to cracking than those made in the electric steelmaking process. The charged raw materials for steelmaking have been considered as being influential on crack susceptibility, but no strong evidence has been obtained for this[4,5]. According to O Werner[6] increasing steelmaking temperature will be likely to reduce weld cracking tendency, and the experiments of P Bardenheuer[5] showed the same results. This could be explained as the consequence of homogenization of the melt at higher temperatures or in a longer process time. Regarding the effect of steel homogeneity on crack susceptibility one would expect that a large size steel ingot might have an adverse effect due to its conditions for the macrosegregation of sulphur and phosphorus.

Modern steelmaking processes such as vacuum furnace steel melting, controlled atmosphere melting, argon blow melt purification, vacuum degassing, electroslag melting etc will modify steel quality in various ways. It can be speculated that such processes may produce steels with different crack susceptibility, even if their composition is similar. For example, HV Huxley[7] showed that some vacuum melted high purity steels have a markedly reduced crack susceptibility.

2.1.4 Heat treatment conditions

Steels are heat treated to obtained the best combination of mechanical properties. For example, SAE4130 steels might be oil quenched

from 900°C and tempered at about 500°C before welding, however, this heat treatment is designed for a better tensile strength rather than for the crack prevention. According to HS George[8], heating steel above or below its critical temperature with a subsequent air cooling could prevent cracking, however, no detailed explanation for this was given. In contrast, EJ Morgan-Warren[3] showed that heat treatment has no significant effect on cracking for his particular steels and heat treatment conditions. The reported effect of heat treatment on crack prevention might possibly be explained as the consequence of decarburizing during heat treating, for steels reheated to over 800°C are subject to oxidation and decarburization if the heat treating atmosphere in not controlled.

Even preheating the parts to be welded has the effect of reducing crack susceptibility, as consequences of stress releasing or homogenization, this practice is not economical and sometimes impractical, especially when the construction is large and complicated.

2.2 Concepts of solidification cracking

In the early work of P Bardenheuer and W Bottenberg[5] they concluded that the steel weld cracks were due to the internal stresses caused by the pearlite or martensite transformation. It was later discovered that cracks are formed at temperatures much higher than pearlite or martensite transformation. This theory must therefore be discarded in favour of high temperature mechanisms. In the following sections some concepts of solidification cracking are reviewed.

2.2.1 Portvin model of solidification stages

A Portvin[9] was the first to consider the metal solidifica-

tion stages and relate them to solidification cracking. His ideas have been widely used and modified by later research workers. According to his view the solidifying metal proceeds in three stages:

Stage 1: Crystals of the solid phase are not sufficiently developed to touch one another and float in the liquid. In this stage the solid phase is discontinuous, therefore both liquid and solid phase are capable of relative movement.

Stage 2: Crystals of the solid phase are sufficiently developed to touch one another. They form a solid mesh through which liquid can circulate like water in a sponge. Both liquid and solid phases are continuous, but only the liquid phase is capable of relative movement.

Stage 3: The solid crystals are so far developed as to form barriers restricting movement of the liquid. In this stage the solid phase is continuous while the liquid discontinuous, and consequently no relative movement of the two phases is possible.

According to this model a crack does not developed until the beginning of the second and the third stages. This model explains that no actual crack is developed within the weld pool, and if cracks are formed, they must form at the weld pool boundary or behind the weld pool where the third stage solidification process takes place. As this model gives only a qualitative description of the solidification process, no quantitative approach being used, its application is therefore limited.

2.2.2 The concept of crack susceptible temperature interval

It has been agreed that there is a particular temperature interval in which the solidifying weld is susceptible to cracking. It is also reasonable to assume that the wider the crack susceptible temperature interval of a material, the higher its susceptibility to soli-

dification cracking. If the developed stress does not exceed the critical rupture stress in this interval, the solidified metal is free from solidification cracks. However, there is no settled agreement about at what stage the metal becomes crack susceptible.

Coherent temperature is defined as the temperature at which the growing dendrites are interlocking with one another and forming a network. Based on the studies of aluminium castings many investigators [10-12] have agreed that a crack could developed in the temperature interval between the coherent and solidus temperature, being termed "the brittle range". JC Borland [13] argued that the actual crack formation begins at a later stage when the grain boundaries are being developed, and termed this interval between the temperature of grain boundary formation and solidus temperature "the critical solidification range".

Not arguing the particular stage of solidification for the crack formation, NN Prokhorov [14] and T Senda [15] actually measured the crack susceptible temperature interval. The former used equipment similar to the Gleeble machine, while the latter applied the Trans-Varestraint test machine to determine the ductility and strain condition at various temperatures, thus to obtain the information for the crack susceptible temperature interval. They called this interval "the brittle temperature range". In the case of steel, this interval lies between about 1400°C and 1200°C, and is dependent on the composition, especially on the contents of sulphur and phosphorus. A steel with a higher content of sulphur or phosphorus tends to have a wider brittle temperature range than a steel with a lower content of sulphur and phosphorus. Fig 1 shows schematically the brittle temperature range together with the ductility curve of a material. It also shows that the starting temperature of the brittle temperature range lies below the liquidus and the end of the range below the solidus temperature.

2.2.3 The concept of crack susceptible length

The crack susceptible length, or the length of the crack susceptible zone, is the length behind the weld pool which is vulnerable to stress and susceptible to cracking. This depends not only on the crack susceptible temperature interval, but also the welding parameters. Theoretically the crack susceptible length can be calculated if the crack susceptible temperature interval is known. EJ Morgan-Warren[3] has attempted to calculate this length by using Rosenthal heat flow equation[16]. Practically this length can be determined by the sudden imposition of augmented strain on the weld immediately after the weld run.

With the same magnitude of a stress on the crack susceptible zone, a weld with a larger crack susceptible length is expected to be more crack susceptible. However, for the same material, a weld with a larger crack susceptible length may not necessarily mean that it is more susceptible to cracking then that with a smaller crack susceptible length, because as the weld pool and the crack susceptible length are elongated by using a higher welding speed, the stresses acting on the crack susceptible length are reduced. This concept is therefore only good for the comparison of materials, but not valid for the comparison of welding parameters. Performing Varestraint test at welding speeds ranging from 1 mm/S to 10 mm/S, EJ Morgan-Warren[3] discovered that: 1) crack resistant steels would have a crack susceptible length equals to zero; 2) less crack susceptible steels would have a crack susceptible length of about 1 mm, being not much affected by the welding speed; 3) for most of the crack susceptible steels the crack susceptible length increased as the welding speed was raised.

2.2.4 The concept of crack susceptible time interval

TW Clyne[17] studied the relationship between crack suscepti-
bility and the changes in local liquid fraction with time. and defined
the crack susceptibility coefficient (CSC) as:

$$CSC = \frac{t_V}{t_R} \qquad (2.1)$$

where t_V is the vulnerable time period and t_R is the time available
for the stress relaxation process. t_R is thought to be the time availa-
ble for mass and liquid feeding or the time period in which the local
liquid fraction (f_L) is between 0.1 and 0.6 approximately, whereas t_V
is the time for interdendritic separation when the local liquid fraction
is between 0.01 and 0.1. This is illustrated in Fig 2. With the Scheil
equation[18] and the phase diagram data it is possible to calculate the
theoretical CSC.

The above treatment has a more theoretical character, and for
the calculation of CSC it assumes the knowledge of liquidus as well as
solidus temperature , and relies on the correctness of the Scheil equa-
tion. It does not take account of the size of strain imposed during
the solidification process. In practice the alloy has multiple compo-
nents and its solidification data are not readily available, which
makes the calculation of CSC hardly possible.

If the Clyne concept is valid for the weld, a low weld crack
susceptibility can be achieved by the combined effect of increasing t_R
and reducing t_V . In the general practice, increasing the heat input
of the welding arc will simultaneously raise both t_R and t_V , which may
not have the effect of reducing t_V/t_R . However, by applying an
auxiliary electrode some distance behind the welding arc for additional
heat input may increase t_R but not much affect t_V , and thus reduce
weld crack susceptibility.

2.2.5 The concept of critical strain rate

This concept originated from the study of the brittle tempe-
rature range and the hot ductility curve of materials by NN Prokhorov[14]
and later expanded by T Senda et al[15]. According to NN Prokhorov the
weld strain begins to develop at the upper limit of the brittle tempe-
rature range with an approximately constant rate (see Fig 1). If the
strain development of the weld bead exceeds the weld ductility, or the
strain line intersects the ductility curve of the material, a solidifi-
cation crack is formed. The slope of the strain line in Fig 1 represents
the strain rate $d\varepsilon/dT$. The minimum strain rate with respect to tempe-
rature which causes a crack (represented by line 2 in Fig 1) is called
the critical strain rate. This depends on the alloy composition, welding
parameters and the rigidity of the welded structure.

T Senda et al[15] made a distinction between the critical
strain rate to time (CSS) and the critical strain rate for temperature
drop (CST) required to cause cracking, and established the relationship
between CSS and CST by

$$CSS = CST \times \text{Mean Cooling Rate} \qquad (2.2)$$

where the mean cooling rate is that between the upper brittle tempe-
rature and the temperature at which a crack initiats.

Both CSS and CST can be measured experimentally by the Trans-
Varestraint cracking test. T Senda et al measured them and pointed out
that CSS is a good crack susceptibility index and the smaller the CSS
the more crack susceptible is the weld.

2.3 Steel composition and the solidification cracking relationship

Earlier research work done by German investigators[1,4,5,6] and the later reports by CLM Cottrell[27], FJ Wilkinson et al[19], JC Borland[20] and HV Huxley[21,22] have shown the various effects of composition on the solidification cracking in the welding of high tensile steels or carbon manganese steels. It has been generally accepted that the effects of carbon, sulphur and phosphorus in steels are harmful, though HV Huxley[22] indicated that an increase of carbon content to a maximum of 0.15% confers improved resistance to weld solidification cracking.

Regarding the effect of manganese or Mn/S on the weld cracking many empirical formulae have been claimed to be able to predict crack formation . These formulae are often different from one another. For example, by an investigation of solidification cracking in low alloy steel welds with the Murex cracking test PW Jones[23] indicated an Mn/S ratio of about 50 in steel would prevent crack formation. CF Meitzner and RD Stout[24] showed that HY80 steels with Mn/S ratios from 144 to 175 would prevent the HAZ cracking even under severe test conditions. CT Anderson[25] found the concentration of manganese required to prevent red-shortness in hot working could be represented by the empirical formula: %Mn = 1.25 x %S + 0.03.

The effect of oxygen in steels has been also reported to be significant. T Boniszewski[26] indicated that the propensity of sulphur to cause solidification cracking in the mild steel welds in influenced by the degree of oxidation. EJ Morgan-Warren[3] based on his statistical analysis, reported a strong effect of oxygen in alloy steels in preventing solidification cracking. Though the effect of oxygen in steels

in modifying sulphide inclusion shape has been documented by CE Sims[28], W Craft[29], W Dahl[30] and PP Mohla et al [31], some workers have not confirmed the beneficial effect of oxygen in reducing the weld cracking tendency in alloy steels. Earlier German work[5,32] did not show the direct relationship between oxygen content and crack susceptibility in the welding of aircraft steels. Furthermore, recent investigations by N Bailey[33] on the solidification cracking in C-Mn steels by submerged arc welding have not supported the view that oxygen reduces weld cracking. Because of such different views on the composition effects, it seems necessary to review the fundamental iron-based systems and the theories of inclusion formation.

2.3.1 Fe-S system

The Fe-S system phase diagram according to ET Turkdogan[34] is shown in Fig 3. Relating to the sulphide inclusion formation four features are very important for solidification cracking and these are as follows:

1) Delta iron has the highest sulphur solubility of 0.18% at 1365°C.

2) The highest solubility of sulphur in gamma iron is only 0.050% at 1365°C. It decreases with decreasing temperature.

3) Due to its low solubility in gamma, a sulphur rich liquid will precipitate from the solid upon cooling.

4) Liquid phase will be present in the system for temperatures over 988°C.

It is assumed that so long as the liquid sulphide is present in a sufficient amount, the solidifying Fe-S alloy is susceptible to solidification cracking. However the Fe-S phase diagram should be

used only as a guideline for the further study of crack susceptibility in carbon and alloy steels, because commercial steels, being always multi-component systems, might behave quite differently from the Fe-S system.

2.3.2 Fe-Mn-S system

The Fe-Mn-S phase diagram was constructed by H Wentrup[35] and R Vogel[36]. Wentrup's version disagrees with Vogel's in a small detail, and recent work by LK Bigelow and MC Flemings[37] has been in favour of Vogel's diagram, which is schematically represented in Fig 4. The iron-rich, low sulphur Fe-Mn-S alloy melt may solidify in two distinct ways:

1) First case: The melt begins to solidify when it reaches its freezing point. On cooling more primary solidification of iron occurs until the liquid melt is so enriched with manganese that a solid MnS phase (containing FeS) is precipitated. The liquid composition reaches the right of the point R in the Ee_3' eutectic curve and moves toward e_3' (see Fig 5 the path of $A_1b_1e_3'$). The solidification is finished when the remaining liquid has vanished.

2) Second case: The melt solidifies as in the first case till the liquid composition reaches the left of R in the Ee_3' eutectic curve, the remaining liquid changes the composition along this curve toward E and it might persist until $988^{\circ}C$ (see the path of A_2b_2E in Fig 5). In this case the last solidified phase is FeS.

The solidification which proceeds as in the second case is not desirable because the persisting liquid of FeS weakens the solid and might lead to solidification cracking. By adding more manganese to alloys which would solidify as in the second case, they might

change the solidification path to the first case. This means that the
formation of FeS-Fe eutectic liquid can be suppressed by adding more
manganese to the steel. Based on the study of FeS-MnS phase relation-
ships in the presence of excess iron, GS Mann and LH van Vlack[38]
deduced that in order to avoid liquid FeS in a low sulphur steel, the
manganese content required would be:

$$\%Mn > 0.40\% + 2 \times \%S \qquad\qquad (2.3)$$

With this argument, they explained why the Mn/S ratio is not a good
index of manganese requirement for the suppression of solidification
cracking.

Research work on the effect of sulphur on solidification
cracking in the weld metal of low carbon and low nickel alloy steels
by H Nakagawa et al[39] showed a very interesting effect of Mn^3/S or
Mn^5/S ratio on the solidification cracking. Based on Scheil equation
they deduced the solidification path of the Fe-Mn-S alloy with respect
to the change of its liquid composition and concluded that all alloys
with a similar Mn^3/S ratio share the same solidification path if the
primary phase is delta ferrite. If the primary phase is austenite,
alloys with a similar Mn^5/S ratio have the same solidification path.

The relationship between solidification cracking and com-
position according to their conclusions can be shown in Fig 6. With
steels in region A, whose Mn^3/S is less than 0.83, FeS inclusions are
formed together with MnS, and therefore the crack susceptibility is
extremely high. With steels in region B, whose Mn^3/S is between 0.83
and 6.7, MnS only is generally formed, but the crack susceptibility
is high, since the eutectic temperature is relatively low. With steels
in the region C, whose Mn^3/S is greater thatn 6.7, the eutectic tempe-
rature of Mn-MnS is high, and consequently the crack susceptibility
is sufficiently low. The above mentioned is valid for ferritic steels.

As to austenitic steels it was also reported by the same investigators that $Mn^5/S > 370$ is required to prevent crack formation.

It should be emphasized that these conclusions were based on the experiments of very low carbon steels with a higher sulphur content than in high tensile alloy steels. It is doubtful that such conclusions are also valid for the alloys at present under investigation.

2.3.3 Fe-O-S system

Because sulphur and oxygen are always present in steel and because oxygen modifies inclusion shape, the Fe-O-S system will be investigated in some detail. DC Hilty and W Crafts' Fe-O-S phase diagram (see Fig 7)[40] gives basic hints on how sulphide and oxide inclusions are formed. According to the phase diagram the solidification path of an iron-rich Fe-O-S alloys depends on the ratio of oxygen to sulphur.

Two cases of solidification paths are illustrated in Fig 8 and Fig 9. Fig 8 refers to the solidification paths of an alloy not saturated with oxygen but having a high O/S ratio, as indicated by the line of I on the diagram. When this melt reaches liquidus upon cooling, relatively pure iron solid is formed, and the concentration of the liquid phase will gradually shift to c upon further cooling. At the point of c, a second liquid will appear, having its composition at the opposite end of the tie line cd. The melt then will continue to solidify with a solid concentration from c to f, but simultaneously precipitate driplets of an oxide-rich phase with a composition from d to g. According to J Yarwood et al[41] such droplets will be trapped or isolated by growing dendrites and will eventually become solid inclusions at the eutectic temperature.

Fig 9 relates to tne soliaification of an alloy having a relatively low ratio of O/S and saturated with oxygen at the start of solidification. As the alloy is cooled, it will separate into two liquids represented by i and j, where i is metal rich liquid and j oxide and sulphide rich liquid phase. By forming a metal phase upon further cooling, i will shift along the line to k, meanwhile the other liquid will vary its composition from j to l. At this stage the growing dendrites are more or less enveloped by the liquid of composition l. In addition the dendrites themselves will contain droplets of liquid varying in composition from j to l. The solidification process is continued by additional metal crystallization from the last droplets and ends with the formation of FeS-Fe or FeS-FeO-Fe eutectic.

In the first case, the inclusions are oxide rich and spherical, while in the second case the inclusions are mainly sulphide or FeS-Fe eutectic, which are filmlike. Therefore, the ratio of O/S is very crucial in deciding the inclusion type.

The solidification process of Fe-O-S alloys just mentioned has been confirmed by JC Yarwood et al[41], however, all the work done was based on alloys with quite a high sulphur and oxygen content (about 0.3% S and 0.1% O). In normal steels sulphur or oxygen content will not be so high and therefore the applicability of this Fe-O-S system to commercial steels needs careful consideration.

2.3.4 Fe-Mn-S-O system

It is not easy to construct a Fe-Mn-S-O quarternary phase diagram. However ET Turkdogan and GJW Kor[42] have made an extensive study of phase relations in this system. The most important features of their study relating to solidification are explained here.

There are two distinct invariant equilibria in the Fe-Mn-S-O system and the estimated data for them are given in Table 1. According to Table 1, one invariant is at about 900°C and the other at about 1225°C. It can be seen that so long as the alloy contains Mn(Fe)O and Mn(Fe)S in equilibrium with the metal, a liquid oxysulphide phase can still be present between 900°C and 1225°C.

A convenient way of representing the phase equilibria in the Fe-Mn-S-O system is to use the univariant equilibria involving four condensed phases. This is shown in Fig 10 for the part of the system involving the solid metal and manganese sulphide with ternary Fe-Mn-S and Fe-S-O and binary Fe-Mn terminal phase fields. For simplification, the delta to gamma transformation is omitted in this equilibrium diagram.

According to Fig 10 and assuming the absence of a liquid oxysulphide is the condition for crack resistant steels, then three important features can be pointed out:

1) The higher the manganese content in a steel, the higher is the temperature below which no liquid oxysulphide is present, or the less crack susceptible is the steel.

2) The liquid oxysulphide vanishes at temperatures between 900 and 1225°C, this means that the lowest temperature at which sulphur-induced cracking can take place is 900°C for Fe-Mn-S-O alloys.

3) For steels with a manganese content of more than 1%, the temperature at which the liquid oxysulphide disappears is almost constant, being very close to 1225°C. This implies that steels with a manganese content of over 1% have no additional benefit of reducing sulphur-induced cracking as steels with a manganese content of just 1%.

The foregoing points could apply to a rimmed or semi-killed steel containing manganese as the major alloying element. For killed

alloy steels, the oxygen content is low and the sulphur will be pre-
dominately in the form of MnS, manganese oxysulphide inclusions are
only formed in the solute-enriched interdendritic liquid during the
solidification of steel.

2.4 Solidification process and its effects on solidification cracking

Cracking occurs in the weld metal because the weld metal is
brittle at a stage during the solidification and cooling process and
is subject at the same time to severe stresses. The control of the
weld pool solidification in favour of crack-free sound welds can be
achieved if the basic principles of metal solidification are well
understood. For this reason some important features of metal soli-
dification are reviewed here.

2.4.1 Solidification morphology of a single phase alloy

According to WA Tiller and JW Rutter[43] the solidification
types of a single phase alloy are fixed by three parameters C_o ,
G and R, where C_o represents the solute concentration at the solidi-
fication front, G the temperature gradient and R the growth rate.

1) Under the same cooling conditions the solidification type
will shift from plane front to dendritic, and from dendritic to endo-
genous equiaxed solidification with increasing solute concentration.

2) With an alloy of the same solute concentration, the soli-
dification type shifts from exogenous globulitic to dendritic and
from dendritic to plane front solidification by increasingly retarded
cooling conditions.

In the solidification of a weld, G depends mainly on the heat input, while R depends on the welding speed. If the welding speed is not exceedingly high, the growth rate R is approximately the same as the welding speed in the central region of the weld bead.

2.4.2 Weld solidification and its effect on cracking

Weld solidification has been investigated by GJ Davies and JG Garland[44], F Matsuda et al[45] and WF Savage and CD Lundin[46] etc. Important features of weld metal solidification are summarized as follows:

1) The columnar grains in the weld metal grow epitaxially from the half-melted grains in the parent metal at the fusion boundaries.

2) The columnar grains grow competitively toward the centre. Only the grains with orientations conducive to growth would grow to the central region of the weld bead.

3) Constitutional supercooling takes place in front of the growing interface, and with an increase in constitutional supercooling, the interface solidification substructure changes in term from planar to cellular dendritic and dendritic modes. If constitutional supercooling progresses sufficiently, equiaxed grains will form in front of the growing interface.

4) Depending on the welding speed, the weld pool shape can be tear-shaped or elliptical. The latter is associated with a higher welding speed.

5) Solidification cracking occurs at the point of impingement of the columnar grains growing from the opposite sides of the weld pool.

6) Welds made with a tear-shaped weld pool, where the angle

of abutement between the columnar grains is steep, are more susceptible to solidification cracking than welds with an elliptical weld pool.

7) Solidification cracking is favoured by factors which decrease the solid-solid contact area during the last stage of solidification. These factors include the presence of low melting segregates and the solidified grain size.

8) The larger the solidifying grain size, the smaller the area of grain boundary contact is for a given liquid content, consequently the more susceptible to cracking is the weld.

9) Equiaxed weld solidification tends to occur in the central region of the weld bead, where solidification rates are highest and the thermal gradients the smallest due to the distance from the arc.

10) Equiaxed weld pool solidification might also be promoted by increasing welding speed.

11) Due to their fine sizes and isotropic character the equiaxed grains are favourable for better mechanical properties. In the same thermal conditions equiaxed weld solidification is less susceptible to cracking than the weld with a columnar structure. This is partly due to the smaller area of grain boundary contact.

12) For some alloys the equiaxed grains are not obtainable without an artificial control of the weld pool.

13) Equiaxed grains may form on the surfaces of the weld, this suggests that these grains are nucleated hetereogeneously at the gas/liquid surface[47].

2.4.3 Control of weld pool solidification

The control of weld pool solidification by changing welding parameters is very limited. However, for the freedom of solidification

cracking and better weld qualities, it is sometimes required to control the weld pool solidification by artificial means. Some possible methods for weld pool solidification control are listed as follows:

    1) Using inoculants to induce the nucleation of new grains.

    2) Directing streams of argon on the weld pool surface to stimulate surface nucleation.

    3) Using transverse or longitudinal arc vibration to cause grain refinement.

    4) Introducing ultrasonic vibration into the weld pool.

    5) Inducing weld pool stirring by a magnetic field.

    6) Using pulsed arc or modulation of the arc current to generate thermal fluctuation.

For the improvement of the weld pool solidification in the steel sheet, the application of pulsed arc welding seems to be very promising. It requires only the power source which supplies pulsed and modulated current. G Aichele[48] reported the reduction of cracking severity by the application of pulsed arc welding.

2.5 Methods for assessing solidification crack susceptibility

Numerous methods have been developed for assessing the solidification crack susceptibility of weld metal, most of them having been designed to fulfill a specific purpose rather than for general applicability. Some test methods have been documented by JC Borland[2] and K Wilken and W Schoenherr[49,50]. Tests may be classified broadly by the method used to impose the stress on the solidifying metal. On the one hand the stress may be applied mechanically by an external force, as in the Murex[23], varestraint[51,52] and Trans-varestraint[53] tests; on the other hand the stress may be induced thermally by the

specimen design as in the Houldcroft[54] and Pellini[55] tests. For the TIG arc welding , the material concerned is often in a sheet form, therefore only test methods using thin sheet or plate will be reviewed here.

2.5.1 Focke-Wulf Test

In this test a specimen of about 50 mm x 70 mm, 1 to 2 mm thick is firmly clamped by a commercial apparatus originally made by Focke-Wulf Flugzeugbau AG, Bremen. A butt weld is made along the centreline with or without a filler wire. After cooling, the specimen is bent backwards and forwards until it is fractured. Weld metal crack susceptibility is then determined by estimating the percentage of oxidized fracture surface on the broken edges. Extensive work on the weld crack susceptibility of aircraft steels using this test was reported[1,4,5,6,32,56]. The results will be analysed and discussed in later sections.

2.5.2 Pellini cracking test

The test has been described by WR Apblett and WS Pellini[55]. It involves the laying of a weld bead with full penetration over a number of strips of fixed width (see Fig 12). The interface of adjacent strips lies at right angles to the direction of welding and acts to increase locally the strains imposed on the freezing weld metal, thus under certain conditions causing cracks to occur. By the use of strips of different widths it is possible to vary the degree of severity of straining. The crack lengths in various straining conditions due to the strip width variation are the measure of the crack susceptibility.

2.5.3 Houldcroft cracking test

The test described by PT Houldcroft[54] does not require a clamping fixture. The test piece is made from a rectangular plate of about 45 mm x 77 mm, by cutting slots in either side, their depth increasing progressively along the length of the sheet. The specimen is placed on a carbon block and a TIG weld is made without a filler wire starting at the edge of the specimen where the slots are widest aparrt. A full penetration weld with a constant bead width should be obtained in this test. A crack initiates at the edge and then propagates until there is insufficient stress to cause cracking. The crack length measured is regarded as a measure of the solidification crack suscep-tibility. The design of the specimen is shown in Fig 13.

FJ Wilkinson et al[57] used the Houldcroft test in a miniature form to assess the crack susceptibility of high tensile steels.

2.5.4 Huxley cracking test

This test, developed by HV Huxley[7], is similar to the Houldcroft cracking test, but it uses a specimen with a different geometry and slotting arrangement, and requires a special jig. The specimen is in the form of a strip of 506 mm long by 38 mm wide, usually about 2 mm thick (Fig 14). The strip has opposite slots, approximately 0.8 mm wide and 15 mm deep, let into each edge, the distance between each pair of opposing slots being 38 mm. The slots serve as thermal insulators between the segments and give an edge starting effect for the initiation of a crack. The test is effected by making a melt-run along the length of the specimen, running between but not intersecting the base of the slots. The cracking tendency of a steel is given by

expressing the mean crack length as a percentage of the segment length.

2.5.5 <u>Circular patch test</u>[59]

By this type of test a 150 mm x 150 mm square sheet is firmly held in a test jig with four bolts at each corner and one at the centre (see Fig 15). A circular weld bead of 50 mm diameter is then made starting from any point. The weld run is made by TIG process in one pass. Centreline or transverse cracks are formed due to radial and circumferential strains imposed on the solidifying metal. The length or the angle of a centreline crack is normally measured and referred as crack susceptibility.

2.6 <u>Indicators and predictors of solidification crack susceptibility</u>

The concepts of indicator and predictor must be distingui-shed first before going into any detail. Crack indicators are those which describe the severity or manner of cracking, and they are easily measurable in weld production or in some welding tests. On the other hand, the predictors are those which may more or less predict the severity of solidification cracking. Composition, metallurgical and welding process parameters, which have a correlation with crack indi-cators, may be regarded or used as crack predictors. The relationships between crack indicators and predictors are usually thought to be capable of explanation but sometimes the explanations are not very satisfactory. Some crack indicators and predictors are reviewed in the following sections.

2.6.1 Crack indicators

There are many types of crack indicators, but not all of them are good criteria for crack susceptibility. Possible crack indicators are listed as follows:

1) Crack length: In a designed crack test, usually with severe test conditions, crack length can be measured. It is especially suitable for the centreline cracks, because the number of these cracks in a test is few and the cracks are continuous. Crack length becomes difficult to measure when the cracks are numerous and irregular, as is the case with the Varestraint test. The length of a fine crack or subsurface crack is also very difficult to assess.

2) Crack number: In some tests, only a crack or a crack-free condition is recorded as the test result. In other tests the crack number can be estimated, such as in the Trans-Varestraint test.

3) Crack area: There is some justification for using the crack area as a crack indicator when the crack area is measurable and indicative of the real situation. In the Focke-Wulf cracking test the crack area or the percentage of crack area is measured and taken as a crack indicator.

4) Required strain to cause cracking: In the tests involving the application of external restraints the required strain to cause cracking may be measured. This serves as a useful guide for the comparison of materials or welding procedures.

5) Derived crack indicators: This is based on a series of tests under varying test conditions. Examples are UCS or units of crack susceptibility derived by JG Garland and N Bailey[60], based on the gradient and intercept in the plotting of crack length against strain, CSS and CST (the critical strain rate) described in section 2.2.5. Using the experimental results in the Gleeble hot tension test,

G Wellnitz[61] also derived a crack indicator RF (Rissfaktor). The
application of the derived crack indicator is only justified when it
can indicate the crack severity more precisely, or when other simple
indicators fail to reflect the real crack situation.

2.6.2 Crack predictors

Only the predictors based on alloy composition will be
considered here. A predictor may consist of only one variable, or it
may be derived from many variables. Its predicability is more essential
than its theoretical background. Some values thought or claimed to be
predictors of crack susceptibility are presented as follows:

1) Carbon content: Sometimes the carbon content alone in steel
can indicate the solidification crack susceptibility quite successfully,
especially when the steels are not alloyed or specially treated.

2) Carbon equivalent: Various carbon equivalent formulae are
available, some designed for the prediction of solidification cracks,
some actually designed for other purposes, such as hardness prediction,
estimation of martensite temperature and cold crack prediction. SA
Ostrovskaya[62] defined carbon equivalent to be:

$$CE(Ostrovskaya,1) = C + 2S + \frac{P}{3} + \frac{(Si-0.4)}{10} + \frac{(Mn-0.8)}{12} + \frac{Ni}{12} +$$

$$+ \frac{Cu}{15} + \frac{(Cr-0.8)}{15} \quad (2.3)$$

(for C between 0.09 and 0.14%)

$$CE(Ostrovskaya,2) = C + 2S + \frac{P}{3} + \frac{(Si-0.4)}{7} + \frac{(Mn-0.8)}{8} + \frac{Ni}{8} +$$

$$+ \frac{Cu}{10} + \frac{(Cr-0.8)}{10} \quad (2.4)$$

(for C between 0.14 and 0.25%)

$$CE(\text{Ostrovskaya}, 3) = C + 2.5S + \frac{P}{2.5} + \frac{(Si-0.4)}{5} + \frac{(Mn-0.8)}{8} + \frac{Ni}{6} +$$

$$+ \frac{Cu}{8} + \frac{(Cr-0.8)}{10} \qquad (2.5)$$

(for C greater than 0.25%)

Crack susceptibility is said to be the function of the carbon equivalent thus calculated. The correlation between CSF of the Huxley cracking test and this carbon equivalent was poor according to EJ Morgan-Warren[3].

Realizing the detrimental effects of carbon and nickel in the high tensile steel, H Nakagawa et al[39] proposed the carbon equivalent to be:

$$CE(\text{Nakagawa}) = C + \frac{Ni}{23} \qquad (2.6)$$

This carbon equivalent has a good correlation with the maximum crack length in the Trans-Varestraint cracking test for steels containing P and S less than 0.010%, C being between 0.04 and 0.14% and Ni up to 9%.

A common equivalent based on the end of transformation temperature (M_f), much used for the prediction of the heat affected zone cracking is as follows:

$$CE(M_f) = C + \frac{Mn}{6} + \frac{Ni}{20} + \frac{Cr}{10} - \frac{Mo}{50} - \frac{V}{10} + \frac{Cu}{40} \qquad (2.7)$$

Similar equations for carbon equivalent are plenty in number. More detail is given in the reports by K Winterton[63] and I Hrivnak[64].

3) <u>Sulphur</u>: If the contents of alloying elements and carbon in steels are comparable, the sulphur content is a very good crack predictor. However, there is no agreed sulphur level above which solidification cracks occur.

4) <u>Mn/S</u>: A high Mn/S ratio has been thought to be effective in controlling the hot workability or solidification and HAZ crack susceptibility. Many authors[23,24,25,29] have studied the effect of

Mn/S on cracking, however, no universal trend for this ratio can be concluded. It seems that the effect of Mn/S depends on the carbon content in the steel.

5) Mn^3/S or Mn^5/S: H Nakagawa et al[39] argued that the conventional Mn/S for crack susceptibility indication should be replaced by Mn^3/S for the ferritic steel or Mn^5/S for the austenitic steel, based on the consideration of the solidification process and some experimental results. The steels used for their study of solidification cracking were almost pure Fe-Mn-S alloys with a very low carbon content and a relatively high sulphur content. Therefore, the Mn^3/S or Mn^5/S may not reflect crack susceptibility for technical steels.

6) O/S: The investigations of DC Hilty[40], JC Yarwood[41] and ET Turkdogan[42] encourage the belief that a high oxygen to sulphur ratio will be beneficial for crack prevention, but no reliable figure is available for the minimum O/S required to suppress the formation of filmlike sulphide inclusions or cracks.

7) Phosphorus: When other alloying elements have similar contents, the solidification crack susceptibility can be predicted by the amount of phosphorus in the steel. This fact was recognized by JC Borland[20] and HV Huxley[21], the latter realizing the mutual effect of phosphorus and carbon on solidification cracking, quoted two tentative crack predictors:

$$PCE(Huxley,1) = P \times (C + \frac{Ni}{30}) \qquad (2.8)$$

$$PCE(Huxley,2) = P \times (C + \frac{Ni}{30} - \frac{Mo}{10} - \frac{Cr}{100} - \frac{V}{100}) \qquad (2.9)$$

8) Hot crack susceptibility(HCS): The equation for HCS was obtained from the miniature Houldcroft cracking test carried out on a number of low alloy steels by FJ Wilkinson et al[57]. It is expressed by:

$$HCS = \frac{C \left(S + P + \frac{Si}{25} + \frac{Ni}{100}\right) \times 1000}{3Mn + Cr + Mo + V} \qquad (2.10)$$

The HCS was found to correlate with the test results and was in good agreement with production welding. Steels with a HCS value of less than 4 would show resistance to weld solidification cracks.

9) Crack susceptibility factor according to CLM Cottrell[27]:

The crack susceptibility factor (CSF) measured by the Huxley cracking test, can be predicted by the following equation:

$$P(CSF, Cottrell) = (P(C + 0.142Ni + 0.282Mn + 0.2Co - 0.14Mo - 0.224V) + \\ + 0.195S + 0.00216Cu) \times 10^4 \qquad (2.11)$$

Cottrell found this expression has a correlation of 0.92 with the actual CSF value, though the equation looks complicated.

10) Crack susceptibility factor according to HV Huxley[22] :

In his study of the influence of composition on weld solidification cracking in carbon manganese steel, Huxley attempted to establish an equation to predict the crack susceptibility factor. Various regression equations were obtained, but none appeared to be good enough for prediction purposes. One of his equations is as follows:

$$P(CSF, Huxley) = 7836C \times S - 1145S + 13.3 \qquad (2.12)$$

The above equation is based on 22 observations with a carbon content ranging from 0.10 to 0.30% and has a correlation of 0.74.

11) Crack susceptibility factor according to Morgan-Warren[3]:

With 82 observations of steel composition and the Huxley cracking test data, EJ Morgan-Warren made a regression analysis of the crack susceptibility factor based on composition and found an equation with a correlation of 0.82, which is given as follows:

$$P(CSF, Morgan-Warren, 1) = 36C + 12Mn + 5Si + 540S + 812P + 3.5Co - \\ - 20V - 13 \qquad (2.13)$$

With 42 observations of crack susceptibility and composition (inclu-ding oxygen analysis) he discovered another regression equation:

$$P(CSF,Morgan-Warren,2) = 42C + 847S + 265P - 10Mo - 3042(O) + 19$$

(2.14)

For this expression the correlation has improved from 0.82 to 0.9 with 95% confidence limits of $\pm$ 11. The mean oxygen content in those steels was, however, only 0.0054%. It can be argued that the apparent effect of oxygen is obstructed in the second equation by the introduc-tion of a much higher sulphur coefficient and a higher intercept constant.

12) Units of crack susceptibility (UCS) predictor: the UCS is a derived indicator of crack susceptibility according to JG Garland et al[60] and the UCS in the submerged arc welding of carbon-manganese steels can be expressed as being equal to:

$$P(UCS,Garland,1) = 184C + 870S - 188P - 18Mn - 4760CxS - 12400SxP +$$
$$+ 501PxMn + 326000CxSxP + 12.9 \qquad (2.15)$$

In their later investigation[66], however, another equation was reported in which the various terms of interactions were disregarded. The equation then is:

$$P(UCS,Garland,2) = 223C + 187S + 100P + 48Nb - 14.3Si - 6Mn -$$
$$- 16Al + 0.5 \qquad (2.16)$$

Based on the later work of N Bailey[33] a revised equation of UCS is given by:

$$P(UCS,Bailey) = 230C^{*} + 190S + 75P + 45Nb - 12.3Si - 5.4Mn -$$
$$- 14Al - 1 \qquad (2.17)$$

where C^{*} is the corrected carbon content (the carbon contents less than 0.08% are to be treated as equal to 0.08%).

There is another possibility of predicting crack susceptibi-lity based on composition. Instead of using a straight-forward equa-tion, a decision flow chart according to some criteria can be constructed

as carried out by K Orths et al[67] for the prediction of solidification cracking in the steel cast. In their decision flow chart, deoxidation products, P+S, P, S and other factors are considered one by one, details of which are shown in Fig 16.

From the various expressions of predictors as introduced before, it can be seen how difficult it is to find an applicable and universal crack predictor. It would be worthwhile to point out that the following questions have not yet been clearly answered:

1) How do the alloying elements interact with each other?

2) Does Mn/S or O/S have a real effect on cracking?

3) Can a single equation reflect the effect of a wide range of composition on cracking?

4) To what extent has composition an overriding effect compared to solidification conditions and welding parameters?

2.7 Summary of the literature survey

Of the various factors which affect solidification cracking, stresses are clearly the direct cause for the occurrence of cracks. Unsuitable plate geometry and poor selection of welding parameters intensify stresses and hence have a direct adverse effect on cracking. The steelmaking process may confer unfavourable properties on the material and affect the crack susceptibility of material in some cases.

There are many conceptual variables of solidification cracking, such as crack susceptible temperature interval, crack susceptible length, crack susceptible time and the critical strain rate etc. If these can be experimentally measured it will be very helpful for the understanding of the relationships between cracking and composition or welding variables.

Instead of using these conceptual variables as criteria for crack susceptibility, the results of a simple cracking test are more conveniently used as crack indicators. They may be crack length, crack area, number of cracks, or required strain to cause cracking in certain tests. There are two approaches for the test of crack susceptibility: one with externally imposed restraints and the other with thermally induced restraints. Among the numerous cracking tests, the Huxley cracking test is regarded as the most suitable one for the crack susceptibility assessment of steel sheet.

The Huxley cracking test has the advantages of requiring no special test apparatus, relatively easy specimen preparation, a high test sensitivity and reproducibility. Moreover the test results have been correlated with the real production welding[7]. Numerous Huxley cracking test data have been available in the literature, which can be taken as reference for the study of cracking and composition relationships.

Theories of the effect of composition on solidification cracking are based on the metallurgical conditions for the formation of filmlike sulphide inclusions. The study of the iron-based alloys, such as Fe-S, Fe-Mn-S, Fe-O-S and Fe-Mn-S-O systems, leads to the belief that the manganese and oxygen content, or Mn/S and O/S ratios could be important factors for the control of crack susceptibility. However, their effects have not yet been verified. None of the above mentioned systems can be directly applied to the technical steels, because of the presence of carbon and the relatively low amounts of oxygen and sulphur in them.

Various equations for the prediction of crack susceptibility from composition are available, but they seem to contradict each other. This reflects the uncertainty about the effects of composition on crack

susceptibility. Clearly more work is needed to identify the limits and conditions for the effects of Mn/S, O/S and other compositional factors. This would assist the establishing of a rational and realistic cracking and composition relationship.

The solidification cracking of weld metal is closely associated with the solidification process. A solidification process producing fine equiaxed grains with less segregation would reduce crack susceptibility. However, the control of weld pool solidification is limited without using artificial menas. Using inoculants, or vibrating or stirring the weld pool may also refine the grains in the weld metal and hence reduce the crack susceptibility, but these measures may not be required if crack-proof steels with required properties are readily available.

The objectives of this work are to extend the knowledge about solidification cracking in steel welds in general and to investigate the cracking and composition relationship in particular. Particular problems to be solved are:

1) To avoid cracks in the weld, what amounts of sulphur and phosphorus are tolerable in the various types of steels?

2) What factors can raise the tolerable amount of sulphur in steels?

3) Is the effect of manganese or Mn/S on solidification cracking significant? If so, what level of Mn/S or manganese content is required for the prevention of cracking?

4) Can the oxygen content reduce the sulphur-induced solidification cracking? What is the necessary level of oxygen to counteract the harmful effect of sulphur?

5) Can it be assumed that the effect of each alloying element is linear and additive? Is it possible to find a linear regression

equation on this assumption for the prediction of crack susceptibility?

6) To what extent has composition an overriding effect on cracking compared to solidification conditions and welding parameters?

7) Which of the existing theories of solidification cracking can explain the crack behaviour in the TIG arc welding of thin steel sheet?

3. EXPERIMENTAL INVESTIGATION AND RESULTS

The Huxley cracking test was chosen as the main method for the assessment of solidification crack susceptibility. In order to ensure the reliability and similarity of testing results under various testing conditions, the general aspects of the Huxley cracking test were re-examined. These included:

1) Reproducibility.

2) The effect of surface conditions.

3) The effect of plate thickness.

4) The right conditions for a full penetration of weld bead.

5) Possibility of modifying the specimen design.

6) The effect of jig.

Two sets of experimental steels were then tested with the Huxley cracking test in order to see the effects of carbon, manganese, sulphur, oxygen, Mn/S and O/S. Additional steels were also tested, so the crack susceptibility of a wide range of steels can be compared.

All the test data were used for the regression of crack susceptibility based on composition. The data from each set of experiment was treated separately first, then pooled to reveal the general trend. Numerous Huxley cracking test data from previous research investigators were also collected for regression analysis. This effort enabled the conclusions of the general trend of cracking and composition relationship to be established.

As this work had a special interest in evaluating the effect of oxygen, more experiments were undertaken, these included:

1) Closed box welding tests.

2) Welding with an argon-oxygen mixture as a shielding gas.

3) Oxygen analysis of parent and weld metals of various tests.

To determine the mechanism of weld solidification cracking as well as the effect of inclusions, the fractured crack surfaces were examined under a scanning electron microscope. Fresh crack surfaces obtained from the closed box welding revealed the general features of solidification cracking. In addition, the actual crack development during welding was studied during some runs of the Huxley cracking test, so as to gain more information of cracking development.

3.1 General aspects of the Huxley cracking test

The Huxley cracking test has already been described in section 2.5.4 and the test conditions of the present research have adhered as closely as possible to those chosen by HV Huxley and EJ Morgan-Warren. Concerning the reproducibility of the test results of CSF values, HV Huxley[68] reported 95% confidence limits for a mean of 8 crack lengths being 1.75 mm (equivalent to a CSF value of 4.6), and for a mean of 24 crack lengths 1.02 mm (equivalent to a CSF value of 2.7). Similarly EJ Morgan-Warren[3] reported the 95% confidence limits for 24 crack lengths to be 0.91 mm (equivalent to a CSF value of 2.4). In this research the reproducibility of the Huxley cracking test has been checked constantly throughout the research period. Some of the typical reproducibility test results are shown in Table 2. It appears that steels with a higher crack susceptibility tend to have a wider scatter of the test results. However, in any case, the 95% confidence limits for the mean of 24 crack lengths will not exceed 2 mm or 5 CSF units as can be seen in Table 2.

The original plate thickness of various research materials was not uniform, and the surface conditions of them were also different.

For these reasons, the effect of surface conditions and the testing conditions for various plate thicknesses was studied. Four types of surface condition of the Huxley cracking test specimens have been used for the comparison of Huxley cracking test results, namely:

1) Heavily scaled.

2) Pickled in a mixed acid (mainly HCl).

3) Shot-blasted or abrasive-ground (linished).

4) Brightly milled.

The test results are shown in Table 3. Generally speaking the test results were not affected by surface conditions if there were no heavy scale on the surfaces. A specimen with a heavy scale on the surface may affect the arc stability during welding, and if the arc wanders away from the centreline, the test result must be discarded. A bright surface is not required for the test, though the test result would not be affected by this condition. During the experimental programme many plates were taken down to 2.0 mm by milling, therefore their surfaces were bright. To remove surface scales, shot-blasting is not so effective as abrasive-grinding. Because surface grinding by abrasive took a considerable time to remove scales, attempts to pickle the specimen in a mixed acid were made. The quick scale removal by pickling was offset by the required drying process and the quickly developed new scales on the surfaces. In the later tests, specimens with brightly milled or abrasive-ground surfaces were used.

The sheet thickness of the experimental steels was not constant, consequently a slight variation of the welding conditions was required. In accordance with the experiments done by HV Huxley and EJ Morgan-Warren, the rules applied in this research for the variation of test conditions were as follows:

1) Keeping the welding speed constant at 2 mm/S.

2) Choosing a suitable current to yield a 6 mm weld bead
with a full penetration.

In all of the tests, the arc length was kept at about 2.2 mm
and it was found that a slight variation of arc length within the limits
of $\pm$ 0.2 mm did not change the test results. The electrode was a clean
thoriated tungsten electrode having a tip with an angle of about 55°.
For all current settings the arc voltage remained very close to 11V.
The current required to produce a 6 mm weld bead by using various sheet
thickness was found experimentally and is given in Table 4. The re-
lationship between arc current and sheet thickness can also be repre-
sented by the following equation:

$$\text{Current(A)} = 3.8 + 4.19 \times \text{Thickness (mm)} \qquad (3.1)$$

The specimen design for the Huxley cracking test used in this
research was the same as used by previous investigators, which is shown
in Fig 14. Because the number of segments in a test coupon has no
effect on test results, some test specimens were cut so as to have only
five segments in order to save material. The original design allowed
a 51 mm run-in and 51 mm run-out margin in the test specimen. However,
most of the specimens were cut to have a 38 mm run-in and 38 mm run-out
margin, because it was found that such arrangement has no effect on test
results and saves material.

The thickness of the test sheet was ideally 2 mm, and some
thicker plates were taken down to 2 mm by milling. The effect of
sheet thickness on the Huxley cracking test results was checked by the
available sheets of various thicknesses, and the results are shown in
Table 5. It can be seen that the variation of thickness between 1.68
and 2.51 mm has a negligible effect. Most of the specimens had a
thickness very close to 2 mm; in any case it was within the range
between 1.6 to 2.5 mm.

To carry out a test the specimen was set up on a Huxley jig consisting essentially of two round bars 12.7 mm diameter by about 420 mm long. The specimen was laid on the jig in such a way that line contact only was maintained between specimen and jig; this ensured a minimum loss of heat to the jig by conduction. The specimen was held loosely at the edges by screws let into the jig at suitable intervals, the point of retention being at the ends of each test section. During welding, the specimen held in the jig was moved at a constant speed of 2 mm/S, while the elctrode was held vertically above the specimen with a gap of about 2.2 mm. It was found that the centreline of the specimen must strictly follow the welding line in order to avoid bridging the ends of the slots. However, the way of holding specimen was found to be not essential. Tests with other type of jig were experimented. In the simplest case it involved putting a specimen on a metal block which has a groove along the centreline, without any clamping. The test results were identical to that using Huxley jig.

In case there was difficulty in starting the welding arc, the electrode was slightly lowered for striking the arc and quickly adjusted to the required level, or alternatively, a small piece of graphite was used to assist starting the arc. Generally speaking, starting the arc was not a problem if the specimen was free from scale.

When the weld proceeded toward the end of the run-out margin in the specimen the welding current as well as the travelling device was switched off. In case crater cracking was to be avoided, a slope down current was used at the end of welding.

The crack lengths of each tested specimen were measured visually, a stereo-microscope with a low magnification being used where necessary. Measuring the crack length in the Huxley cracking test was not found to be a problem in this research.

3.2 <u>The effects of carbon, manganese, sulphur and oxygen on crack</u>
<u>susceptibility</u>

First of all, two series of experimental steels were made
for the welding test. One of these series of steels belongs to the
SAE4130 specification with intended variation of manganese, sulphur
and oxygen contents while keeping the contents of other alloying elments
at the same levels. By comparing the test results of this series of
steels, it was anticipated that the effects of manganese, sulphur, oxy-
gen, Mn/S and O/S could be assessed. The other series of steels basically
belongs to the Fe-Mn-S-O alloy system. The variation of manganese,
sulphur and oxygen contents in the latter series of steels enables a
fundamental study to be made of the sulphide inclusions and their effect
on solidification cracking. Comparing the two series of steels, one
with 0.30% carbon and the other with practically no carbon content, the
effect of carbon on solidification cracking can also be examined.

3.2.1 <u>SAE4130 steels</u>

The plan of 2^3 factorial experiment with manganese, sulphur
and oxygen each at low and high levels for SAE4130 steels is shown in
Table 6. The chosen high and low levels of manganese were 0.70 and 0.20%
respectively, being slightly beyong the specified manganese range (0.40
to 0.60%) so as to show the effect of manganese more clearly. The high
sulphur level of 0.040% is equivalent to the specified maximum value
for SAE4130 steel, while the low sulphur level of 0.007% represents
the amount of sulphur in a quality steel. The chosen levels for oxygen
contents, 0.020 and 0.005% , were thought to be the upper and lower
limits of oxygen content in high tensile steels. By such arrangement

it also provided a wide range of O/S and Mn/S ratios, which enabled
study to be made of whether O/S and Mn/S has an effect on solidifica-
tion cracking.

According to the plan a series of special casts was made at
the BSC Material Research Laboratory and the resulting analysis is given
in Table 7. The resulting casts had a manganese content between 0.17
and 0.80%, a sulphur content between 0.007 and 0.042%, an oxygen con-
tent between 0.004 and 0.016%, an O/S ratio between 0.17 and 2.00, and
an Mn/S ratio between 5 and 80. Because their composition agreed rea-
sonably with the plan, the casts could be suitably used for the experi-
ment. The casts were hot-rolled to 15 mm plates and then cold-rolled
to approximately 2 mm thick sheets. The 2 mm sheets of each steel were
flattened and cut into Huxley specimens. The specimens were tested
repeatedly on different occasions in order to avoid systematic errors.
The test procedures were in accordance with that described in section 3.1,
the current used being about 90 A and the voltage measured 11 V.

The oxygen content of each parent sheet was analysed at
least five times by the fusion method and the composition was determined
by a routine spectro-analysis. The results of the chemical analysis
and cracking test for this series of steels are shown in Table 7. It
can be seen that a wide range of CSF values (0 to 62), or a good spread
of cracking behaviour, was obtained.

The eight steels with composition most close to the 2^3 factorial
plan, MA1 to MA8, were arranged in a manner suitable for factorial
analysis as shown in Table 8. For further treatment, the three factors,
manganese, sulphur and oxygen are represented by A, B and C respectively.
The appropriate small leter a, b and c is used when the corresponding
factor is at high level, The absence of a letter means that the corres-
ponding factor is at the low level. Thus ab represents the steel in

which manganese and sulphur are at the high level but oxygen is at the low level. The symbol (1) is used when all factors are at the low level.

The Yates method[69] is a simple technique for the analysis of a 2^n factorial experiment, which relies on a specific arrangement and order of calculation. In this investigation this method was applied to show the effects of Mn, S, O and their interactions, and the calculation is shown in Table 9. In the Table, the observation column gives the observed CSF values, and columns I, II and "Effect Total" are calculated from the preceding columns in the same way: The first 4 numbers in a column (I, II or Effect Total column) are the sums of successive pairs of numbers in the preceding column, the next 4 numbers are the differences of successive pairs in the preceding column, the first number being substracted from the second one. By dividing the values in the "Effect Total" column by 4, the corresponding effects can be obtained. The sum of squares for each effect is obtained by squaring the effect total and dividing by 8, From the results of calculation as shown in Table 9, it can be seen that sulphur (b) has the largest effect on cracking; the interaction of Mn and S (ab) as well as the interaction of S and O (bc) has only a negligible effect comparing with the extremely large effect of sulphur (b).

In addition to this factorial analysis, a multiple regression of CSF values based on composition was made in which the variables Mn, S, O, O/S and Mn/S etc were considered. This analysis also showed that only sulphur has a 5% level of significance and the regression equation was found to be:

$$P(CSF, MA) = 1681S - 6 \tag{3.2}$$

with a correlation coefficient of 0.95 and a residual error of 8. A comparison of the observed values and the estimated ones using the above equation is shown in Table 10 and Fig 17.

3.2.2 Fe-Mn-S-O alloys

The plan of 2^3 factorial experiment with manganese, sulphur and oxygen each at high and low levels for this series of alloys is shown in Table 11. The high and low levels of manganese were 0.80 and 0.01% respectively, the low level almost representing the absence of manganese in the alloy. The high sulphur level of 0.20% is slightly higher than the solubility of sulphur in delta ferrite (0.18%) in the Fe-S binary system. The high level of oxygen content 0.20% was thought to be a possibly meaningful upper limit for the present investigation. This plan also provided a very wide range of Mn/S and O/S ratios, ideally for the study of the effects of Mn/S and O/S on cracking. Because of the uncertainty and difficulties of having the required composition, 12 ingots were made by the BSC Corporate Laboratory. The chemical analysis of the resulting casts is shown in Table 12. It can be seen that the first eight casts had the high and low levels of Mn, S and O contents conforming to the plan, and the other four casts were additional alloys with an intermittent level of oxygen content. The ranges of O/S and Mn/S ratios were wide, being between 0.03 and 3.15 for the former, and between 0.1 and 51.8 for the latter. Therefore, the suitability of these casts for experiments could be expected.

Slices of about 10 mm thick were cut from the ingot, which having a 75 mm x 75 mm cross section and weighing approximately 10 kg, then cold-rolled to a 2 mm sheet. Due to the limited size of the rolled sheet, each Huxley specimen contained only five test segments. The specimens normally had a clean surface, but required hammering to restore the flatness.

The test procedures for this series of steels were the same as described in the previous section. The details of composition and

the Huxley cracking test results are shown in Table 12. Factorial analysis for this series of steels with the Yates method as described in section 3.2.1 is shown in Table 13 and 14. Table 14 indicates that only the effect of sulphur is significantly large, other effects negligibly small. This fact can also be observed quite readily from Table 12, since the five alloys with high CSF values correspond exactly to the alloys with a high sulphur content. A multiple regression of CSF values based on compositional factors including Mn, S, O, Mn/S and O/S was made and the results showed that sulphur only has a 5% level of significance, and the regression equation for this series of steels being:

$$P(CSF,MC) = 431S - 9 \qquad\qquad (3.3)$$

with a correlation coefficient of 0.98 and a residual error of 8.

It is interesting to notice that Mn/S and O/S ratios in this series as well as in the previous SAE4130 series had no significant effect despite their wide ranges. Comparing the sulphur coefficients in equation 3.2 and 3.3, it can be seen that the effect of sulphur on cracking is more severe in the SAE4130 steels than in the Fe-Mn-S-O alloys, this is presumably due to the higher carbon content in the SAE4130 steels.

3.2.3 Other steels

In order to check the effects of oxygen, manganese, carbon, sulphur, O/S, Mn/S ratios on the crack susceptibility of commercial high tensile steels and to extend the scope of the test data for the study of composition and cracking relationship, more steels were collected for the Huxley cracking test. The steels collected included six additional SAE4130 steels (designated as MB series), four EN24, four ASTM A387B, one each of HY130, HY80, ASTM357, EN5, EN19, EN353,

Corten A, Creusabro 32, Hypress 23, BS4360-50B and SAE1006. Except for SAE1006 all other steels are high tensile low alloy steels. For further reference all steels(except for the 6 additional SAE4130 steels) are called MD series of steels in this research, and each steel has its series number beginning with MD (see Table 15).

Table 16 shows the composition and cracking test data for the six additional SAE4130 steels (MB series). It can be seen that the variation of composition, especially carbon and phosphorus, in this series was wider than in the previous SAE4130 experimental steels (MA series). Table 17 shows the composition and Huxley cracking test data for the miscellaneous steels in the MD series. As can be seen from the Table, in this series of steels the carbon content lied between 0.06 and 0.50%, sulphur content between 0.010 and 0.040%, manganese content between 0.30 and 1.48%, and other elements had also a considerable scatter of contents. Except for MD9, which contained 0.052% O_2, most steels had an oxygen content of less than 0.015%, as could be expected, most high tensile steels being killed steels. A wide range of cracking behaviour was also observed in this series of steels, for the CSF values lied between 0 and 68.

Without a statistical analysis of the results, the effects of sulphur and phosphorus can be directly seen from the data shown in Tables 16 and 17, but the effects of other elements as well as the Mn/S and O/S ratios can only be revealed by a suitable statistical analysis. An analysis of the results will be described in the following section.

3.3 Statistical analysis of the composition and cracking relationship

Details of the statistical methods adopted in the present investigation are expounded in such standard texts as "Statistics for Technology" by C Chatfield[69], and some important terms are explained

in the appendix of this thesis.

Altogether 47 steels have been studied in this research. The test results have already shown many interesting features of the composition and cracking relationship. In order to have more understanding of the effect of each single element and their interactions the results have been systematically analysed by means of a computer statistical package programme (ICL Statistical Analysis XDS3). Many regression equations have been obtained consequently.

In order not to draw conclusions from limited observations, and to take full advantage of the documented cracking test data, an attempt has been made to collect as much cracking test data as possible. Altogether 170 Huxley cracking test data are collected, most of them belonging to the high tensile low alloy steels of interest to the aircraft construction industry. In addition 131 Focke-Wulf cracking test data and 49 Trans-Varestraint cracking test results have been collected for analysis, and this enables the comparison of testing methods and shows if composition has an overriding effect on solidification cracking.

In the following sections the data sources, statistical procedures and the analytical results are presented. At the end there is a brief summary of the findings. The effect of each single element, and their interactions, will be discussed in the next chapter.

3.3.1 Data sources

Four series of steels have been tested in this research as described before. They are:

1) <u>MA series</u>: This series of steels fall into the specification of SAE4130 with designed variation of Mn, S, O, O/S and Mn/S, details of composition and cracking test results are shown in Table 7.

2) <u>MB series</u>: This series contains six SAE4130 steels with a wider variation of C, S and P, and its details are shown in Table 16.

3) <u>MC series</u>: Twelve experimental Fe-Mn-S-O steels with a vey low carbon content are in this series, whose composition and CSF values are shown in Table 12. The sulphur contents in this series of steels are higher than in any other series of steels, the highest being 0.180%. The oxygen contents are also higher than in other series, the highest being 0.066%.

4) <u>MD series</u>: This series includes many miscellaneous commercial steels, in which the carbon level varies from 0.06 to 0.50% (details in Table 17).

The following series of steels have been investigated by previous investigators. For the convenience of identification, a series name and number are given to each steel according to data source. The first letter in the series name stands for the initial of the author's name, additional letters follow if the data originated from more than one author or an author had various sets of data. Except for steels in the HD series, all are high tensile steels of interest to the aircraft industry. Unfortunately the oxygen analysis was not given in many series of steels. However, by tracing the steelmaking process records in the original reports or looking at the available oxygen analysis, it can be assumed that most steels had a very low oxygen content, possibly only 0.005%.

5) <u>HA series</u>: The experimental data of this series were supplied by HV Huxley and quoted by EJ Morgan-Warren et al[70]. The steels included in this series were mainly 3%Cr-Mo-V and 1%Cr-Mo steels with a carbon content higher than 0.35%. Because of their high carbon content, the oxygen content might be very low, possibly about 0.005% or even lower. The details of this series are reproduced in Table 18.

6) <u>HB series</u>: The composition and cracking test data of this series of steels were reported by HV Huxley[21] and reproduced in Table 18 of this thesis. The steels included were high tensile steels with various combination of alloying elements. While the sulphur contents were less than 0.010%, the phosphorus contents varied from 0.009 to 0.023%.

7) <u>HC series</u>: The data source of this series of steels is also derived from HV Huxley[7], and the details are shown in Table 20. One interesting point of considerable significance in this report is that both HC8 and HC9 are 2%Ni-Cr steels with a similar composition, one air-melted with 0.012% S and 0.016% P, showing a CSF value of 40, while the other being vacuum-melted high purity steel with only 0.004% S and 0.001% P, showing no cracking tendency at all. This implies that sulphur and phosphorus contents have an overriding effect on solidification compared to other alloying elements.

8) <u>HD series</u>: The data is taken from the report on the influence of composition on weld solidification cracking in carbon manganese steel by HV Huxley[22] and shown in Table 21. This series of steels are almost comparable with those Fe-Mn-S-O alloys in the MC series. While the MC series can be considered as pure Fe-Mn-S-O alloys, the HD series of steels represent contaminated Fe-Mn-S-O alloys.

9) <u>C series</u>: This data is taken from CLM Cottrell's report[27] on factors affecting the fracture of high tensile steels. Among the 55 steels included for the study were 1%Cr-Mo, 3%Cr-Mo-V, 5%Cr-Mo-V, 2%Ni, 12%Cr and Si-Cu alloy steels. EJ Morgan-Warren[3] have already done a regression analysis on this series of steels together with the steels in the HA series. Details of this series are shown in Table 22.

10) <u>MW series</u>: The data, shown in Table 23, is derived from EJ Morgan-Warren[3,70]. Totalling 17 samples, four types of steels were

involved, namely SAE4130, ASTM A387B, EN24 and 3%Cr-Mo-V (RS140). The oxygen analysis for this series of steel is available.

11) MH series: Shown in Table 24, while the crack data is derived from HV Huxley, the oxygen analysis was made available by EJ Morgan-Warren[70]. However, the oxygen content in this series of steels was not very high (all less than 0.006%).

All series of steels mentioned above were tested by the Huxley cracking test under similar test conditions, except that the tested sheets might have different thickness. It has been found in this research that so long as a 6 mm weld bead with a full penetration is obtained, the crack susceptibility of a steel is identical, disregarding the change of sheet thickness between 1.6 mm anf 2.5 mm (see Table 5). For this reason, the test results in various series should be fully comparable, and the variation of crack value can be thought as the effect of composition only.

Two series of steels have been assessed by JG Garland and N Bailey[60,66] by using the Trans-Varestraint cracking test, which are:

12) GBA series: This data, shown in Table 25, is quoted from the report by JG Garland and N Bailey[60]. The compositions were specially designed by the original authors to suit a 2^4 factorial analysis. By using plates containing 0.10 or 0.25% C with 0.007 or 0.05% each of S and P, and 0.5 or 1.5% Mn and welding with a 1% Mn steel wire and a neutral flux giving a bead of 70% dilution, it was possible to study the crack susceptibility and composition relationship.

13) GBB series: The data, reproduced in Table 26, is from the report of JG Garland and N Bailey[66]. The test and the evaluation of crack susceptibility are the same as in the GBA series, however, more steels were involved in this series.

14) Focke-Wulf or FW series: This series contains 131 Focke-Wulf cracking test data collected from German documents[1,6,32]. Most

of the steels are aircraft steels . The test procedures have been
described in section 2.5.1. Full details of each steel composition
and cracking test result are not listed in this report, but the sta
tistics of this series are given in Table 27.

3.3.2 Procedures of statistical analysis

An ICL statistical package programme was used for the statis-
tical analysis of the collected data. Each set of data was treated
separately, but in the later stage various sets were pooled or a set
of data was divided for analysis according to the alloy composition.
No matter how the data was combined or divided, the following tests
were usually made:

1) Regression analysis of crack susceptibility with the
variables of C, S and P only, where C, S and P representing the weight
percentage of carbon, sulphur and phosphorus in the steel (parent metal).
Other alloying elements were not considered.

2) Regression analysis of crack susceptibility with all
single term variables: C, S, P, Si, Mn, Ni, Cr, Mo, V, Al, O, attempting
to find a regression equation with variables at a 5% or 10% level of
significance, having the form:

$$CSF = a_0 + a_1 \cdot C + a_2 \cdot S + a_3 \cdot P + a_4 \cdot Mn + \cdots$$

In case the values of a variable is not known, the inclusion of such
a variable is omitted or a typical value is assigned to the variable.

3) Regression analysis of crack susceptibility based on
single term as well as cross term variables. Cross term variables inclu-
ded were: CS (the product of carbon and sulphur percentage), CP (the
product of carbon and phosphorus percentage), Mn/S and O/S ratios, etc.

Accompanying the finding of regression coefficients, the sum

of squared errors, residual, correlation coefficient and t statistics
are simultaneously calculated. These statistical values provide infor-
mation to evaluate the suitability of the equation.

The higher the correlation coefficient for a regression
equation, the better is the fitness of this equation in relation to
the values observed. With more variables in the regression set, the
correlation coefficient becomes higher. However, it is only meaningful
to include the variables which are really significant. Variables with
a high t statistic value are significant, for example, a variable with
a t value of greater than 2 is significant at a 5% level. The selection
of variables to be included in the regression is done by the computer
according to t statistic values; no human calculation is required, thus
the accuracy of the selection is assured.

After finding a regression equation a prediction of the crack
susceptibility based on composition can be made by the computer programme
if it is required.

3.3.3 Results of statistical experiments

For the Huxley cracking test data, the crack susceptibility
factor (CSF) is treated as a dependent variable of compositional variables.
For the Trans-Varestraint cracking test, the units of crack susceptibi-
lity (UCS) are the dependent variable; for the Focke-Wulf cracking test,
the crack factor (CF) is the dependent variable. Regression analysis
based on variables at various levels of significance have been made in
the statistical experiments, however, it is impossible to include all
the test results in this report. For the sake of clarity and economy
of space, only the regression equations with variables at 10% level
of significance are given here. In order to distinguish various regres-

sion equations, the predicted value of CSF is represented by $P(CSF, SN)$, where SN is the series name of the observations.

1) <u>MA series</u>: This series, shown in Table 7, has ten SAE4130 experimental steels with a designed variation of Mn, S and O contents and a wide range of Mn/S and O/S ratios. The effects of oxygen, manganese, O/S and Mn/S are however not significant at 10% level in this series. Because the contents of carbon, phosphorus and other alloying elements were not varied, their effects were not discovered by the regression analysis, thus the regression equation contains only one variable, sulphur. The equation is:

$$P(CSF, MA) = 1681S - 5 \qquad (3.2)$$

With a correlation coefficient of 0.95 and a residual error of 8, more details have been described in section 3.2.1

2) <u>MB series</u>: This series contains six SAE4130 steels with a wide range of sulphur, phosphorus and carbon contents as can be seen in Table 16. The regression equation for this series is:

$$P(CSF, MB) = 1060S + 333P + 18 \qquad (3.4)$$

with a correlation coefficient of 0.95 and a residual error of 4.

3) <u>MC series</u>: The study of this series (Fe-Mn-S-O alloys) has been already described in section 3.2.2. Although the variation of Mn, O, Mn/S and O/S is quite substantial, these variables have no significant effect on cracking. The regression equation is:

$$P(CSF, MC) = 431S - 9 \qquad (3.3)$$

with a correlation coefficient of 0.98 and a residual error of 8.

4) <u>MD series</u>: This series includes many miscellaneous steels as can be seen in Table 17. Though this series has a wide range of composition, the regression analysis showed that only carbon and sulphur are the variables at the 10% level of significance. The regression equation

$$P(CSF,MD) = 114C + 1035S - 23 \qquad (3.5)$$

has a correlation coefficient of 0.83 and a residual error of 15. The comparison of the observed and predicted values is shown in Fig 18.

5) <u>HA series</u>: As shown in Table 18 this series contains only two types of steels, 3%Cr-Mo-V and 1%Cr-Mo (SAE4130) steels. The regression equation for this series is:

$$P(CSF,HA) = 84C + 404S + 509P - 20 \qquad (3.6)$$

The regression equation has a correlation coefficient of 0.63 only, much less than the other. This might imply that the 1%Cr-Mo and 3% Cr-Mo-V steels have less comparable cracking and composition relation-ships (comparing equation 3.12 and 3.17 for each type of steel).

6) <u>HB series</u>: This series contains a mixture of many types of steels as can be seen in Table 19. The sulphur contain in this series of steels is less than 0.010%, probably because of this, sulphur appears not a significant variable in the regression. A wide range of carbon content in this series of steels reveals the importance of the mutual effect of carbon and phosphorus on cracking as can be seen in the following regression equation:

$$P(CSF,HB) = 4Ni - 5Mo - 316CP + 7 \qquad (3.7)$$

The above equation also shows the harmful effect of nickel and the beneficial effect of molybdenum on solidification cracking. Surpri-singly this regression equation has a very high correlation coeffi-cient of 0.96 and a very small residual error of 4.

7) <u>HC series</u>: With a similar carbon content but various phosphorus contents, the steels in this series are very susceptible to cracking, except for HC9, which is a vacuum-melted high purity steel(Table 20). Cracking appears to be influenced by the phosphorus content only as can be seen in the following equation:

$$P(CSF,HC) = 1919P - 3 \qquad (3.8)$$

with a correlation coefficient of 0.89 and a residual error of 10.

8) HD series: This series contains 22 experimental steels with data shown in Table 21. The steels are carbon manganese steels, in which the manganese and sulphur contents were deliberately varied. However, the regression did not show that sulphur, manganese and Mn/S are significant at the 10% level. The equation

$$P(CSF, HD) = 6749CP - 16 \qquad (3.9)$$

with a poor correlation coefficient of 0.65 and a large residual error 18 implies that factors other rhan CP have effects on CSF value, but do not behave linearly in such kind of steels.

9) C series: This series contains a wide variety of composition and cracking behaviour as can be seen in Table 22. The best regression equation with variables at the 10% level of significance is:

$$P(CSF, C) = -18C + 1001P + 4Si + 29Mn + 6Ni - 7Mo +$$
$$+ 4716CS - 1462\ MnxS - 10 \qquad (3.10)$$

with a correlation coefficient of 0.91 and a residual error of 5. Because of the wide scatter of alloy contents in this series of steels, many variables are revealed as being enfluential on the cracking tendency; however, the occurrence of MnxS as a variable at the 10% level of significance might be explained due to some chance effect of the regression.

10) MW series: Shown in Table 23, this series contains four types of steels. The oxygen analysis is available in this series of steels, however, the oxygen content varied only between 0.003 and 0.015%. The regression equation is:

$$P(CSF, MW) = 6Ni - 2078(0) - 30(0/S) + 55 \qquad (3.11)$$

with a correlation coefficient of 0.96 and a residual error of 5. The apparent large negative coefficients of oxygen and 0/S are in fact balanced with a large intercept of 55.

11) <u>MA and MB series</u>: This set combines the MA and MB series, both are SAE4130 steels. The regression equation for this combined set of data is:

$$P(CSF,MA+MB) = 1587S + 657P - 5 \qquad (3.12)$$

with a correlation coefficient of 0.94 and a residual error of 8. Figs 10 to 21 show that carbon, manganese and oxygen contents have no effect on the CSF value in this combined series with only one type of steel involved. Fig 22 and 23 show the effects of sulphur and phosphorus contents on CSF values respectively. Fig 24 shows the observed values against estimated values by using the above equation.

12) <u>MA+MB+MD series</u>: This set contains a variety of high tensile steels with a known oxygen analysis, which were experimentally investigated in the present research. The regression equation is:

$$P(CSF,MA+MB+MD) = 121C + 1320S + 373P - 36 \qquad (3.13)$$

with a correlation coefficient of 0.86 and a residual error of 13. The effects of oxygen, Mn/S and O/S were not significant at the 10% level despite the inclusion of oxygen analysis for regression.

13) <u>MA+MB+MC+MD series</u>: This set combines all steels which have been investigated in this research. All the 47 steels in this set have a known oxygen analysis and the regression equation for this set is:

$$P(CSF,MA+MB+MC+MD) = 278S + 3602CS + 2077CP - 5 \qquad (3.14)$$

with a correlation coefficient of 0.88 and a residual error of 13. A summary of this set of data is given in Table 28 for reference.

14) <u>MW+MH series</u>: This set combines the steels of the MW and MH series. The same set has been analysed by EJ Morgan-Warren[3]. The results of the regression in the present research are slightly different from those quoted by him (see equation 2.14). The present regression equation for this set is:

$$P(CSF,MH+MW) = 40C + 833S + 260P - 10Mo - 3266(0) + 21 \qquad (3.15)$$

with a correlation coefficient of 0.92 and a residual error of 5. This is the only equation to show that oxygen has a powerful effect on cracking.

15) MC+HD series: This set combines 12 Fe-Mn-S-O alloys in the MC series and 22 carbon manganese steels in the HD series and has a regression equation as follows:

$$P(CSF, MC+HD) = 157C + 453S - 20 \qquad (3.16)$$

with a correlation coefficient of 0.79 and a residual error of 17.

16) 3%Cr-Mo-V series: This set contains 44 steels with a composition close to the 3%Cr-Mo-V steel (RS140) and its statistical data is shown in Table 29. The regression equation for this type of steel is:

$$P(CSF, 3\%Cr-Mo-V) = 175S + 523P + 29Si + 17Ni - 17Mo + 22 \qquad (3.17)$$

with a correlation coefficient of 0.87 and a residual error of 4. It is interesting to see that Si, Ni, and Mo appear to have some effects on cracking.

17) All Huxley cracking test series (H217 series): This set includes all known Huxley cracking test data from the literature and the present investigation, totalling 217 observations. A statistical summary of this set of data is shown in Table 30, and the regression equation is:

$$P(CSF, H217) = 272S - 620P + 5Si + 2Ni + 1.3Cr - 9Mo +$$
$$+ 2037CS + 3735CP + 5 \qquad (3.18)$$

with a correlation coefficient of 0.76 and a residual error of 12. This shows that when the number of steel types increases or when the composition range widens, the correlation between CSF and composition becomes poorer, and the prediction of crack susceptibility by means of regression becomes more difficult.

18) <u>GBA series</u>: The Trans-Varestraint cracking test data
and composition of this set are shown in Table 25 and the regression
of UCS (units of crack susceptibility) yields following equation:

$$P(UCS,GBA) = 224C + 418S - 19Mn + 4 \qquad (3.19)$$

with a correlation coefficient of 0.82 and a residual error of 5. This
is quite different from the one given by the original work and quoted
in equation 2.15, as a result of not including the less significant
cross term variables.

19) <u>GBB series</u>: This series contains 32 carbon manganese
steels tested by the Trans-varestraint method; the details of which are
shown in Table 26. The regression equation is:

$$P(UCS,GBB) = 130C + 142S - 93Al - 1 \qquad (3.20)$$

with a correlation coefficient of 0.92 and a residual error of 5.

20) <u>FW series</u>: This series contains 131 Focke-Wulf cracking
test data, a summary of which is given in Table 27. The regression
equation for this set of data is:

$$P(CF,FW) = 6777CS + 1215CP - 8Cr - 1283S - 4 \qquad (3.21)$$

where the dependent variable CF is the crack factor (Rissfaktor) or the
percentage of crack area in the Focke-Wulf cracking test. The regres-
sion has a poor correlation coefficient of 0.62 and a residual error
of 16. This shows that the Focke-Wulf cracking test reflects poorer
cracking and composition relationship than the Huxley cracking test.

21) <u>Mixed series</u>: This set combines 131 Focke-Wulf cracking
test data and 141 Huxley cracking test data, assuming that CSF and CF
are comparable and identical. With the means and ranges of observations
shown in Table 31, the regression of the dependent variable(CSF or CF)
yields the equation:

$$P(CSF,CF) = 245C + 17Si + 853P + 917S + 5Cr - 56 \qquad (3.22)$$

With a very poor correlation coefficient of 0.53 and a very large

residual error of 18. The results imply that the Huxley cracking test is not comparable with the Focke-Wulf cracking test, and the scale and the sensitivity of the both tests are quite different.

In addition to the above regression analyses, the correlation between the CSF value and single terms variables as well as the derived crack indicators as described in section 2.6.2 was studied and the results are shown in Table 32. Among all the variables, C(S+0.5P) has the best correlation with CSF value, based on 203 observations of the Huxley cracking test.

3.3.4 Summary of the analytical results

Numerous regression equations of crack susceptibility based on composition have been obtained for various sets of data. These included not only the Huxley cracking test data, but also the Focke-Wulf and Trans-varestraint cracking test data. Twenty two equations with variables at the 10% level of significance are shown in this report. It was possible to summarize as follows the results of the extensive statistical experiments:

1) The regression equations for various sets of data are not always in harmony. The compositional variables join or leave the regression equation depending not only on their effects on crack susceptibility, but also on the combination of samples.

2) Crack promoting elements recognized by most of the regression equations are: C, S, P; in some cases also Si and Ni. S and P are the most distinct ones.

3) Molybdenum appears often as a beneficial element, for its presence in steel is associated with a reduction of cracking tendency.

4) The effect of oxygen content appears to be significant in

regression of the MW and MW+MH series (see equations 3.11 and 3.15). In other sets of regression with a known oxygen analysis, the effect of oxygen appears to be not significant at the 10% level of significance.

5) Cross term variables CP and CS appear on many occasions as very significant variables, especially when the steels with a wide range of sulphur and carbon contents are included for the regression analysis. Mn/S and O/S do not appear as significant variables (except for the MW series).

6) Al and Mn have a significant effect on cracking in the Trans-varestraint test series (GBA and GBB) for the submerged arc welding of carbon manganese steels. Their effect is not significant in the series of TIG arc welding under investigation.

7) With the number of samples increased or the range of composition widens, the correlation between crack susceptibility and composition tends to become poorer by using a linear regression model. This may imply that the effect of each alloying element is not linear and additive.

8) Prediction of crack susceptibility with composition by using a linear regression model can be carried out with fair accuracy only for limited types of steels or for steels with a small range of composition.

9) The correlation between the observed CSF value and single term variables as well as crack predictors is shown in Table 32. The expression of $C(S+0.5P)$ has the best correlation with CSF value, based on 203 Huxley cracking test data.

3.4 The effect of oxygen in weld metal

In the statistical analysis the regression of CSF was based on the parent metal composition, and the parent metal composition was assumed to be the same as the weld metal composition. This assumption might be true for the alloying elements, but might not be true for the oxygen and carbon contents, because oxygen pick-up could occur during welding in the open air without backing gas. As a consequence of oxygen pick-up, weld metal decarburization could also be expected. The oxygen pick-up might vary from steel to steel, and the degree of oxygen pick-up might have the effect on weld metal crack susceptibility. For this reason the oxygen contents in the weld and parent metal were analysed and compared. Furthermore, two extreme approaches in addition to the normal Huxley cracking test were applied in order to investigate if oxygen has a real effect on cracking. One approach was to carry out cracking tests in an argon-atmospheric closed box to limit the oxygen source, and the other one was to carry out cracking tests with a 2% oxygen-argon shielding gas. By comparing the differences of oxygen absorption to the differences of weld crack susceptibility, the effect of oxygen on cracking could be seen if any.

3.4.1 Open air welding

The so-called "open air " welding in this research is the normal TIG arc welding carried out in the atmosphere, in which the top side of the weld pool is protected by the shielding gas, but the bottom side of the weld is not protected by a backing gas or any other means. The tests involved in the open air welding were the Huxley cracking test and a simple bead on plate welding test, the latter is carried out for

the comparison of the weld metal oxygen analysis, because some part of the weld bead in the unslotted sheet would be free from cracking , thus more suitable for the oxygen analysis.

The Huxley cracking test and results have been already reported in sections 3.2.1, 3.2.2 and 3.2.3. The weld metal oxygen analysis will be given in section 3.4.4.

3.4.2 Closed box welding

Two techniques have been employed and both have been used with appreciable success. In the first series of experiments a well sealed box of about 1m x 1m x 0.5m was purged with argon gas for 16 hours at 8 l/min. The Huxley cracking test was then carried out inside the box using a stationary torch and a traction device to move the test piece. The welding conditions were the standardized values as described in section 3.1. With a view to show the degree of oxidation and decarburization on the one hand, and to see the variation of cracking behaviour on the other, materials used for tests included both crack susceptible and crack resistant steels, with a wide range of carbon and oxygen contents. These included 10 SAE4130 experimental steels (MA series), 12 Fe-Mn-S-O alloys (MC series), 4 ASTM A387B steels etc. The cracking test results of these steels in the closed box condition as well as in the open air conditions are shown in Table 33. It can be seen that the two sets of CSF values are almost identical. The weld appearance in the closed box welding was, however, greatly improved and the crack area correspondingly less oxidized.

There was some trouble in the operation of the first series of experiments, because the efficiency of the purge and the degree of oxygen contamination inside the box were not uniform and were unknown.

Therefore, an alternative method was developed, in which an industrial vacuum chamber with a volume of about 2000 litres was evacuated to about 5×10^{-3} torr and then filled with pure argon to about 1 atmosphere for welding. The whole set-up of the stationary torch and the traction device for the specimen was put inside the chamber for the welding test. The welding conditions applied in this series of experiments were also the same as mentioned before. More steels have been tested with this technique and the crack susceptibility factors obtained in this way are shown in Table 34 together with those welded in open air. The second technique did not modify the crack susceptibility, but the weld appearance was better than from the first technique.

3.4.3 Oxygen-argon shielding gas welding

The Huxley cracking tests with oxygen-argon shielding gas were carried out. The mixtures of argon and 2% or 5% oxygen were supplied by the gas producer in cylinders, therefore no laboratory gas mixing was required. The introduction of oxygen in the argon shielding gas changed the arc characteristics, therefore the welding current and voltage were altered so that a full penetration of weld bead with about 6 mm bead width could be obtained. The required arc current and voltage for the welding with 2% oxygen-argon shielding gas were 85A and 12V respectively (otherwise 95A and 11V).

In the welding test with 5% oxygen in the argon shielding gas, the arc stability and the smoothness of the welding run were so difficult to control that the results could not be properly evaluated. Therefore, most experiments were concentrated on the tests with an argon + 2% O_2 mixture. The cracking test data with the pure argon, and with the argon + 2% O_2 mixture, are shown in parallel in Table 35.

The CSF values were generally less in the case of the oxygen-argon shielding gas welding than in the case of the pure argon welding experiments. However, the weld metal oxygen content was much higher in the case of the former than in the case of the latter, as can be seen in Table 36.

3.4.4 Analysis of weld metal

Samples of parent and weld metals were taken for the analysis of oxygen content by the vacuum fusion method using the Balzer Exhalograph apparatus. A sample of about 1 g is introduced to the graphite crucible by a special loading device. Within a very short time (less than one minute) the sample is fused and the oxide in the melt is reduced by the graphite of the crucible. The oxygen content is then determined by measuring the carbon mono-oxide developed by infrared absorption. This method is standardized and an analysis can be made in a few minutes.

The problem with the oxygen analysis of parent and weld metals was the technique of sampling. If the oxidized scale of the parent plate is removed by filing and rinsing with acetone, the oxygen content in the parent metal can be successfully determined. However, the weld metal requires a very careful preparation before the actual analysis can be made because of the oxidized surface and crack area.

In this series of experiments, the Huxley cracking test weld of each steel was cut through the centreline and the oxide in the crack area removed. Both sides of the weld metal surfaces were also cleaned by filing. Finally, care was taken to remove any parent metal from the weld metal. The resulting sample of the weld metal for the oxygen analysis was therefore small, so that sometimes two or three pieces of

weld metal were used for one analysis. For the analysis of oxygen at least four replicate tests were required in order to have a good estimate of the real oxygen content.

Table 36 shows the results of the oxygen analysis for the parent and weld metals tested by the open air, and by the close box welding. Table 37 shows the oxygen analysis for the weld metal welded with argon + 2% O_2 gas mixture. All figures given are the mean values of more than four tests.

In order to examine the extent of decarburization due to welding, the weld metal carbon content of the 10 SAE4130 steels in the MA series and 2 steels in the MD series (HY80, EN353) were analysed by means of a conventional laboratory procedure, in which samples were taken from the weld of the Huxley cracking test specimen without including crack area and oxidized surfaces. The parent metal carbon contents were also determined in the same manner for a comparison. The results are shown in Table 38. It can be seen that only slight decarburization can be traced during the normal TIG arc welding. However, as a result of the welding with an argon-oxygen mixture, the decrease of carbon content in the weld metal was very obvious.

3.5 Metallographic study of weld metals

Weld metal can be studied both by the optical and scanning electron microscope. A polished, but unetched specimen can give a general impression of the inclusion type and distribution under the optical microscope. A polished specimen etched with a suitable solution can reveal the microstructure of the solidified weld metal. However, the most powerful instrument for this subject might be the scanning electron microscope, although in that case a clean solidification

crack surface is required. Many crack surfaces were obtained by the
closed box welding, which were good enough for the SEM investigation
of the crack morphology. The following sections will show the inves-
tigational procedures and the results. A discussion of the results is
reserved for the next chapter.

3.5.1 Solidification microstructure of the weld metal

Some well polished but unetched specimens have been examined
under the optical microscope. Randomly distributed fine inclusions
could be seen by using a 200 or 500-fold magnification. The inclusion
number per unit area has been counted for the SAE4130 experimental steels
in the MA series, and the results are given in Table 39. The inclusion
number has no direct association with the crack susceptibility factor,
but appears to be related to the sum of sulphur and oxygen contents in
the parent metal.

Liquated sulphide films were rarely seen in the SAE4130 ex-
perimental steels, even in the case of the specimen with more than 0.03%
S, such as MA3, MA4, MA7 and MA8. If the sulphide films of the SAE4130
steels were to be seen, they were very thin and not very long, more
often in the form of a chain.

For the Fe-Mn-S-O alloys in the MC series, the polished and
unetched specimen showed many liquated films of sulphide. The presence
of about 0.060% of oxygen did not prevent the formation of liquated
films in this research.

Weld metal etched with picric acid or 2% nital showed the
general features of the transformed microstructure of bainite and
martensite, but the solidification structure of the weld metal could
not be revealed. A saturated solution of picric acid with sodium tri-
decylbenzene sulphonate as a wetting agent has been successfully applied

to reveal the primary solidification structure of high tensile steels.
Figs 25 to 28 show typical micrograph of the weld metal solidification
structure. For the SAE4130 steels, the primary and secondary dendrite
arm-spacing have been estimated from the micrograph, being about 50μm
for the former and about 20μm for the latter. Because the basic com-
position of the weld and heat input were similar for all SAE4130 weld
specimens in the MA series, the primary, and the secondary arm-spacing
for them were also identical. According to K Schwerdtfeger[71] the
local solidification time in seconds could be calculated from the pri-
mary dendrite arm-spacing L in μm by using the following equation:

$$L = 29.5 \ t^{0.39} \tag{3.23}$$

Therefore for $L = 50 \mu$m, the corresponding local solidification time t
would be 3.9 seconds. This would mean that for a welding speed of 2 mm/S
in the Huxley cracking test, about 8 mm behind the weld pool is in the
process of solidification, or in other words, about 8 mm behind the
weld pool is the "crack susceptible length".

Columnar grain growth was generally seen in the weld metal
specimens under investigation; a columnar to equiaxed transition in the
weld metal was rarely found in the high tensile low alloy steel speci-
mens welded under the Huxley cracking test conditions.Near the weld
centre the dendritic columns may grow in parallel with the welding di-
rection, as can be seen in Fig 28. This phenomenon is, however, not
directly associated with a higher or lower crack susceptibility.

3.5.2 Solidification crack morphology

The scanning electron microscope has been widely applied for
the study of the weld metal solidification, crack surfaces, mechanical
fracture of the crack extension, and the surface phenomena of the crack

surfaces, in order to trace how solidification cracks occur and factors affect their formation. In the majority of the tests the crack surfaces were so oxidized that many of their features were obscured. An attempt has been made to overcome this problem in the present work by preparing the specimens under closed box argon atmospheric conditions and examining them as soon as possible after the welding operation.

All the test specimens were taken from the Huxley cracking test pieces. The SAE4130 steels were more extensively studied than the others.

A stereomicrograph of a typical weld surface is shown in Fig 29, where it can be seen that it has markings which follow the growth directions of the weld metal crystallites. A close-up view (Fig 30) reveals that the growth markings consists of continuous ridges, and the ridges are more or less faceted. Fig 31 is the stereomicrograph of the weld metal surface of MA3 (SAE4130, 0.042% S, CSF = 62), slightly etched, which shows not only the characteristic growth markings but also the relief of the instantaneous shape of the weld pool, or solid-liquid isotherms. The crack is located along the centreline where the grains meet together. By a careful examination of Fig 31 it can be seen that the grains near the centreline show a random orientation. The fine crack in the lower part of the micrograph would have been very difficult to detect if the original specimen had been examined by the naked eye alone.

Gas pores were found on many surfaces where C x O value exceeds 0.004, the condition for the CO gas formation. Fig 32 shows the interior of a gas pore with a leading channel or pipe (specimen of MB4 with a weld metal oxygen content of 0.023% and C x O = 0.008). The Co gas which was evolved through the pipe to form the bubble. The bubbles could be as small as 100 μm in diameter or as large as the

thickness of the sheet to be welded. As seen in Fig 32 the pore interior surface looks rather like the weld metal surface but with radial markings.

The extended fracture surfaces of solidification cracks caused by mechanical rupturing at room temperature were bright and therefore they could be clearly observed with the SEM. Basically there are two types of mechanical fracture surfaces, one with an obvious honeycomb-like structure as shown in Fig 33, and the other with a smoother appearance in general as shown in Fig 34. The more the sulphur content in steel, the more distinct is the honeycomb-like structure, and this structure is thought to be the fractured FeS-MnS-Fe eutectic.

The weld surface and the crack interior of the open air TIG welded specimens have been always oxidized. The crack surface was seen to have an oxidation skin which obscured the original solidification structure, though the dendritic columnar pattern of solidification may still be recognized. Figs 35 to 37 are typical examples of such oxidized crack surfaces. Because of the secondary oxide skin on the original crack surface, the actual crack morphology and inclusions on the crack surface could not be evaluated. For this reason fresh solidification crack surfaces were obtained from the test pieces prepared in the closed box argon atmospheric TIG arc welding experiment as described in section 3.4.2. Many typical features were found on the crack surfaces:

1) <u>Dendritic columns</u>: such dendritic columns can be seen in Fig 38 and such a columnar structure is the most typical feature of the crack surface.

2) <u>Round dendritic tips</u>: This could be seen locally in the high tensile steel weld crack specimens, and quite often seen in the

low carbon Fe-Mn-S-O alloy specimens. Such round dendritic tips were also found in the pore interior surface. Fig 39 shows an example of this structure.

3) <u>Distorted or ill-defined dendrites</u>: This type of crack surfaces has been quite frequently observed. Examples are shown in Figs 40 and 41, also shown in some area of Fig 38. The ill-defined dendritic structure seems to have been distorted by thermal stresses, or seems to have been covered by a flooding liquid phase after cracking (see Fig 41).

4) <u>Crack surface with globules</u>: As shown in Figs 42 and 43, the globules may have a sunk cavity or a projection of a non-metallic phase protruding out from the centre of the globule (clearly shown in Fig 44). The straight projection implies that it was formed after cracking, otherwise it would have been bent. The sunk cavity can be interpreted as the shrinkaage of the liquid phase in the open, namely after cracking, without a resupply of the liquid to fill the cavity.

5) <u>Dendrites with extended tips</u>: This type of structure can be seen occasionally on some part of the crack surfaces. These extended tips were more often found in the low carbon steels than in the high tensile steels. As shown in Figs 45 and 46, the extended parts seem to have been liquid or glutinous while they were stressed.

6) <u>Broken dendritic columns</u>: It is possible for dendritic columns to break off in a brittle manner without a significant deforma-tion. The dendritic columns may be broken individually as shown in Fig 47, or as a group as shown in Fig 48. This brittle fracture on the crack surface is a proof of sub-solidus cracking.

7) <u>Crack surface with liquated inclusions</u>: Figs 49 and 50 show the presence of liquated inclusions on the crack surface. Liquated inclusions as shown in fig 49 could be found on the crack surfaces of

MA3 and MA4, whose weld metal contains 0.04% sulphur. Fig 50 shows the extreme case in the high sulphur steel of MC8 (containing 0.16% S and 0.06% O). This kind of crack surface is associated with a very high crack susceptibility (more than 40 CSF value).

8) Crack surface with an apparent liquated iron phase: Some parts of the weld in Figs 51 and 52 seem to be in a liquid or musty state while cracking is taking place. This could be found occasionally on a small scale in the high tensile steels. Figs 51 and 52 are the stereomicrograph of the crack surface of MB6 (SAE4130, 0.40% C, 0.012% S, CSF = 31). The presence of the liquid iron phase during cracking seems to have a connection with a wider solidification range of weld.

9) Crack surface with ridges: As shown in Fig 53 and 54, the ridges on crack surfaces seem to be original, not caused by the exposure to the atmosphere after welding, and they seem to match the groove of the opposite side of the crack surface. An occurrence of such a crack surface is associated with a very low crack susceptibility weld. The micrographs in Figs 53 and 54 are from the SAE4130 steel specimen MA2 with a CSF value of 12.

10) Crack surface with striation: As shown in Fig 55a, this type of crack surface is very clean with very few inclusions on it. The striation on the crack surface implies that there might be only a very small amount of film in the grain boundaries. A crack surface having such an appearance is always associated with a less crack-sensitive weld. Fig 55a shows the crack surface for MA5 weld (SAE4130, 0.007% S, 0.006% P, CSF = 1).

11) Freely solidified iron ball: As shown in 55b, the solidified ball seem to grow from a liquid drop which fell onto the crack ssurface, and during its suspension in the air, it solidified to a nearly perfect ball. Such ball was rarely found.

In a single piece of a crack surface it is quite often the case that more than one of the above mentioned phenomena can be observed. The general tendency is that the cleaner the crack surface appearance (the clearer the striation),and the fewer the liquated inclusions, the less crack susceptible is the weld.

3.5.3 Microsegregation and inclusion identification

Inclusions and matrices on the crack surfaces were studied by means of the KEVEX X-ray energy spectrometer together with the SEM. The purpose of this study was to see the extent of micro-segregation and to identify the inclusion types, so as to find some clues for the composition and cracking relationship. Whenever an inclusion of appreciable size (larger than $30 \mu m$) or a cluster of inclusions, or a liquated film was found on the crack surface by the SEM, an attempt was made to identify it. For each crack surface under investigation, the degree of microsegregation was checked. Consequently more than 200 KEVEX charts were obtained. Thirty typical charts resulting from this survey are reproduced in Figs 56 to 85. Figs 56 to 67 are the KEVEX charts of the inclusions believed to be oxide inclusions because they showed either only a minor amount of sulphur or none. These inclusions have a relatively large size, being about $50 \mu m$ or even larger, and their shapes are not well defined, apparently resulting from particle coalescing and sintering in the liquid weld. As the charts show, these inclusions may also have sulphur dissolved in them, It has been found that the presence of such oxide inclusions has no direct association with weld crack susceptibility.

Figs 68 to 73 are the KEVEX charts of inclusions believed to be sulphide or oxysulphide. They were taken from the liquated films or globular particles on the crack surfaces. Due to the iron matrix,

it was not possible to establish if they were manganese sulphide or iron sulphide. However, it is certain that the sulphur peak in a chart is accompanied by the peaks of iron, manganese and chromium. These inclusions were found in the specimens with a sulphur content of more than 0.030% in the parent metal, and such steel weld is always susceptible to cracking.

Figs 74 to 81 are the KEVEX charts of more complicated inclusions. Inclusions revealed by such charts are randomly located and their shapes are not in a crystal form. Such inclusions seem to be a complex of sulphide and oxide. The presence of such inclusions would be harmful to the mechanical properties, but have no direct influence on weld crack susceptibility.

Inclusions containing phosphorus were only detected by the KEVEX on the crack surface of MD16 (Hypress 23, 0.058% P, CSF = 21), the specimen with the highest phosphorus content in this research. The KEVEX chart in Fig 82 shows the presence of phosphorus on the matrix of the crack surface in the case of the specimen with a phosphorus content of more than 0.035% (such as in MD16 and MD 19). Fig 83 shows the KEVEX chart of an inclusion containing phosphorus in the specimen of MD16 (Hypress 23, 0.058% P).

Fig 84 shows the KEVEX chart of the iron matrix of the crack surface with almost no sulphur content and Fig 85 shows that with an appreciable sulphur content. The latter is associated with the weld with a high crack susceptibility (CSF > 20).

3.6 Miscellaneous experiments

In order to understand the initiation and propagation of solidification crack, the welding arc and the weld pool were occasionally

observed through a less tinted shield during the Huxley cracking test. It has been observed that: 1) The weld pool is tear-shaped rather than elliptical, having an estimated length of about 9 to 12 mm; 2) A crack initiates behind the weld pool and gradually lags behind the weld pool until it stops.

In the evaluation of crack length for the Huxley cracking test results, normally only continuous centreline cracks were observed, in some cases, minor cracks may follow the continuous crack as shown in Fig 31. It has been possible to produce a continuous crack through a piece of steel sheet (38mm x 305mm x 2mm, without slot pairs), such a continuous crack has been observed in the specimens of MD7 (EN24), MB3, MB4 and MB5 (SAE4130), etc, whose crack susceptibility being very high (CSF value about 60). A crack through the whole segment between two pairs of slots in the Huxley specimen was found occasionally in the specimen of MC8 which contains 0.16% S and 0.064% O and has an average CSF value of 70, the highest value obtained among all steels investigated.

4. DISCUSSION

The investigational work of this research included weld cracking experiments and statistical analyses. The experimental parts included the Huxley cracking tests in the open air, in the closed box , and in the open air with an oxygen-argon shielding gas, and the successive evaluation of crack suceptibility, oxygen analysis and microscopic studies of weld metals and inclusions. This investigation yielded a great deal of information on solidification cracking in the TIG arc welding of steels and showed the effects of composition on weld cracking.

The statistical survey in this research was very extensive. it included the regression analysis of crack susceptibility based on composition for the present and previous observations obtained by the Huxley cracking tests. In addition it also included for comparison the regression analysis for the 131 Focke-Wulf cracking test observations and 49 Trans-Varestraint test data for the submerged arc welding.

In this chapter the results are discussed with a particular reference to the effects of carbon, sulphur and oxygen on crack suscep- tibility. The value of regression analysis and the validity of its application are re-examined in a more stringent way on the basis of the available data.

Finally the crack morphology seen in this investigation is compared with the existing theories on solidification cracking and comments are given to these theories.

4.1 Cracking and composition relationships based on linear regression

The aim of the regression of crack susceptibility based on composition is to trace the effect of each single alloying elements on

weld crack susceptibility in an unknown steel using the available
data of composition. Comparing the regression experiments for the
MA, MB and MC series, it was realized at once that the linear effects
of carbon, sulphur and phosphorus cannot be assumed. The change of
the sulphur coefficient from 1681 in equation 3.2 for the MA series(SAE4130)
to 431 in equation 3.3 for the MC series (Fe-Mn-S-O) indicates that the
effect of sulphur is dependent on the carbon and other alloying factors.
For this reason, CS and CP (the product of carbon and sulphur, and the
product of carbon and phosphorus) were included as variables in the
regression study for the mixed series of MA, MB, MC and MD, the vari-
ables of CS and CP were readily detected as variables at the 5% or 10%
significance level. However, the correlation of the regression was not
much improved by the introduction of CS and CP variables in the regres-
sion set.

Mn, O were considered in the regression analyses for the
MA, MB and MD series (all being high tensile steels investigated in the
present research), but Mn and O did not appear in the regression equa-
tion for lack of significance. Mn/S and O/S ratios could not be included
for the same reason. Regression equations for the MW and MH series (data
from Morgan-Warren and Huxley) have O and O/S as significant variables
(see equation 3.11 and 3.15), and surprisingly have a very high cor-
relation coefficient (r = 0.96 and 0.92 respectively), which contradict
the findings in the MA, MB, MC and MD series. To ascertain if the oxygen
and O/S ratio has a real effect on crack susceptibility, a closed box
welding and weld metal analysis were carried out. The results showed
oxygen has no real effect on crack susceptibility in the steels under
investigation, as will be discussed in the following section. The
inclusion of the variables O and O/S in equation 3.11 and 3.15 should
be considered as rare cases of statistical coincidence rather than

the true effects of oxygen and O/S ratio.

The effects of alloying factors Si, Mn, Cr, Ni, Mo etc could only be detected by the series with a wide variation of such alloying factors. It is impractical to design and use samples in a planned series with each factor at both high and low levels (full 2^n factorial design), for too many samples are involved. If 10 factors are considered and each factor has a high and low level, then 2^{10} or 1024 samples would be required. If an intermidiate level were introduced in addition, 3^{10} or 59040 samples would be required for a full scale factorial experiment. Because such extensive factorial experiment is not likely to be carried out, published data relating to composition and cracking (which have a random rather than an intended variation of composition) are taken up for regression analyses with a view to seeing if this can also shed some light on the understanding of cracking and composition relationship.

According to the regression of CSF value for many sets of data, the effect of Mn is very close to zero. Ni, Ni and Cr slightly increase CSF value, while Mo reduces it. On the whole, their effects are not very large compared with that of C, S and P. It is therefore suggested that the sulphur and phosphorus contents should be controlled rather than alloying elements in the production of crack resistant steels.

Reviewing all the regression equation, one hesitates to use a regression equation for the prediction of crack susceptibility, not only because of their variety, but also the error of prediction encountered. If the equation based on the largest number of observations (equation 3.18) is used for the prediction of the crack susceptibility factor, one must bear in mind that the predicted value of CSF is only a rough estimate, for the true value can be any value within the inter-

val of $\pm$ 24 of its estimate (95% confidence limits).

For the following reasons it is believed that a versatile equation for the prediction of the CSF value in steels with a wide range of composition cannot be obtained:

1) The relationship between CSF and each alloying content may not be linear.

2) The effect of each alloying element may reach a saturated value or its effect may be only distinct above a certain level.

3) The alloying elements may interact with each other, in other words, the effect of an element depends on the presence of other elements.

4) Types of steels may affect the cracking and composition relationship.

However, for a particular group of steels, with a narrow range of composition, the non-linearity of the alloying variables can be treated as approximately linear and the interaction of them can be neglected, thus a fairly good regression equation may be found and applied for the prediction of crack susceptibility. Two examples of regression equations for a particular group of steels are:

1) <u>For SAE4130(1%Cr-Mo) steels</u>

$$P(CSF, 1\%Cr-Mo) = 1587S + 657P - 5 \qquad (3.12)$$

(with $r = 0.94$)

2) <u>For 3%Cr-Mo-V steels</u>

$$P(CSF, 3\%Cr-Mo-\bar{V}) = 175S + 523P + 29Si + 17Ni - 17Mo + 22$$

(with $r = 0.87$) $\qquad (3.17)$

More work on the regression of crack susceptibility based on composition should be encouraged, especially with controlled levels of variables, because then the effect of the variables can be more firmly and easily assured. A descriptive model of the cracking and composition relation -

ship for the prediction of solidification cracking can be constructed on the basis of regression analyses as well as on other information which is available in the literature. For the construction of a tentative model of cracking and composition relationship, following facts have been considered:

1) Most steels showing a CSF value of less than 20 is weldable and free from cracks in real production welding[7].

2) Low carbon steels (such as that in the MC series) tolerate more sulphur and phosphorus content without showing cracks.

3) The expression of C(S+0.5P) has the highest correlation with CSF value (see Table 32), and is relatively simple.

4) The effect of sulphur on cracking is about twice as much as the effect of phosphorus.

5) Alloying elements such as Ni, Cr, Mn, Si, Mo have only a negligible effect on cracking.

6) The level of carbon in steel is an important factor for the sulphur and phosphorus-induced cracking.

As a consequence of these considerations and using the available regression data and cracking results, the model of cracking and composition is proposed as follows:

1) For carbon or alloy steels with a carbon content of more than 0.40%

Crack susceptible if (S+P) > 0.010%;

Crack susceptible or resistant if (S+P) between 0.005 and 0.010%, depending on alloying contents;

Crack resistant if (S+P) < 0.005%.

2) For carbon or alloy steels with a carbon content of between 0.20 and 0.40%

Crack susceptible if C(S+0.5P) > 0.0050;

Crack susceptible or resistant if C(S+0.5P) between 0.0033 and 0.0050, depending on alloying contents;

Crack resistant if $C(S+0.5P) < 0.0033$.

3) <u>For carbon and alloy steels with a carbon content of less than 0.20%</u>

Crack resistant if $C(S+0.5P) < 0.0033$;

Crack susceptible if $S > 0.160\%$,

Crack resistant or susceptible if $S < 0.160\%$, depending on

alloying factors including Mn/S and O/S ratios.

Referrring to the data collected as well as the present data, it can be seen that this model is a good quide for the prediction of weld crack susceptibility. Figs 86 and 87 show the curves of $C(S+0.5P)$ = 0.0033 and $C(S+0.5P)$ = 0.0050, and the influence of $(S+0.5P)$ and C on the crack susceptibility of steel welds. Steels with a $C(S+0.5P)$ value of less than 0.0033 (under the curve of $C(S+0.5P)$) are crack resistant in the most cases except for that with a carbon content of more than 0.40; steels with a $C(S+0.5P)$ value of more than 0.0050 are crack susceptible except for that with a carbon content of less than 0.20%.

4.2 The effect of oxygen and O/S ratio on crack susceptibility

It has been shown that oxygen and O/S ratio have no significant effect on cracking by means of the results of various experiments carried out in this research. The main points relating to the effect of oxygen and O/S ratio are given as follows:

1) Regression analysis for the ten SAE4130 experimental steels in the MA series with a systematic variation of oxygen level from 0.004 to 0.016% did not show that oxygen content is a significant variable of crack susceptibility.

2) Regression analysis for the twelve planned Fe-Mn-S-O alloys in the MC series with an oxygen level from 0.007 to 0.066% and an O/S

ratio of between 0.03 and 3.15 showed neither oxygen nor O/S ratio has an effect on crack susceptibility.

3) Regression analysis of miscellaneous steels in the MD series with varying oxygen content and O/S ratio also did not show their effect on cracking.

4) The open air and closed box welding of 32 research steels showed that the CSF values for each steel in both welding tests are almost identical, though the weld metal oxygen contents are quite different.

5) As shown in Table 36, the weld metal oxygen content is not the same as that of the parent metal, and this change of oxygen as a result of welding is not regular. This shows that the practice of including the parent metal oxygen content of steels as a variable for the regression analysis of CSF value is not permissible.

The evidence for the conclusion that oxygen does affect crack susceptibility is only seen in the welding test with an argon-oxygen shielding gas, and is mentioned in the previous reports by EJ Morgan-Warren[3] and T Boniszewski[26]. However, this contradiction can be explained satisfactorily. The fact that the TIG arc welding with an argon-oxygen shielding gas can reduce the crack susceptibility of the weld metal cannot be attributed to the single effect of oxygen, for a welding test with such argon-oxygen shielding gas has a different technical background. The TIG arc welding process using argon-oxygen gas has some particular features:

1) instable arc;

2) uneven penetration;

3) higher arc voltage;

4) substantial decarburization;

5) oxidation of weld metal.

Table 38 shows that welding with an argon + 2% O_2 shielding gas will reduce the carbon content of the weld by as much as 0.10% as in the case of MA2. It is therefore believed that the decarburization of the weld metal was the main cause of crack susceptibility reduction. Both MD13 (HY130) and MD14 (EN353) with a relatively low carbon content (0.15%) did not change their carbon contents significantly as a result of such welding test, and their CSF values also remained practically the same. This very fact also supports the view that it is rather the decarburization than the presence of oxygen that reduces weld metal crack susceptibility.

Considering Morgan-Warren's two regression equation for CSF, it is possible to argue that the apparent effect of oxygen content in the regrssion equation is not a real one. The two equations are:

$$P(CSF, Morgan\text{-}Warren, 1) = 36C + 12Mn + 5Si + 540S + 812P +$$
$$+ 3.5Co - 20V - 13 \qquad (2.13)$$
$$(P, CSF, Morgan\text{-}Warren, 2) = 42C + 847S + 265P - 10Mo -$$
$$- 3042(0) + 19 \qquad (2.14)$$

The change of intercept from -13 to +19 on the one hand and the increase of sulphur coefficient from 540 to 847 on the other hand would cause a higher calculated CSF value in the second equation, and the beneficial effect of oxygen as represented by the negative oxygen regression coefficient might just counteract the given increase of CSF value. Among the 42 steels included for the regression analysis in order to obtain the second equation, only four steels have an oxygen content of between 0.011 and 0.015%, and the rest have an oxygen content of only between 0.003 and 0.006%. Therefore, the argument for the view that oxygen has a beneficial effect on preventing crack formation seems to be too weak.

The appearance of oxygen content in the second equation should

rather be considered as a chance effect due to the regression. There is
another possible explanation for the inclusion of oxygen as a signifi-
cant variable in the regression. Steels with a higher carbon content
would naturally reduce the oxygen content in them, thus steels with a
lower carbon content would be likely to have a higher oxygen content
and those with a higher carbon content would probably have a lower oxygen
content, and furthermore, it is well established that steels with a
higher carbon content are more susceptible to crack than those with a
lower carbon content. This tendency might be falsely interpreted as
due to the presence of oxygen.

According to the Fe-S-O phase diagram of DC Hilty et al[40]
and the experimental results of JC Yarwood et al[41] the O/S ratio
will have some effect on modifying the inclusion shape in the Fe-S-O
alloy with an O/S ratio of greater than 0.1, and the higher the O/S
ratio the more globule oxide-rich inclusions will form. Yarwood's
results further imply that if the formation of FeS film-like inclusions
is to be fully suppressed, an O/S ratio of at least 1.2 is required.
However, this research showed that the O/S ratio has no effect on
crack susceptibility. In the MC series (12 Fe-Mn-S-O alloys) the sulphur
induced cracking was not reduced by a higher O/S ratio (see Table 12
and compare MC3, MC4 with MC7 and MC8). The O/S ratios of 0.37 and 0.40
might be too low to be effective, or the sulphur content of 0.180% or
0.160% in steel is far beyond the scope within which the O/S ratio
can be effective on crack reduction. Though the high O/S ratios of 3.15
and 2.67 in MC5 and MC6 respectively are associated with low CSF values
(both CSF = 0), it cannot be regarded due to the higher O/S ratio; in
fact, it is only due to the effect of low sulphur content. The effect
of the O/S ratio was not found in the SAE4130 steels (MA and MB series)
and miscellaneous steels in the MD series. An O/S ratio of greater than

1.2 might really have an effect of crack reduction, but for a typical crack susceptible high tensile steel with 0.030% S, an oxygen content of at least 0.036% would be required in order to suppress the formation of filmlike inclusions, thus prohibit cracking. On the other hand, it is quite impossible and impractical for killed steels to have such an high oxygen content.

To conclude this section, it can be stated that increasing the oxygen content and O/S ratio within the specified range (0.020% for oxygen content and 1.2 for the O/S ratio) has no potential effect of reducing the sulphur induced solidification crack susceptibility.

4.3 The effect of carbon on crack susceptibility

The carbon content in steel enhances the crack inducing effect of sulphur and phosphorus. Fig 88 and Table 40 show that the higher the carbon content in steel, the higher is the sulphur regression coefficient for the CSF value. It is for this reason that in some regression equations of crack susceptibility factor the product of sulphur and carbon or phosphorus and carbon appears to be more correlated to the CSF value than the contents of carbon, phosphorus and sulphur on their own.

It seems that the presence of carbon content above a certain level would suppress the effects of oxygen and manganese. VV Podgaetskii[72] reported that a high sulphur (0.10% S) and low carbon (0.08%) steel could be rendered crack free by introducing 0.10% oxygen in the weld. In the steel with a carbon content of higher than 0.08%, the effect of oxygen on crack prevention might still be possible, but with an increasing carbon content in a steel the solubility of oxygen gradually decreases, and the required amount of oxygen might thus not be

able to dissolve in the steel. VV Podgaetskii reported[73] that at a

carbon content of 0.16% it is impossible to prevent cracking in the

fillet welds even at an Mn/S ratio of 50 or more. PW Jones[23] also

reported the same. It is not clear why this should be so, the data

included in the Huxley cracking tests have too few steels with a

carbon content of less than 0.16% to show this.

A theoretical study of the carbon effect on solidification

process on the basis of the Fe-C phase diagram might serve to explain

the trend and bridge the knowledge gap about the real effect on carbon

on solidification cracking. According to the familiar Fe-C phase dia-

gram four types of solidification processes can be distinguished:

1) <u>Simple ferritic solidification (for 0.0 to 0.10% C)</u>: Steels

with a carbon content of less than 0.10% will have the delta ferrite

as the primary solidification phase and the subsequent ferrite to aus-

tenite transformation proceeds without the liquid iron phase being

involved, in other words, no peritectic reaction takes place for the melt

of such steels. The crack susceptibility of this type of steel is ex-

pected to be low because of the higher solubility of sulphur and phos-

phorus in the primarily solidified delta ferrite.

2) <u>Hypoperitectic solidification (for 0.10 to 0.16% C)</u>: The

melt of steels with a carbon content of between 0.10 and 0.16% will

undergo a peritectic reaction upon cooling, and when the peritectic

reaction is finished, there is no liquid melt left. A steel with such

solidification is expected to be more crack susceptible than that with

simple ferritic solidification, because of the sulphur and phosphorus

segregation at the austenitic grain boundaries resulted from the peri-

tectic reaction.

3) <u>Hyperperitectic solidification (for 0.16 to 0.50% C)</u>: The

melt of steels with a carbon content of between 0.16 and 0.50% will

undergo a peritectic reaction upon cooling, moreover, after the peri-

tectic reaction there is a remaining liquid phase at the grain boundaries. The microsegregation of sulphur and phosphorus in this type of steel will be higher than in the low carbon steel because of the higher proportion of austenite and the remaining liquid iron at the grain boundaries. Consequently this type of steel is more crack susceptible than the two types of steels mentioned above.

4) <u>Austenitic solidification (with C over 0.50%):</u> Steels with such high carbon contents have direct austenitic solidification and no peritectic reaction is involved. Such steels are expected to be most crack susceptible among the four types of steels discussed in this section, partly because of the severest microsegregation, and partly because of the highest liquid to solid contraction.

Solidification crack susceptibility is a technical property associated with segregation, solidification shrinkage, solidification range and the high temperature ductility of the material. From the Fe-C phase diagram it can be expected that the higher the carbon content, the more crack susceptible is the steel. However, the linear effect of carbon content on crack susceptibility of steels can hardly be assumed as so many metallurgical processes are associated with the carbon content.

The effect of the peritectic reaction on solidification cracking and microsegregation was confirmed by I Matsumoto et al[78]. However, the compositional range for a ferritic and austenitic solidification as well as the range for the peritectic reaction for the technical steels have not been well defined and described in the existing documents.

4.4 <u>The effect of Mn and Mn/S ratio on crack susceptibility</u>

Among the 22 equations obtained in this research as results of regression analysis, only two equations show that the effect of Mn content on crack susceptibility, they are:

$$P(CSF,C) = -18C + 1001P + 4Si + 29Mn + 6Ni - 7Mo +$$
$$+ 4716CS - 1462MnxS - 10 \qquad (3.10)$$
$$P(CSF,GBA) = 224C + 418S - 19Mn + 4 \qquad (3.19)$$

The former equation is for the high carbon alloy steels in the C series. The variables of Mn and MnxS seem to act in the opposite directions. The credibility of this equation is very doubtful, because there is no theoretical basis to support this, and there is no other equations comparable to this. In the factorial analysis for the SAE 4130 experimental steels in the MA series as shown in Table 9, the effect sum square for the factor of manganese is only 22 compared with 5576 for the factor of sulphur. Even if Mn has an effect, it will have only a small effect which is negligible. Table 9 also show a negligible effect of the manganese to sulphur interaction. Based on the results in the MA series of SAE4130 steels, it can be concluded that a variation of manganese content between 0.19 and 0.80%, or a variation of Mn/S ratio between 5 and 80 in the SAE4130 steels has no effect on weld crack susceptibility.

The latter equation (equation 3.19) shows that manganese content has a beneficial effect in the steels of the GMA series. Referring to the data for the GMA series (Table 25) and comparing them with the other, the conditions for showing the effect of manganese on reducing crack susceptibility seem to be:

1) Low silicon content (about 0.05%).

2) Wide range of manganese content (between 0.50 and 1.50%).

3) Relatively low carbon content (0.11 to 0.27%).

4) No alloying elements such as Ni, Cr, Mo.

If such are the conditions for showing the manganese effect, then it is explainable why manganese content has no detectable effect on cracking in most of the high tensile steels, for the above mentioned conditions are not fulfilled in most of the high tensile steels. Under the conditions mentioned above, the steel will be very comparable to the alloy of the Fe-Mn-S system, therefore the harmful effect of a low manganese content can be anticipated according to the Fe-Mn-S phase diagram. Under other conditions, however, the harmful effect of having a low manganese content might be cancelled by the effect of various alloying elements present in steels.

The above mentioned conditions are fulfilled in the Fe-Mn-S-O alloys of the MC series, however, neither the effect of manganese, nor that of Mn/S ratio can be confirmed. A possible explanation for this might be that the manganese content of about 0.80% is still too low for a steel with 0.16% sulphur.

4.5 The effects of S and P on crack susceptibility

Experiments and regression analyses of crack susceptibility have shown clearly that the presence of sulphur and phosphorus is responsible for the solidification cracking of weld metal. However, the harmful effects of sulphur and phosphorus in various steels are not the same. The general tendency is that by increasing the carbon content in steel the tolerable contents of phosphorus and sulphur for a crack resistant steel decrease. This has been already discussed in many of the previous sections. Some particular findings concerning the effects of sulphur and phosphorus are pointed out as follows:

1) In the SAE4130 steel, the harmful effect of sulphur on cracking could not be reduced by either increasing the manganese content up to 0.80% or by allowing oxygen content to go up to 0.015% in the steel.

2) The maximum tolerable sulphur in the SAE4130 steel with a low phosphorus content (0.005%) is about 0.020%, if the CSF value is expected to be lower than 20.

3) The tolerable sulphur and phosphorus content for a crack resistant 3%Cr-Mo-V steel is less than 0.010%, and this fact is associated with the presence of a much higher carbon content in it (0.34 to 0.58%) as can be seen in Table 18.

4) The correlation between CSF and CS is 0.58, while the correltaion between CSF and CP is 0.32 based on 203 cracking test observations. However, the expression of $C(S+0.5P)$ has a correlation coefficient of 0.63 with CSF. Therefore , $C(S+0.5P)$ could be used as an index for the weld crack susceptibility of high tensile steels (especially for steels with a carbon content between 0.20 and 0.40%). If the $C(S+0.5P)$ value of a high tensile steel is less than 0.0033, it is positively crack resistant; if this value is greater than 0.0050, the steel is crack susceptible in welding.

5) For predicting weld crack susceptibility, the phase diagrams of Fe-S, Fe-Mn-S, Fe-S-O and Fe-Mn-S-O are very suggestive, but none of them could be used with safety. One reason for this is that most technical steels have a composition with a low sulphur and low oxygen content, which are not covered sufficiently by the studies of such phase diagrams.

4.6 Solidification crack morphology and crack mechanism

The metallographic examination of the weld solidification microstructure and detailed investigation of weld metal crack surfaces by using the scanning electron microscope have revealed many basic facts about solidification cracking. From the direct observation of the arc and crack development with a shield during TIG arc welding it can be seen that a crack initiates behind the weld pool and gradually lags further behind the weld pool until it stops. This implies that crack initiation occurs at a higher temperature than crack development does, and the speed of crack development cannot catch up the weld pool. The slow-down of the crack development speed is partly due to the release of thermal stresses as a result of cracking and partly due to the fact that the further the weld is behind the weld pool, the stronger it is. When the accumulated thermal strain is released, the crack will come to a stop. However, as a result of crack arrest, thermal stresses may accumulate again; if a sufficient strain is reached, the crack may re-initiate. In the Huxley cracking test, such crack re-initiation was not often observed and the observed ones were fine and short after the main centreline crack. During the welding in the Huxley cracking test, a crack initiates from the position where both sides are slotted. A possible explanation for this phenomenon is that as the welding arc comes to the position of paired side slots, the slots act as a thermal insulator and restraint insulator, and the cooling rates in the neigh-bourhood are thus lower, in other words, the crack susceptible time is longer, or the strain to be accumulated at that position is greater. As a continuous crack through the whole segment between two pairs of slots in the Huxley cracking test specimen was observed, it cannot be accepted that there is an "end effect" to restrict the maximum crack length in the Huxley cracking test.

According to the investigation of crack interior surfaces by using the scanning electron microscope and KEVEX spectro-analyser four distinct phases may participate in the solidification cracking process. They are:

1) <u>Low melting non-metallic phase</u>: The low melting phase contains sulphur and the amount of this low melting phase is proportional to the content of sulphur in the steel. It has been shown that the higher the amount of low melting liquid present, the higher the crack susceptibility of the weld. If the low melting film has only a negligible amount at the grain boundaries, cracking may not occur; if the low melting film is just sufficient to cause the crack, the striation on the crack surface can still be recognized; if the amount of a low melting liquid is further increased, a thin film is formed between the grain boundaries and cracking occurs along these weak grain boundaries filled with liquid films. The liquid film is normally so thin that it cannot be seen on the crack surface by the SEM. However, the smooth surfaces and the absence of striation betray the presence of such a thin liquid film. Were there no liquid film present, the crack surface would be more complicated, being either a solid to solid rupture or having original faceted grain boundaries. When the low melting liquid is in an abundant quantity, not only the liquid film is formed, but also the liquated inclusions, granules or the localized flow of a liquid phase can be traced on the crack surfaces (see Figs 42, 43, 44, 49 and 50). In this research the majority of the low melting liquids contain sulphur, and the microsegregation of sulphur on the crack surfaces can also be detected on the crack surfaces by the KEVEX. The liquid phase containing phosphorus was not detectected, probably because the majority of the specimens available for this research were not rich in phosphorus content.

2) <u>Liquid iron phase</u>: The extended tips or neckings as shown in Fig 45 and 46 are thought to be in the liquid state while they were being pulled apart. The ill-defined area in Fig 38 and the middle parts in Figs 51 and 52 seem to show crack areas with an incompletely solidified metal phase. A liquid metal phase is expected to be present locally in the area where the thermal extraction and grain growth are most unfavourable. There is no reason to exclude the possibility of liquid iron participating in the crack formation. One more piece of evidence to show that the liquid iron phse is present during solidification cracking can be seen in Fig 89. The spherical ball on the crack surface grew independently from a liquid drop which fell onto the crack surface, and during its formation in the air, it solidified to a nearly perfect ball.

Back-filling of the liquid iron into the crack area is thought to be possible, but no clear SEM micrograph of such crack surface has been found to show this. If the original solidification crack is refilled with the liquid iron completely and no secondary cracking takes place, no crack surface can be seen. If however, the crack is refilled completely or a secondary cracking occurs after refilling, it can be seen and may be distinguished from the crack not being refilled. Some ill-shaped crack surfaces observed on many occasions might be the secondary cracks being partly filled previously with liquid iron (see Fig 38).

3) <u>Solid phase (interlocked dendritic columns)</u>: When the solid bridges begin to form in the solidifying weld, they connect the grains growing from two sides of the fusion boundaries, therefore thermal stresses begin to grow and are imposed on the solid bridges. If the liquid coverage of the boundary surfaces is extensive, and the number of solid bridges is small, the solid bridges may not sustain the excessive stress imposed on them, and thus will break apart. The breaking

of solid bridges may begin with their deformation and end with their rupture, or it may just occur without an appreciable deformation(see Figs 47 and 48). If the solid bridges are strong enough and in a sufficient number, a crack should not be able to initiate or propagate, even if there is liquid film present. For this reason it is suggested that crack susceptibility can be reduced by:

a) increasing the number of interlocking dendrites;

b) increasing the area of any kind of solid to solid contact;

c) increasing the hot ductility of the solid bridges;

d) reducing the liquid to solid contact area.

The first two factors seem to be controlled by the welding process, while the last two factors are thought to be controlled by the weld composition. The brittle rupture seen in Fig 48 might be avoided if the solid phase were stronger at cracking temperature.

4) Gas phase: Gas porosity has been occasionally found on the weld crack surfaces. Apparently hydrogen is not the cause of porosity in the weld, because there is no source of hydrogen in the TIG arc welding process if the parent sheet to be welded is dry. The nitrogen content in the weld is about 0.004%, which is not the reason for porosity. The gas porosity in the steel weld of the TIG arc welding process is more likely due to the high absorption of oxygen and its reaction with the carbon in steel. In the steel of MB4 (SAE4130), $C\% \times O\%$ in the parent metal is only 0.35×0.007 or 0.0025, much less than the required value of 0.004 for CO gas formation, but gas porosity was found in the weld of this steel. To find out the reason for gas porosity, the composition of MB4 steel is compared with that of other SAE 4130 steels and it is discovered that MB4 differs from other SAE4130 steels in the silicon content, being 0.07% agaist about 0.30% for the others (see Tables 16 and 7). It is therefore conjectured that the absence of silicon or other oxidizing elements in the high carbon

steel may induce oxygen absorption during TIG arc welding and form gas pores. The actual oxygen content in the weld of MB4 was 0.023%, representing an absorption of 0.016% oxygen, its C% x O% being already in excess of the required value of 0.004 for CO gas formation.

The formation of gas pores might be beneficial for crack prevention if the pores are very small and well distributed, because the high-pressure in the pores may cancel out the accumulated thermal stress and reduce the danger of cracking. However, for a sound weld, porosity in the weld cannot be considered as being desirable. If the pores are large and plentiful, they might accelerate crack formation because the presence of pores reduces the solid to solid contact area.

Besides the above mentioned four phases which participate in the solidification cracking process, various oxide inclusions are also involved. However, the presence of well distributed fine oxide particles in the weld has no direct association with cracking.

4.7 Theories on solidification cracking

A number of theories on solidification cracking have been summarized by JC Borland[13,74] and F Matsuda[75]; three of the most popular ones are described here for the further discussion in connection with findings of this research.

1) Shrinkage and brittleness theory: This theory was mainly developed from studies of cracking behaviour in aluminium alloy casting and welds[10-12,14] and it suggests that solidification cracking is due to the exhaustion of ductility of a solid-liquid mass within a temperature interval (brittle temperature range, see Fig 1) where solid-solid bridges have been established. Cracking is presumed to involve the

breaking of these bridges.

2) <u>Strain theory</u>: Proposed by WS Pellini[55] this theory suggests that solidification cracking is caused by localized strains, set up by thermal gradients tending to tear apart metal consists of dendrite structures separated by essentially continuous films of liquid. It occurs at temperatures slightly above the solidus.

3) <u>Borland's generalized theory</u>: A revised version of Borland's generalized theory of solidification theory in the recent literature[74] described that cracking can occur in regions where high stresses can be built up between grains or where by reasons of lack of constraints at free surfaces a parting of the liquid phase can occur as a result of the development of highly localized strains. Three different situations were said to be apparent: a) necking of liquid films open to external (free) surfaces and subsequent void (crack) formation (eg, crater cracks, weld centreline cracks and sheet edge initial cracks); b) separation (rupture) of highly stressed thin liquid films separating adjoining grains while no solid to solid bonding occurs; c) Breaking of solid to solid bonds in regions where the liquid coverage of grain surfaces is sufficiently extensive to allow "breaking stresses" to be imposed on the solid to solid bridges.

In this research, necking of liquid phase, smooth or distorted parting of grains, rupture surfaces have been observed, therefore, it is believed that Borland's generalized theory most closely described the cracking behaviour in the TIG arc welding of a thin sheet.

JC Borland[74] believed that the initiation of solidification cracking during welding is most likely to occur in the brittle temperature range involving the breaking of solid to solid bridges, and crack propagation is most likely to occur by the separation of a continuous liquid film at the rear of the weld pool. However, it can be argued

the opposite is true, in other words, crack initiation is more likely to occur by the separation of grains along the grain boundary where a continuous liquid phase is present, and crack propagation is more likely to occur by the deformation and breaking of solid to solid bridges. A strong argument for this is that a crack initiates at the rear of the weld pool and gradually lags behind the weld pool until it stops. As the crack initiation is so close to the rear of the weld, the presence of a continuous liquid film rather than the presence of solid to solid bridges is expected.

A report on solidification crack in the Varestraint test of fully austenitic steel by F Matsuda et al[76] also support the view that crack initiation is due to the separation of grains along a liquid film. In their work they discovered that the crack area in the high temperature region had a dendritic surface full of fine protuberances, and the crack area in the low temperature region had a flat surface, and the crack area in the medium temperature region had a surface which was partly dendritic and partly flat in appearance. These regions were termed D, F and D-F regions respectively. The transition from D type (dendritic) crack surface to the F type (flat) crack surface was discovered by them to be due to the gradual decrease in liquid phase at the original columnar solidification grain boundary and due to the gradual migration of grain boundary. In fact the grain boundary migration, so called by them, includes the mechanisms of grain distortion and a transverse breaking of established cellular dendrites.

In the present research, many of types D, D-F and F crack areas were observed in the solidification crack, however, they were not orderly distributed. An explanation for this is that the centreline crack observed in the Huxley cracking test specimen is a continuous crack while the crack of the Varestraint test is a sudden crack with an

augmented strain. The former crack proceeds gradually at almost a
constant temperature, while the latter crack proceeds suddenly along
a length of different temperatures and thermal gradients. The discre-
pancy of grain growth directions, the localized thermal fluctuation and
a slight wandering of the welding arc might be the causes for the mixed
mode crack mechanism of the centreline solidification crack observed
in the welding of thin sheet. If a continuous liquid film is present
in front of the crack tip, a smooth parting along the grain boundary,
with or without an occasional necking of liquid phase, is conceivable.
If a continuous liquid film almost vanishes in front of the crack tip,
the crack may still propagate by separating solid to solid bridges, or
may come to a temporary halt till a sufficient stress is built up to
cause further cracking. In this case, some of the solid to solid
bridges or the established grains must be broken and deformed. If a
sufficient stress is available in front of the crack tip, even the solid
mass can be torn apart, because this solid just solidified is still
very brittle. In overcoming a short length of a solid barrier, the
crack tip may again reach an area where an essentially continuous film
is present, thus the crack can keep on developing easily. In some stage
of crack progress, cracking will become more difficult as a result of
having more solid contact area and less stresses. In this case, cracking
slows down and finally come to an end.

All the existing theories seem to simplify the real situation
or tell part of the truth, or they are valid only for a particular type
of cracking, Therefore, this work will not deny any of them. However,
the Borland's generalized theory on solidification cracking is found
more acceptable for the description of cracking behaviour of centre-
line cracks observed in the welding of thin steel sheet.

4.8 Practical implications

As the Huxley cracking test is sensitive and requires small demands in terms of material and specimen preparation, the welder can use this test to assess the crack susceptibility of steel sheet before real welding production. The steel designer may apply this in order to test and to compare the crack susceptibility of a series of steels to find the suitable grades of steels. The welding process engineer may also use the Huxley cracking test under various technical conditions to enable the selection of an optimum welding speed, current and other welding parameters.

There might be more scope for the modification of testing conditions and specimen design in order to have more sensitive testing results or to meet other purposes. However, potential research workers in this field are recommended to test the steels under the same conditions as described by HV Huxley, to take advantage of comparing the test results with the abundant cracking test data already available in the relevant literature.

For steels with a known composition, there might be no need to carry out such cracking tests, because their crack susceptibility may already have been documented in the literature or it may also be easily predicted. For the prediction of weld crack susceptibility based on composition, though there is not an versatile equation for all kinds of steels, the model of the cracking and composition relationship as described in section 4.1 might be a simple and reliable guide. The value of $C(S+0.5P)$ is a good indicator for crack susceptibility especially when the carbon content is between 0.20 and 0.40%. For steels with a carbon content between 0.20 and 0.40%, if their value of $C(S+0.5P)$ is greater than 0.0050, it is almost certain that

they are crack susceptible. Such steel should not be selected for the
production welding, or if they are selected, their crack resistance
must be measured by the Huxley cracking test or other tests. Assuming
0.0050 is the maximum tolerable value of C(S+0.5P), then for a steel
with a carbon content of 0.40%, the tolerable amount of (S+0.5P) is only
0.013%. For a steel with a carbon content of 0.20%, on the other hand,
the tolerable amount of (S+0.5P) is double, or 0.025%.

For steels with a carbon content between 0.20 and 0.40%, and
with a value of C(S+0.5P) between 0.0033 and 0.0050, their crack suscep-
tibility may be influenced by alloying elements to a certain degree.
Whether they are crack resistant is not certain according to this model,
though in the majority of the cases they are crack resistant (CSF less
than 20).in the Huxley cracking test. If their crack susceptibility is
in doubt, the Huxley cracking test is strongly recommended.

For steels with a carbon content between 0.20 and 0.40%,
and with a value of C(S+0.5P) less than 0.0033, it can be certain that
they are not crack susceptible. The cracking test for such steels may
be omitted, because a steel with a C(S+0.5P) of less than 0.0033 is
guaranteed to be crack resistant.

For steels with a carbon content of over 0.40%. their crack
resistance can only be expected if (S+P) is well below 0.005%. As re-
gards steels with a carbon content of less than 0.20%, they are not
crack susceptible even with a sulphur content of as high as 0.030%.
The certainty of crack resistance can be expected if C(S+0.5P) is less
than 0.0033. However, a steel with a C(S+0.5P) value of greater than
0.0033 is crack resistant in many cases, conditioned by the presence
of a higher manganese content.

It is the task of steel producers to produce crack resistant
steels for welding application. As regards the low C(S+0.5P) condition

required, it might be very difficult for them to do so with the conventional steelmaking processes, especially when the carbon content in steel is higher than 0.35% as for the 3%Cr-Mo-V steels. The steelmaking in a controlled atmosphere (such as in an argon atmosphere) may yield better and more crack resistant steels. The addition of cerium or other rare earth metals in steel has been reported to be very effective for the modification of sulphide inclusions. Though the effect of cerium addition to the steel is not covered in this research, it is believed that by the presence of cerium in steel, the tolerable sulphur content for a crack free steel will be much higher.

Since the presence of oxygen in steel, especially high tensile steel, would not improve the weld crack resistance, the oxygen content in steels should be kept at a low level for a better impact strength. Though an addition of 2% oxygen in the argon shielding gas slightly reduces weld crack susceptibility, it should not be applied because of the arc instability and the decarburization associated with this process. Hence contrary to expectations of previous investigators there is no scope for reducing cracking by using oxygen addition to the arc atmosphere.

The modification of weld metal solidification might be a good way of improving weld quality and reducing weld crack susceptibility, but in the TIG arc welding of thin sheet there is not so much room for this modification, since a suitable arc voltage and current are fixed by the welding speed and sheet thickness. Alternative welding processes may be employed for the welding of very crack susceptible steels. The pulsed TIG arc welding with a periodic change of the fusion and solidification phases, offers more variety for the manipulation of weld pool solidification, as a result of such manipulation, solidification cracks might be prevented. In the case of multiple electrode TIG

welding, one electrode serves the purpose of fusion, the other electrodes are positioned before and after the main fusion electrode for preheating or postheating of the weld. W Vanschen[77] reported a two cathodes TIG welding of thin sheet is ideal for mass production with a production rate much higher than with one electrode TIG welding. In the above mentioned process the welding speed is much higher, and consequently the weld pool becomes longer, and a forced columnar to equiaxed transition in the weld central region can be expected. In the case of plasma arc welding, even a thinner sheet can be welded and the risk of solidification cracking is lower due to the reduced heat input and the smaller weld bead size. The alternative welding processes just mentioned are not dealt with in this research, but their attractive features have been recognized. It is hoped that the relationships of solidification cracking and the welding processes mentioned will receive more attention.

Reducing the carbon content in steel is one way of tackling the problem of sulphur and phosphorus induced cracking, however, this is restricted by the strength requirement of steel. If carbon content in the steel can be substituted partly by other alloying elements and the required mechanical and heat-treating properties can be maintained, the replacement of carbon with other alloying elements is recommended from the point of view of crack prevention. This might be a subject for future study.

Regression analysis is a powerful tool for the study of various relationships, and with the availability of a computer access this can be done easily. However, the results of regression analysis with a limited number of observations might not be representative. It is suggested that a regression equation can only be accepted if it is based on a large number of observations or verified by theories.

5. CONCLUSIONS

As a result of this investigation the following conclusions can be drawn:

1) It is confirmed that the most important elements in high tensile steels which affect solidification cracking are carbon, sulphur and phosphorus.

2) The presence of carbon alone in steel without a significant content of sulphur and phosphorus is not a sufficient cause for solidification cracking. The main effect of carbon in steel is to intensify the harmful effects of phosphorus and sulphur.

3) In the case of high tensile steels, weld crack resistance is not improved by a higher manganese content or a higher Mn/S ratio. In the case of low carbon steels, in which the alloy composition approaches Fe-Mn-S system, a higher manganese content or a higher Mn/S ratio may improve weld crack resistance.

4) Increase of oxygen content of up to 0.016% in high tensile steels has no effect on solidification cracking, and there is no evidence for a beneficial effect of a higher O/S ratio in high tensile steels.

5) Welding of high tensile steels with a 2% oxygen-argon shielding gas may reduce weld crack susceptibility, however, it is not a viable technique because of the arc instability and its effect attributed to decarburization.

6) The presence of silicon, nickel and chromium in high tensile steels may slightly increase weld cracking susceptibility, while the presence of molybdenum may reduce it. On the whole their effects are not very large compared with that of sulphur and phosphorus.

7) No single regression equation has been found to be

versatile enough for the prediction of crack susceptibility in the range of low alloy steels. A model of cracking and composition relationship based on the criteria of carbon content and the C(S+0.5P) value can be proposed as a guide for crack prediction. The proposed model is found to fit the 203 observations fairly well.

8) The presence and amount of the low melting liquid phase is accountable for solidification cracking. This low melting liquid phase is confirmed to contain sulphur.

9) Based on investigation of fresh solidification crack surfaces, four phases may participate in the solidification cracking process, these being: low melting liquid films, localized liquid metal, solid bridges and gas pores.

10) The general features of solidification crack surface are: smooth dendritic grain boundaries, distorted and broken dendrites, and traces of liquated and globular inclusions.

11) Borland's generalized theory on solidification cracking is more acceptable for the description of the cracking behaviour for the centreline crack observed in the welding of thin steel sheet.

6. RECOMMENDATIONS FOR FURTHER RESEARCH WORK

With the increase of material strength and ductility required, and with the decrease of sheet thickness for the fabrication of high duty components, the problem of weld cracking becomes more serious and the demand for a crack free welding performance becomes more urgent. For this reason it is considered that the areas required further research are as follows:

1) The possibility of cerium addition to high tensile steels to avoid sulphur-induced crack susceptibility.

2) The possibility of replacing carbon partly with other alloying elements in favour of increasing the tolerable amounts of sulphur and phosphorus under such conditions that the required material properties are not impaired.

3) The study of weld crack susceptibility in other alternative welding processes used for the fabrication of sheet materials, such as pulsed TIG welding, multiple electrode TIG welding, plasma and micro-plasma arc welding.

4) More Huxley cracking tests for planned series of steels with controlled compositions in order to extend the knowledge of cracking and composition relationships.

5) Collecting Huxley cracking test data and comparing them with the records of actual production welding to establish and confirm their close relationships.

7. ACKNOWLEDGEMENTS

8. REFERENCES

1) F Bollenrath and H Cornelius: Luftfahrtforschung 1936, Vol 13, pp118-124.

2) JC Borland: British Welding Journal 1960, Vol 7, pp623-637.

3) EJ Morgan-Warren: "Solidification Cracking in Low Alloy Steel Weld Metals", PhD Thesis of the University of Aston in Birmingham, 1972.

4) KL Zeyen: Technische Mitteilung Krupp 1936, Vol 4, pp115-122.

5) P Bardenheuer and W Bottenberg: Archiv für das Eisenhüttenwesen 1938, Vol 11, pp375-383.

6) O Werner: Archiv für das Eisenhüttenwesen 1939, Vol 12, pp449-458.

7) HV Huxley: British Welding Journal 1961, Vol 8, pp514-519.

8) HS George: Mechanical Engineering 1931, Vol 53, pp433-439.

9) A Portvin: Journal of the Institute of Metals 1948-49, Vol 75, pp949-971.

10) DCG Lees: Journal of the Institute of Metals 1946, Vol 72, pp343-364; ibid 1947, Vol 73, pp537-540.

11) ARE Singer and SA Cottrell: Journal of the Institute of Metals 1946, Vol 73, pp35-54.

12) WI Pumphrey and PH Jennings: Journal of the Institute of Metals 1948, Vol 75, pp235-256.

13) JC Borland: British Welding Journal 1960, Vol 7, pp508-512.

14) NN Prokhorov: Welding Production 1962, Vol 4, pp1-5.

15) T Senda, F Matsuda et al: Transactions of the Japan Welding Society 1971, Vol 2, pp45-66.

16) D Rosenthal: Transactions of ASME 1946, pp849-966.

17) TW Clyne: Sheffield International Conference on Solidification and Casting 1977, Preprint pp875-888.

18) E Scheil: Zeitschrift für Metalkunde 1942, Vol 34, pp70.

19) EJ Wilkinson and CLM Cottrell: Welding and Metal Fabrication 1958, pp171-184.

20) JC Borland: British Welding Journal 1964, Vol 11, pp634-640.

21) HV Huxley: Welding and Metal Fabrication 1963, pp29-32.

22) HV Huxley: Metallurgia 1970, Vol 82, pp167-174.

23) PW Jones: British Welding Journal 1959, Vol 6, pp282-290.

24) CF Meitzner and RD Stout: Welding Journal 1966, Vol 45, pp393S-400S.

25) CT Anderson: Transactions of AIME 1954, Vol 200, pp835-837.

26) T Boniszewski: British Welding Journal 1966, Vol 13, pp558-577; ibid Vol 14, pp131-144.

27) CLM Cottrell: Journal of the Iron and Steel Institute 1965, Vol 203, pp597-604.

28) CE Sims: Transactions of AIME 1959, Vol 215, pp367-393.

29) W Craft and Hilty: Proceedings of the Electric Furnace Steel Conference 1953, pp121-145.

30) W Dahl, H Hengstenberg and C Düren: Stahl und Eisen 1966, Vol 86, pp782-795.

31) PP Mohla and J Beech: Journal of the British Foundryman 1968, Vol 61, pp453-460.

32) W Eilender and R Pribyl: Archiv für Eisenhüttenwesen 1837/38, Vol 11, pp443-448.

33) N Bailey: The Welding Institute Research Report Dec 1976, Effect of wire composition and flux type on solidification cracking when submerged arc welding C-Mn steels.

34) ET Turkdogan, S Ignatowicz and J Pearson: Journal of the iron and Steel Institute 1955, Vol 180, pp349-354.

35) H Wentrup: Technische Mitteilung Krupp 1937, Vol 5, pp131-173.

36) R Vogel and Hotop: Archiv für Eisenhüttenwesen 1937, Vol 11, pp41-54.

37) LK Bigelow and MC Flemings: Sulphide Inclusions in Steel. CR70-13, Army Materials and Mechanics Research Center, Cambridge USA, 1970.

38) GS Mann and LH van Vlack: Metallurgical Transactions B, 1976, Vol 7B, pp469-475.

39) H Nakagawa, F Matsuda and T Senda: Transactions of Japan Welding Society 1974, Vol 5, pp39-45, pp84-89, pp26-33, pp18-25; ibid 1975, Vol 6, pp3-6 and pp10-16.

40) DC Hilty and C Crafts: Transactions of AIME 1952, Vol 194, pp1307-1312.

41) JC Yarwood, MC Flemings and JF Elliot: Metallurgical Transactions 1971, Vol 2, pp2573-2582.

42) ET Turkdogan and GJW Kor: Metallurgical Transactions 1971, Vol 2, pp1561-1570, pp1571-1582; ibid 1972, Vol 3, pp1269-1278.

43) WA Tiller and JW Rutter: Canadian Journal of Physics 1956, Vol 34, pp96.

44) GJ Davies and JG Garland: International Metallurgical Reviews 1975, Vol 20, pp83-106.

45) F Matsuda, T Hashimoto and T Senda: Transactions of the National Research Institute of Metals 1969, Vol 11, pp43-58.

46) WF Savage and CD Lundin: Welding Journal 1965, Vol 44, pp175-181S.

47) T Ganaha and HW Kerr: Metals Technology 1978, pp62-69.

48) G Aichele: Schutzgasschweissen, Messer Griesheim GmbH, Hanauer
    Landstrasee 300. 6 Frankfurt am Main, Germany.

49) K Wilken: Chemie Ingenieur Technik 1972, Vol 44, pp777-783.

50) K Wilken and W Schoenherr: Welding in the World 1975, Vol 13,
    pp238-248.

51) WF Savage and CD Lundin: Welding Journal 1966, Vol 45, pp497-
    503S.

52) M Inagaki, J Nishikawa and R Kohno: Transactions of Japan
    Welding Society 1973, Vol 42, pp29-39.

53) D McKeown: Metal Construction and British Welding Journal 1970,
    Vol 2, pp351-352.

54) PT Houldcroft: British Welding Journal 1955, Vol 2, pp471-475.

55) WR Apblett and WS Pellini: Welding Journal 1954, Vol 43, pp83-
    90S.

56) F Bollenrath and H Cornelius: Archiv für das Eisenhüttenwesen
    1937, Vol 10, pp563-576.

57) FJ Wilkinson, CLM Cottrell and HV Huxley: British Welding
    Journal 1958, vol 5, pp557-562.

58) PW Jones: British Welding Journal 1957, Vol 4, pp189-197.

59) JC Borland and JH Rogerson: British Welding Journal 1962, vol 9,
    pp 494-499.

60) JG Garland and N Bailey: Welding Research International 1975,
    Vol 5. No 3, pp1-33.

61) E Schmidtmann and G Wellnitz: Archiv für das Eisenhüttenwesen
    1976, vol 47, pp101-106.

62) SA Ostrovskaya: Automatic welding 1964, Jan, pp6-11.

63) K Winterton: Welding Journal 1961, Vol 40, pp253-258S.

64) I Hrivnak: Welding in the world 1978, Vol 16, pp130-151.

65) CLM Cottrell and MJ Turner: Journal of Iron and Steel Institute 1962, vol 200, pp380-388.

66) JG Garland and N Bailey: The Welding Institute Report 1976, Dec, Solidification Cracking during the Submerged Arc Welding of Carbon Manganeses Steels-- A detailed Assessment of the Effect of Parent Plate Compositions.

67) K Orths, W Weiss and A Kolorz: Giessereiforschung 1974, Vol 26, pp95-108.

68) HV Huxley: Welding and Metal Fabrication 1967, pp498-502.

69) C Chtfield: Statistics for Technology, Chapman and Hall, London, 1974, Chapter 11, pp257-287.

70) EJ Morgan-Warren and MF Jordan: Metals Technology 1974, Vol 1, pp271-278.

71) K Schwerdtfeger: Archiv für das Eisenhüttenwesen 1970, Vol 41, pp923-937.

72) VV Podgaetskii, GI Parfessa and SM Litvinchuk: Automatic Welding 1969, No 3, pp19-23.

73) VV Podgaetskii: Pori, vklyuchennya i trishchini v svarnikh shvakh (Pores, inclusions and cracks in weld metal), Kiev, 1970, pp159-201.

74) JC Borland: Welding and Metal Fabrication 1979, pp19-29 and pp99-107.

75) F Matsuda: Welding Metallurgy, Nikan Kogyo Shinbunsha, Tokyo, 1975 fourth edition, pp143-157.

76) F Matsuda, H Nakagawa, S Ogata and S Katayama: Transactions of JWRI (Japan Welding Research Institute) 1978, Vol 7, pp59-70.

77) W Vanschen: Baender Bleche Rohre 1978, Vol 9, pp354-358.

78) I Masumoto and K Imai: Transactions of Japan Welding Society 1970, Vol 1, pp104-111.

9. APPENDIX

Statistical terminology

Confidence limits: When an estimate of some quantity has been made it is desirable to know not only the estimated value but also how precise this estimate is. A convenient way of expressing the precision is to quote confidence limits. These represent the upper and lower limits within which it can be stated with a given degree of confidence that the true value lies. The degree of confidence may be very high at, say, 99% certainty when there is a probability of only 1 value in 100 being outside the limits or at 90% when there is a probability of 10 values in 100 being outside the limits.

Correlation coefficient r: This is a means of showing the significance of an apparently linear relationship. It has the characteristics such that if the relationship between the data can be represented exactly by a straight line $r = \pm 1$, whereas if no relationship at all $r = 0$. The value of r lies between -1 and $+1$, and the higher the absolute value of r the better is the correlation.

Level of significance: This is the probability of getting a result which is as extreme, or more extreme, than the one specified. If a 5% level of significance is chosen in designing a test of hypothesis, then there are about 5 chances in 100 that the hypothesis would be rejected when it should be accepted.

Null hypothesis: The hypothesis which is to be tested is called the null hypothesis, and is denoted by H_o . Any other hypothesis is called

the alternative hypothesis, and is denoted by H_1. The null hypothesis normally takes the form that a parameter does not differ from a particular value. A numerical method for testing such hypothesis is called a significance test (see t statistic).

Regression: The problem of finding the most suitable form of equation to predict one variable from the values of one, or more, other variables is called the problem of regression. A linear regression equation is of the form:

$$y = a_0 + a_1x_1 + a_2x_2 + \cdots + a_nx_n$$

where y is the dependent variable, and x_1, x_2, $\cdots$ x_n are independent variables, and a_0, a_1, a_2, $\cdots$, a_n are the regression coefficients. With a suitable computer programme, the regression equation can be readily obtained.

Residual: A residual is defined as the algebraic difference between the predicted and observed value. There is one residual for each of the original observed values, and the regression coefficients are estimated by minimizing the sum of squares of these residuals. Residuals are therefore a form of error which cannot be explained in terms of the independent variables used in the regression equation.

Significance test: See null hypothesis and t statistic.

Sum of squared errors: A measure of the overall disagreement between the predicted and observed values. See also residual.

t statistic: A calculated value which is used to test the null hypothesis that a parameter does not differ from a particular value. For

example, it can test the null hypothesis that the slope of the regression line is 0. As a rule of thumb it can be said that if the calculated t statistic is greater than 2 in absolute value, the null hypothesis can be rejected at the 5% level of significance.

Variance and standard deviation: They are measures of spread. The sample variance s^2 of n observations, x_1, x_2, $\cdots$, x_n, is given by

$$s^2 = \frac{(x_1 - \bar{x})^2 + (x_2 - \bar{x})^2 + \cdots + (x_n - \bar{x})^2}{(n - 1)}$$

The standard deviation s of the sample is obtained by taking the square root of the variance. If the values of x are all identical, there are no differences and the estimate of the variance is zero; if they differ slightly from each other, the variance is small; if they differ widely, the variance is large.

Yates method: A systematic method of estimating the effects and of performing the analysis of variance for the 2^n factorial experiment as proposed by F Yates. The details of this method is explained in many books of the applied statistics such as "Statistics for Technology" by C Chatfield[69].

Table 1. Estimated Data for Invariant Equilibria in Fe-Mn-S-O
Quarternary System according to ET Turkdogan et al [42].

Invariant Temperatures	Invariant Phases	Invariant Phase Composition
900°C	Gamma Iron	about 10 ppm Mn
	Solid Mn Sulphide	$a_{MnS} \cong 0.4$
	Solid Fe Sulphide	$a_{FeS} \cong 1$
	Fe(Mn) Oxide	$a_{MnO} \cong 0.5$
	Liquid Oxysulphide	about 26% FeO, 54% FeS, 15% MnS and 5% MnO
	Gas	$p_{O_2} \cong 3.8 \times 10^{-18}$ atm
		$p_{S_2} \cong 1.4 \times 10^{-4}$ atm
about 1225°C	Solid Fe/Mn	about 90% Mn
	"MnS"	$a_{MnS} \cong 1$
	"MnO"	$a_{MnO} \cong 1$
	Liquid oxysulphide, l_1	about 0.1% FeO, 0.3% FeS, 65.2% MnS and 34.4% MnO
	Metallic Liquid, l_2	O/S for l_2 less than O/S for l_1.

Table 2. Reproducibility of Crack Susceptibility Factor in Huxley Cracking Test.

Steel	Individual Crack Lengths in mm, x_{ijt}		x_{ij}	x_i	CSF	SE of CSF	95% Confidence Limits ± CSF
EN353	21 21 24 24 19 15 22 24 27 20 23 24 24 26 27 27 24 22 23 25 24 27 27 22		20.9 24.8 24.3	23.4	61	11	4.4
EN19	24 20 18 16 20 24 18 16 18 25 22 16 23 22 18 24 20 18 17 24 20 19 21 21		19.5 21.0 20.0	20.2	53	7	2.8
HY80	10 10 10 10 13 13 14 12 18 12 10 15 10 8 7 11 7 6 11 15 16 15 10 11		11.5 11.4 11.4	11.4	30	8	3.2
HY130	0 0 0 0 0 0 0 0 0 0 0 0 0 0 0 0 0 0 0 0 0 0 0 0		0 0 0	0	0	0	0
BS4360 -50B	0 0 0 0 0 3 0 2 0 0 0 0 0 2 4 0 0 0 0 0 0 0 0 0		0.6 0.8 0	0.4	1	3	1.2
Corten A	3 2 2 0 0 0 0 0 2 4 0 3 2 0 2 0 2 2 3 0 0 0 1 1		0.9 1.6 1.1	1.2	3	3	1.2
Hypress 23	8 11 14 13 18 11 4 10 12 3 2 2 4 3 8 5 6 4 11 13 11 9 3 3		11.1 4.9 7.5	7.8	21	12	4.8
EN5	25 27 30 27 25 27 27 25 26 27 27 22 26 26 24 27 21 24 25 27 29 24 25 25		26.6 25.6 25.0	25.8	68	5	2.0

x_{ij}: mean crack length for a specimen of 8 test segments in mm.

x_i : mean crack length for three specimens in mm.

Table 3. The Effect of Surface Conditions on the Crack Susceptibility in the Huxley Cracking Test.

Cast Number	Specimen Number	Surface Conditions	CSF
SV299	MA1-A	Brightly milled	17
	MA1-B	Abrasive ground	16
	MA1-C	Pickled	16
	MA1-D	Shot blasted	17
SV309	MA2-A	Brightly milled	9
	MA2-B	Abrasive ground	12
	MA2-C	Pickled	8
	MA2-D	Heavily scaled	25
SV307	MA3-A	Brightly milled	62
	MA3-B	Abrasive ground	60
	MA3-C	Pickled	63
	MA3-D	Heavily scaled	65
SV306	MA4-A	Brightly milled	56
	MA4-B	Abrasive ground	57
	MA4-C	Pickled	54
	MA4-D	Heavily scaled	59
AF384	MA5-A	Brightly milled	1
	MA5-B	Abrasive ground	0
	MA5-C	Pickled	0
	MA5-D	Shot blasted	2
SV168	MA6-A	Brightly milled	0
	MA6-B	Abrasive ground	0
	MA6-C	Pickled	0
	MA6-D	Shot blasted	0
SV173	MA7-A	Brightly milled	63
	MA7-B	Abrasive ground	62
	MA7-C	Pickled	66
	MA7-D	Shot blasted	67

Table 4. Required Current to Produce a 6mm Weld Bead with Full
Penetration.

Thickness, mm	Current, A
1.6	70
1.8	80
2.0	87
2.2	97
2.4	105
2.5	110
3.0	130

Table 5. Effect of Sheet Thickness on the Huxley Cracking Test Results.

Steel Number	Sheet Thickness, mm	CSF Value
MA1 (SV299)	2.51	16
	1.96	17
MA2 (SV309)	2.51	12
	2.04	9
	1.68	12
MA3 (SV307)	2.51	60
	2.23	63
	2.00	62
MA4 (SV306)	2.08	56
	1.93	57
	1.87	55
MA5 (AF384)	2.52	0
	2.13	0
	1.97	1
MA6 (SV168)	2.24	0
	2.01	0
MA7 (SV173)	1.98	63
	1.80	62
	1.68	62
MA8 (SV171)	2.00	60
	1.85	62
	1.69	61

Table 6. Planned Series of Composition Levels for SAE4130 Steels

Cast No	Mn %	S %	O %
1	Low 0.20	Low 0.007	Low 0.005
2	High 0.70	Low 0.007	Low 0.005
3	Low 0.20	High 0.040	Low 0.005
4	High 0.70	High 0.040	Low 0.005
5	Low 0.20	Low 0.007	High 0.020
6	High 0.70	Low 0.007	0.020
7	Low 0.20	High 0.040	High 0.020
8	High 0.70	High 0.040	High 0.020

Table 7. Composition* and CSF Value of 10 SAE4130 Steels in MA Series

Series No	Cast No	C	S	Si	Mn	Cr	Mo	O	Mn/S	O/S	CSF
MA1	SV299	0.31	0.011	0.22	0.30	0.95	0.23	0.010	27	0.91	17
MA2	SV309	0.32	0.009	0.31	0.72	0.91	0.22	0.004	80	0.45	12
MA3	SV307	0.31	0.042	0.29	0.23	0.90	0.22	0.006	5	0.14	62
MA4	SV306	0.31	0.041	0.32	0.80	0.93	0.23	0.007	20	0.17	57
MA5	AF384	0.28	0.007	0.22	0.19	0.91	0.20	0.008	27	1.14	1
MA6	SV168	0.29	0.008	0.15	0.61	0.93	0.20	0.016	76	2.00	0
MA7	SV173	0.28	0.032	0.12	0.17	0.93	0.20	0.011	5	0.34	62
MA8	SV171	0.28	0.032	0.18	0.59	0.92	0.20	0.013	18	0.41	60
MA9	SV172	0.28	0.028	0.24	0.67	0.95	0.20	0.010	24	0.36	43
MA10	SV178	0.28	0.039	0.16	0.68	0.93	0.21	0.010	17	0.26	53

* All steels contain 0.005% phosphorus and 0.01% nickel.

Table 8 . Design of 2^3 Factorial Experiment for SAE4130 Steels.

Series No	Code	Observation CSF Value	Levels of Factors Mn, S and O
MA1	1	17	Low Mn, Low S and Low O
MA2	a	12	High Mn, Low S and Low O
MA3	b	62	Low Mn, High S and Low O
MA4	ab	57	High Mn, High S and Low O
MA5	c	1	Low Mn, Low S and High O
MA6	ac	0	High Mn, Low S and High O
MA7	bc	62	Low Mn, High S and High O
MA8	abc	60	High Mn, High S and High O

Table 9 . Analysis of 2^3 Factorial Experiment for SAE4130 Steels.

Code	Observation	I	II	Effect Total	Effect	Effect Sum Square
1	17	29	148	271	67.7	-
a	12	119	123	-13	- 3.3	22
b	62	1	-10	211	52.8	5576
ab	57	122	-3	-1	-0.2	0.1
c	1	-5	90	-25	-6.2	77
ac	0	-5	121	7	1.8	6
bc	62	-1	0	31	7.8	122
abc	60	-2	-1	-1	-0.2	0

Table 10. Comparison of the Observed and Estimated CSF for the ten
experimental SAE4130 steels with a designed variation of Mn, S and O.

Series No	Cast No	S%	Observed CSF	Estimated CSF	Difference
MA1	SV299	0.011	17	13	4
MA2	SV309	0.009	12	10	2
MA3	SV307	0.042	62	65	-3
MA4	SV306	0.041	57	63	-7
MA5	AF384	0.007	1	6	-5
MA6	SV168	0.008	0	8	-8
MA7	SV173	0.032	62	48	14
MA8	SV171	0.032	60	48	12
MA9	SV172	0.028	43	42	1
MA10	SV178	0.039	53	60	-7

Regression Equation: $P(CSF, MA) = 1681S - 6$

$r = 0.95$

Table 11. Planned Series of Composition Levels for Fe-Mn-S-O Alloys.

Cast No	Composition, Wt %		
	Mn	S	O
1	Low 0.01	Low 0.02	Low 0.005
2	High 0.80	Low 0.02	Low 0.005
3	Low 0.01	High 0.20	Low 0.005
4	High 0.80	High 0.20	Low 0.005
5	Low 0.01	Low 0.02	High 0.20
6	High 0.80	Low 0.02	High 0.20
7	Low 0.01	High 0.20	High 0.20
8	High 0.80	High 0.20	High 0.20

Table 12. Composition and CSF value of 12 low carbon Fe-Mn-S-O alloys.

Series No	Cast No	C	S	P	Si	Mn	O	Mn/S	O/S	CSF
MC1	K3027	0.03	0.020	0.007	0.01	0.02	0.011	0.1	0.55	6
MC2	K3045	0.07	0.017	0.009	0.17	0.88	0.005	51.8	0.29	0
MC3	K3044	0.06	0.160	0.008	0.03	0.02	0.005	0.1	0.03	64
MC4	K3030	0.03	0.160	0.006	0.03	0.80	0.017	5.0	0.11	66
MC5	S3128	0.05	0.020	0.008	0.02	0.10	0.063	0.5	3.15	0
MC6	S3130	0.03	0.024	0.007	0.00	0.44	0.064	18.3	2.67	0
MC7	S3129	0.04	0.180	0.005	0.00	0.04	0.066	0.2	0.37	59
MC8	S3131	0.02	0.160	0.005	0.00	0.58	0.064	3.6	0.40	70
MC9	K3043	0.03	0.021	0.006	0.00	0.02	0.033	0.9	1.57	0
MC10	K3029	0.03	0.023	0.007	0.02	0.77	0.011	33.5	0.48	3
MC11	K3046	0.04	0.080	0.006	0.02	0.78	0.007	9.7	0.09	9
MC12	K3028	0.03	0.170	0.006	0.00	0.03	0.016	0.2	0.09	63

Table 13. Design of 2^3 Factorial Experiments for Fe-Mn-S-O Alloys

Series No	Code	Observation CSF Value	Levels of Factors Mn, S and O		
MC1	1	6	Low Mn	Low S	Low O
MC2	a	0	High Mn	Low S	Low O
MC3	b	64	Low Mn	High S	Low O
MC4	ab	66	High Mn	High S	Low O
MC5	c	0	Low Mn	Low S	High O
MC6	ac	0	High Mn	Low S	High O
MC7	bc	59	Low Mn	High S	High O
MC8	abc	70	High Mn	High S	High O

Table 14. Analysis of 2^3 Factorial Experiments for Fe-Mn-S-O Alloys.

Code	Observation	I	II	Effect Total	Effect	Effect Sum Square
1	6	6	136	265	66.3	-
a	0	130	129	7	1.8	6
b	64	0	-4	253	63.2	8001
ab	66	129	11	19	4.8	45
c	0	-6	124	-7	-1.8	6
ac	0	2	129	15	3.8	28
bc	59	0	8	5	1.2	3
abc	70	11	11	3	0.8	1

Table 15. Specification of Steels being tested in this Research

Steel Name	Series No in this Report	Composition
ASTM A357	MD11	0.15%C, 5%Cr, 0.5%Mo
ASTM A387B	MD1, MD2,MD3,MD4	0.15%C, 1%Cr, 0.5%Mo
BS4360-50B	MD15	0.24%C, 0.55%Si, 1.60%Mn, 0.10% Nb
Corten A	MD10	0.12%C, 0.25-0.75%Si, 0.60%Mn, 1%Cr
Creusabro 32	MD17	0.16-0.22%C, 0.40%Si max, 1.1-1.4%Mn 0.15-0.35%Mo, 1.1-1.5%Cr, 0.15-0.35%Cu
EN5	MD18	0.25-0.35%C, 0.05-0.35%Si, 0.1-0.6%Mn
EN19	MD19	0.35-0.45%C, 0.19-1.50%Cr, 0.2-0.4%Mo 0.15-0.35%Si, 0.50-0.80%Mn
EN24	MD5,MD6,MD7,MD8	0.35-0.45%C, 1.0-1.5%Ni, 0.9-1.4%Cr 0.45-0.70%Mn, 0.20-0.35%Mo
EN353	MD14	0.20%C max, 0.35%Si max, 0.5-1.0%Mn 1.0-1.5%Ni, 0.75-1.25%Cr, 0.08-0.15%Mo
HY80	MD13	0.22%C max, 1.90-3.30%Ni 0.90-1.90%Cr, 0.13-0.63%Mo
HY130	MD12	0.12-0.30%C, 0.60-0.90%Mn, 0.02%Ti 4.75-5.25%Ni, 0.40-0.70%Cr, 0.05%V
Hypress 23	MD16	0.10%C, 1.0%Mn, 0.30%Cu, 0.025%Nb
SAE1006	MD9	0.08%C max, 0.25-0.40%Mn
SAE4130	MA1-MA10 MB1-MB6	0.28-0.33%C, 0.20-0.35%Si, 0.40-0.60%Mn 0.80-1.10%Cr, 0.15-0.25%Mo
RS120[*]	see above	0.30-0.35%C, 0.20-0.35%Si, 0.40-0.60%Mn 0.80-1.20%Cr, 0.15-0.25%Mo
Fe-Mn-S-O	MC1-MC12	see Table 12

* RS120: British Aerojet Specification similar to SAE4130.

Table 16. Composition and CSF Value of MB Series SAE4130 Steels

Series No	Specification	C	S	P	Si	Mn	Ni	Cr	Mo	O	CSF
MB1	SAE4130	0.24	0.024	0.028	0.23	0.74	0.18	1.03	0.21	0.006	50
MB2	SAE4130	0.29	0.025	0.029	0.24	0.73	0.18	1.01	0.21	0.006	56
MB3	SAE4130	0.32	0.031	0.036	0.32	0.68	0.01	0.96	0.21	0.006	58
MB4	SAE4130	0.35	0.011	0.051	0.07	0.90	0.02	0.93	0.26	0.007	49
MB5	SAE4130	0.38	0.033	0.010	0.31	0.70	0.01	1.00	0.22	0.010	60
MB6	SAE4130	0.40	0.012	0.009	0.34	0.70	0.02	0.98	0.21	0.005	31

Table 17. Composition and CSF value of MD Series Technical Steels

Series No	Specification	C	S	P	Si	Mn	Ni	Cr	Mo	O	CSF
MD1	ASTM A387B	0.14	0.030	0.023	0.23	0.57	0.13	0.90	0.47	0.015	13
MD2	ASTM A387B	0.15	0.032	0.023	0.23	0.60	0.13	0.95	0.45	0.014	9
MD3	ASTM A387B	0.17	0.035	0.030	0.32	0.51	0.01	0.85	0.36	0.009	43
MD4	ASTM A387B	0.18	0.010	0.010	0.25	0.48	0.01	0.88	0.36	0.012	0
MD5	EN24	0.38	0.043	0.013	0.29	0.73	1.48	1.25	0.22	0.005	62
MD6	EN24	0.39	0.038	0.012	0.29	0.71	1.45	1.23	0.23	0.005	60
MD7	EN24	0.45	0.040	0.009	0.58	0.72	1.36	1.18	0.30	0.007	55
MD8	EN24	0.50	0.014	0.011	0.60	0.70	1.37	1.16	0.24	0.006	41
MD9	SAE1006	0.06	0.021	0.014	0.00	0.29	0.01	0.02	0.00	0.052	0
MD10	Corten A	0.11	0.024	0.011	0.05	0.91	0.12	0.06	0.02	0.004	3
MD11	ASTM A357	0.11	0.021	0.019	0.23	0.59	0.06	4.88	0.55	0.010	11
MD12	HY130	0.12	0.007	0.008	0.30	0.78	5.13	0.59	0.47	0.007	0
MD13	HY80	0.15	0.014	0.019	0.19	0.31	2.64	1.30	0.37	0.010	30
MD14	EN353	0.15	0.040	0.021	0.22	0.80	1.40	1.25	0.10	0.010	61
MD15	BS4360-50B	0.17	0.020	0.028	0.28	1.25	0.03	0.05	0.00	0.004	1
MD16	Hypress 23	0.18	0.019	0.058	0.22	1.48	0.03	0.05	0.00	0.010	21
MD17	Creusabro 32	0.20	0.020	0.014	0.27	1.19	0.20	1.40	0.20	0.004	20
MD18	EN5	0.30	0.030	0.008	0.08	0.74	0.04	0.02	0.00	0.015	68
MD19	EN19	0.34	0.015	0.042	0.23	0.67	0.31	1.11	0.21	0.013	53

Note: MD7 contains 0.12%Al, and MD10 contains 0.17%Al.

Table 18. Steel Composition and CSF values of HA Series.[70)]

Series No	Steel Type	C	S	P	Si	Mn	Ni	Cr	Mo	V	CSF
HA1	3%Cr-Mo-V	0.44	0.003	0.001	1.48	0.60	0.22	2.00	0.59	0.05	23
HA2	3%Cr-Mo-V	0.45	0.004	0.005	0.45	0.71	0.17	3.25	0.97	0.21	29
HA3	3%Cr-Mo-V	0.45	0.004	0.004	0.43	0.78	0.20	3.28	0.96	0.18	28
HA4	3%Cr-Mo-V	0.58	0.008	0.005	1.00	0.74	0.13	3.10	0.95	0.22	42
HA5	3%Cr-Mo-V	0.37	0.005	0.008	0.30	0.57	0.00	2.95	0.98	0.20	29
HA6	3%Cr-Mo-V	0.42	0.008	0.028	0.34	0.78	0.02	2.95	0.98	0.33	33
HA7	3%Cr-Mo-V	0.37	0.009	0.001	0.32	0.66	0.03	3.09	1.03	0.22	14
HA8	3%Cr-Mo-V	0.39	0.004	0.006	0.34	0.64	0.01	3.04	0.90	0.28	20
HA9	3%Cr-Mo-V	0.42	0.015	0.011	0.35	0.70	0.03	3.07	1.06	0.20	23
HA10	3%Cr-Mo-V	0.36	0.012	0.020	0.34	0.78	0.01	3.22	1.04	0.28	27
HA11	3%Cr-Mo-V	0.40	0.010	0.007	0.35	0.63	0.09	3.16	0.94	0.25	19
HA12	3%Cr-Mo-V	0.39	0.010	0.020	0.40	0.81	0.01	3.10	1.02	0.30	33
HA13	3%Cr-Mo-V	0.43	0.008	0.008	0.32	0.66	0.15	3.18	1.04	0.23	22
HA14	3%Cr-Mo-V	0.34	0.010	0.017	0.35	0.78	0.02	3.35	0.95	0.37	23
HA15	3%Cr-Mo-V	0.39	0.013	0.001	0.38	0.67	0.02	3.03	0.99	0.36	17
HA16	3%Cr-Mo-V	0.45	0.012	0.007	0.28	0.66	0.00	3.10	0.92	0.21	14
HA17	3%Cr-Mo-V	0.46	0.018	0.009	0.26	0.65	0.00	2.90	0.97	0.21	21
HA18	3%Cr-Mo-V	0.48	0.024	0.008	0.25	0.65	0.00	3.10	0.97	0.21	31
HA19	3%Cr-Mo-V	0.39	0.008	0.008	0.25	0.70	0.20	3.18	0.93	0.19	4
HA20	1%Cr-Mo·	0.38	0.006	0.005	0.29	0.48	0.00	0.96	1.78	0.00	5
HA21	1%Cr-Mo	0.37	0.006	0.005	0.28	0.50	0.00	0.98	0.90	0.00	16
HA22	1%Cr-Mo	0.38	0.015	0.003	0.36	0.54	0.00	0.98	0.59	0.00	28
HA23	1%Cr-Mo	0.40	0.018	0.006	0.29	0.50	0.00	0.98	1.40	0.00	19
HA24	1%Cr-Mo	0.39	0.024	0.005	0.28	0.55	0.00	0.99	0.47	0.00	19
HA25	1%Cr-Mo	0.35	0.026	0.005	0.24	0.51	0.00	0.99	1.34	0.00	25
HA26	1%Cr-Mo	0.40	0.035	0.005	0.28	0.51	0.00	0.96	0.88	0.00	36
HA27	1%Cr-Mo	0.36	0.033	0.006	0.28	0.50	0.00	0.96	1.75	0.00	34

Table 19. Composition and CSF Value of HB Series Steels[21].

Series No	Steel Type	C	S	P	Si	Mn	Ni	Cr	Mo	V	CSF
HB1	1%Cr-Mo	0.30	0.009	0.016	0.29	0.49	0.18	0.96	0.19	0.00	19
HB2	1%Cr-Mo	0.28	0.006	0.013	0.23	0.51	0.10	1.02	0.17	0.00	18
HB3	2%Ni-Cr	0.38	0.010	0.018	0.15	0.63	1.80	0.82	0.23	0.00	40
HB4	2%Ni-Cr	0.46	0.009	0.011	0.11	0.41	2.10	0.83	0.46	0.26	32
HB5	3%Cr-Mo-V	0.38	0.005	0.014	0.24	0.72	0.14	3.08	0.97	0.20	23
HB6	3%Cr-Mo-V	0.42	0.009	0.010	0.20	0.57	0.12	3.31	1.06	0.18	21
HB7	3%Cr-Mo-V	0.36	0.008	0.009	0.35	0.63	0.16	3.05	2.00	0.39	8
HB8	5%Cr-Mo-V	0.44	0.007	0.011	0.30	0.63	0.15	5.10	2.12	0.43	13
HB9	2%Cr-Mo-V	0.46	0.004	0.017	1.59	0.68	0.00	2.06	0.58	0.07	28
HB10	2%Cr-Mo-V	0.42	0.009	0.016	1.16	0.68	0.09	1.99	0.54	0.06	24
HB11	MVS	0.15	0.005	0.007	0.29	0.52	0.15	0.42	1.13	0.29	1
HB12	A.121	0.40	0.008	0.014	1.58	0.54	0.00	0.04	0.77	0.25	25
HB13	2%Ni	0.73	0.009	0.010	0.26	0.42	2.21	0.07	0.03	0.00	36
HB14	5%Cr-Mo-V	0.43	0.008	0.010	0.92	0.34	0.11	5.31	1.16	0.44	11
HB15	Ni-Cr-Mo	0.44	0.009	0.023	0.28	0.63	1.82	1.31	0.93	0.20	39

Table 20. Composition and CSF Value of HC Series Steels[7].

Series No	Steel Type	C	S	P	Si	Mn	Ni	Cr	Mo	V	CSF
HC1	1%Cr-Mo	0.30	0.009	0.016	0.29	0.49	0.18	0.96	0.19	0.00	20
HC2	1%Cr-Mo	0.30	0.011	0.015	0.24	0.44	0.13	0.90	0.24	0.00	23
HC3	1%Cr-Mo	0.32	0.015	0.030	0.19	0.41	0.09	0.85	0.24	0.00	42
HC4	1%Cr-Mo	0.29	0.016	0.023	0.14	0.51	0.16	0.95	0.20	0.00	54
HC5	1%Cr-Mo	0.31	0.013	0.031	0.19	0.41	0.09	0.82	0.24	0.00	63
HC6	3%Cr-Mo-V	0.38	0.005	0.014	0.24	0.72	0.14	3.08	0.97	0.20	23
HC7	5%Cr-Mo-V	0.37	0.011	0.016	1.11	0.41	0.21	4.84	1.41	0.56	19
HC8	2%Ni-Cr	0.37	0.012	0.016	0.14	0.62	1.82	0.82	0.23	0.00	40
HC9	2%Ni-Cr	0.38	0.004	0.001	0.21	0.59	1.96	0.77	0.27	0.00	0

Table 21. The Composition and CSF Value of HD Series Steels[22].

Name	C	S	P	Si	Mn	CSF
HD1	0.10	0.046	0.033	0.23	0.87	9
HD2	0.16	0.044	0.033	0.26	1.69	0
HD3	0.14	0.044	0.034	0.19	0.89	1
HD4	0.14	0.017	0.034	0.27	0.90	0
HD5	0.20	0.019	0.038	0.20	0.48	24
HD6	0.30	0.019	0.031	0.24	1.16	38
HD7	0.15	0.040	0.025	0.20	1.34	0
HD8	0.22	0.047	0.032	0.23	1.80	50
HD9	0.24	0.043	0.031	0.22	1.40	53
HD10	0.20	0.016	0.029	0.20	0.96	6
HD11	0.30	0.046	0.037	0.22	1.60	71
HD12	0.21	0.046	0.033	0.23	1.35	53
HD13	0.21	0.020	0.034	0.28	0.43	50
HD14	0.13	0.062	0.030	0.25	1.11	1
HD15	0.08	0.017	0.032	0.19	0.42	42
HD16	0.10	0.042	0.028	0.19	0.87	5
HD17	0.15	0.027	0.033	0.19	0.43	1
HD18	0.11	0.040	0.024	0.18	0.31	17
HD19	0.19	0.022	0.028	0.17	0.88	0
HD20	0.15	0.040	0.027	0.18	0.44	11
HD21	0.20	0.022	0.027	0.19	0.87	1
HD22	0.11	0.023	0.027	0.12	0.98	16

Table 22. The Composition and CSF Values of C Series Steels[27]

Series No	Steel Type	C	S	P	Si	Mn	Ni	Cr	Mo	V	Other	CSF
C1	1%Cr-Mo	0.30	0.009	0.016	0.29	0.49	0.18	0.96	0.19	0.00	-	19
C2	1%Cr-Mo	0.30	0.011	0.015	0.24	0.44	0.13	0.90	0.24	0.00	-	21
C3	1%Cr-Mo	0.32	0.015	0.030	0.19	0.41	0.09	0.85	0.25	0.00	-	37
C4	1%Cr-Mo	0.32	0.016	0.023	0.14	0.51	0.16	0.95	0.20	0.00	-	37
C5	1%Cr-Mo	0.32	0.013	0.031	0.19	0.41	0.09	0.82	0.25	0.00	-	41
C6	1%Cr-Mo	0.31	0.014	0.023	0.29	0.49	0.09	0.88	0.22	0.00	-	34
C7	1%Cr-Mo	0.29	0.006	0.013	0.23	0.51	0.10	1.02	0.17	0.00	-	18
C8	1%Cr-Mo	0.30	0.001	0.002	0.20	0.52	0.17	0.99	0.20	0.00	-	0
C9	1%Cr-Mo	0.37	0.001	0.002	0.20	0.52	0.17	0.98	0.21	0.00	-	0
C10	1%Cr-Mo	0.44	0.001	0.002	0.20	0.52	0.17	0.99	0.21	0.00	-	0
C11	1%Cr-Mo	0.29	0.019	0.031	0.22	0.46	0.08	0.95	0.23	0.00	-	39
C12	1%Cr-Mo	0.30	0.007	0.013	0.26	0.56	0.11	0.99	0.21	0.00	-	24
C13	1%Cr-Mo	0.30	0.003	0.010	0.29	0.53	0.12	1.02	0.16	0.00	-	8
C14	1%Cr-Mo	0.31	0.006	0.014	0.38	0.70	0.00	1.19	0.26	0.00	-	26
C15	3%Cr-Mo-V	0.38	0.005	0.014	0.24	0.72	0.14	3.08	0.97	0.20	-	23
C16	3%Cr-Mo-V	0.35	0.005	0.018	0.31	0.60	0.14	2.88	0.94	0.22	-	16
C17	3%Cr-Mo-V	0.39	0.014	0.007	0.03	0.27	0.10	2.93	0.86	0.22	-	20
C18	3%Cr-Mo-V	0.32	0.045	0.015	0.04	0.86	0.28	2.99	0.84	0.21	-	33
C19	3%Cr-Mo-V	0.37	0.029	0.012	0.24	0.47	0.13	2.93	0.85	0.21	-	28
C20	3%Cr-Mo-V	0.38	0.020	0.016	0.11	0.68	0.08	2.89	0.86	0.20	-	21
C21	3%Cr-Mo-V	0.42	0.009	0.010	0.20	0.57	0.12	3.31	1.06	0.19	-	21
C22	5%Cr-Mo-V	0.37	0.011	0.016	1.11	0.41	0.21	4.84	1.41	0.56	-	19
C23	5%Cr-Mo-V	0.40	0.009	0.012	0.88	0.52	0.34	5.13	1.29	1.15	-	8
C24	5%Cr-Mo-V	0.44	0.008	0.010	0.92	0.34	0.11	5.31	1.16	0.44	-	11
C25	2%Ni	0.38	0.010	0.018	0.15	0.63	1.82	0.82	0.23	0.00	-	40
C26	2%Ni	0.46	0.009	0.011	0.11	0.41	2.10	0.83	0.46	0.26	0.55Cu	32
C27	2%Ni	0.53	0.009	0.011	0.19	0.48	2.15	0.90	0.87	0.25	0.43Cu	25

Table 22. Continued

Series No	Steel Type	C	S	P	Si	Mn	Ni	Cr	Mo	V	Other	CSF
C28	2%Ni	0.35	0.012	0.017	0.24	0.72	1.70	0.97	0.29	0.00	0.12Cu	44
C29	2%Ni	0.73	0.009	0.010	0.00	0.42	2.21	0.00	0.00	0.00	-	36
C30	2%Ni	0.44	0.009	0.023	0.28	0.63	1.82	1.31	0.93	0.20	-	39
C31	2%Ni	0.42	0.009	0.020	0.28	0.51	1.83	1.28	0.96	0.20	-	42
C32	2%Si-2%Cu	0.24	0.008	0.015	1.53	0.40	0.00	0.04	1.44	0.33	1.49Cu	17
C33	2%Si-2%Cu	0.37	0.007	0.015	1.86	0.49	0.00	0.00	0.85	0.25	2.12Cu	19
C34	2%Si-2%Cu	0.34	0.008	0.005	1.91	0.93	0.01	0.03	0.75	0.33	1.75Cu	29
C35	2%Si-2%Cu	0.29	0.009	0.009	2.12	0.48	0.01	0.04	0.84	0.35	1.76Cu	20
C36	2%Si-2%Cu	0.35	0.011	0.009	2.12	0.48	0.01	0.02	0.80	0.27	1.75Cu	27
C37	2%Si-2%Cu	0.32	0.008	0.005	2.10	0.42	0.01	0.02	0.80	0.36	1.74Cu	8
C38	2%Si-2%Cu	0.23	0.012	0.008	1.89	1.36	0.01	0.05	1.58	0.66	1.73Cu	19
C39	2%Si-2%Cu	0.40	0.008	0.014	1.58	0.54	0.01	0.04	0.77	0.25	1.94Cu	25
C40	2%Si-2%Cu	0.34	0.019	0.006	1.87	1.04	0.03	0.04	0.77	0.35	1.80Cu	29
C41	2%Si-2%Cu	0.38	0.018	0.007	1.62	1.00	0.04	0.03	0.73	0.30	1.05Cu 2.10Co	30
C42	2%Si-2%Cu	0.33	0.014	0.004	1.74	1.49	0.03	0.03	1.74	0.76	1.80Cu	23
C43	2%Si-2%Cu	0.40	0.005	0.006	1.86	1.30	0.00	0.00	0.93	0.56	1.59Cu	25
C44	2%Cr	0.39	0.007	0.003	1.43	0.92	0.24	2.05	0.47	0.06	-	11
C45	2%Cr	0.46	0.004	0.017	1.59	0.68	0.00	2.06	0.58	0.07	-	28
C46	2%Cr	0.42	0.009	0.016	1.16	0.68	0.09	1.99	0.54	0.06	-	24
C47	12%Cr	0.10	0.008	0.013	0.27	0.84	1.09	11.6	0.57	0.22	-	19
C48	12%Cr	0.09	0.002	0.011	0.54	0.94	0.00	10.2	0.80	0.23	5.94Co	32
C49	12%Cr	0.10	0.011	0.011	0.31	0.79	2.32	11.7	1.38	0.44	-	23
C50	12%Cr	0.14	0.009	0.012	0.33	0.83	0.61	10.9	0.82	0.26	-	9
C51	½Cr-Mo	0.15	0.004	0.007	0.29	0.52	0.15	0.42	1.13	0.29	-	1
C52	5%Cr-Mo-V	0.45	0.007	0.011	0.30	0.63	0.15	5.10	2.12	0.43	-	13
C53	3%Cr-Mo-V	0.37	0.008	0.009	0.35	0.63	0.16	3.05	2.00	0.39	-	8
C54	Cr-Mo-W-V	0.81	0.004	0.014	0.12	1.25	0.17	4.06	5.06	1.96	6.68W	0
C55	3%Cr-Mo	0.63	0.013	0.004	0.08	0.55	0.01	2.76	0.88	0.28	2.01Co	28

Table 23. Composition and CSF Data for MW Series Steels[3,70]

Series No	Steel Type	C	S	P	Si	Mn	Ni	Cr	Mo	V	O	CSF
MW1	RS120	0.35	0.012	0.023	0.30	0.53	0.10	0.93	0.24	0.00	0.005	35
MW2	RS130	0.32	0.007	0.007	0.27	0.49	0.08	1.00	0.19	0.00	0.006	14
MW3	RS140	0.46	0.011	0.018	0.27	0.68	0.17	3.30	1.02	0.25	0.006	23
MW4	ASTM A387B	0.08	0.010	0.008	0.30	0.50	0.01	0.91	0.37	0.00	0.011	0
MW5	ASTM A387B	0.08	0.036	0.031	0.36	0.51	0.01	0.88	0.36	0.00	0.008	38
MW6	ASTM A387B	0.13	0.035	0.025	0.27	0.59	0.13	0.92	0.46	0.00	0.015	5
MW7	ASTM A387B	0.08	0.029	0.035	0.28	0.54	0.24	1.09	0.49	0.00	0.005	37
MW8	EN24	0.35	0.010	0.010	0.53	0.63	1.37	1.07	0.24	0.00	0.006	36
MW9	EN24	0.30	0.036	0.008	0.58	0.64	1.38	1.08	0.30	0.00	0.004	55
MW10	EN24	0.36	0.041	0.014	0.32	0.70	1.54	1.23	0.24	0.00	0.004	49
MW11	EN24	0.35	0.026	0.013	0.29	0.62	1.36	1.09	0.26	0.00	0.003	53
MW12	SAE4130	0.18	0.010	0.008	0.34	0.70	0.02	0.99	0.21	0.00	0.009	0
MW13	SAE4130	0.18	0.034	0.037	0.37	0.69	0.01	0.99	0.22	0.00	0.011	20
MW14	SAE4130	0.19	0.010	0.049	0.06	0.85	0.01	0.92	0.27	0.00	0.007	23
MW15	SAE4130	0.21	0.033	0.010	0.34	0.70	0.01	1.02	0.23	0.00	0.011	30
MW16	SAE4130	0.22	0.026	0.028	0.24	0.67	0.16	0.93	0.20	0.00	0.004	37
MW17	SAE4130	0.28	0.025	0.030	0.17	0.67	0.13	0.92	0.19	0.00	0.005	42

Table 24. Composition and CSF Data for MH Series Steels[70]

Series No	Steel Type	C	S	P	Si	Mn	Ni	Cr	Mo	V	O	CSF
MH1	1%Cr-Mo	0.31	0.014	0.030	0.21	0.40	0.08	0.85	0.24	0.00	0.004	37
MH2	1%Cr-Mo	0.32	0.019	0.022	0.16	0.48	0.13	0.93	0.20	0.00	0.005	37
MH3	1%Cr-Mo	0.31	0.016	0.032	0.22	0.41	0.08	0.87	0.25	0.00	0.005	41
MH4	1%Cr-Mo	0.31	0.014	0.028	0.31	0.48	0.09	0.92	0.23	0.00	0.005	34
MH5	3%Cr-Mo-V	0.35	0.010	0.016	0.30	0.70	0.12	3.15	1.00	0.23	0.004	23
MH6	5%Cr-Mo-V	0.40	0.019	0.019	1.15	0.44	0.20	4.76	1.60	0.60	0.006	19
MH7	3%Cr-Mo-V	0.37	0.013	0.014	0.42	0.63	0.14	3.20	2.10	0.45	0.006	8
MH8	1%Cr-Mo	0.26	0.018	0.024	0.22	0.45	0.06	0.90	0.18	0.00	0.005	39
MH9	2%Si-Mo-V	0.40	0.008	0.003	1.85	1.41	0.25	0.02	0.93	0.55	0.003	25
MH10	2%Si-Cr-Mo	0.44	0.006	0.002	1.55	0.72	0.24	2.10	0.54	0.06	0.002	23
MH11	3%Cr-Mo-V	0.47	0.009	0.006	0.49	0.70	0.17	3.30	1.00	0.22	0.003	29
MH12	3%Cr-Mo-V	0.47	0.009	0.006	0.49	0.82	0.17	3.30	1.00	0.22	0.004	28
MH13	3%Cr-Mo-V	0.59	0.012	0.007	1.02	0.80	0.14	3.35	1.03	0.23	0.003	42
MH14	3%Cr-Mo-V	0.28	0.007	0.011	0.34	0.61	0.00	3.25	0.99	0.21	0.002	29
MH15	3%Cr-Mo-V	0.41	0.010	0.033	0.29	0.65	0.00	3.35	1.05	0.25	0.003	33
MH16	3%Cr-Mo-V	0.37	0.009	0.003	0.29	0.63	0.00	3.20	1.00	0.22	0.003	14
MH17	3%Cr-Mo-V	0.38	0.010	0.008	0.30	0.67	0.00	3.10	1.02	0.23	0.003	20
MH18	3%Cr-Mo-V	0.39	0.010	0.014	0.26	0.61	0.03	3.35	1.01	0.23	0.005	23
MH19	3%Cr-Mo-V	0.35	0.010	0.023	0.31	0.65	0.00	3.35	1.18	0.23	0.004	27
MH20	3%Cr-Mo-V	0.37	0.010	0.010	0.31	0.68	0.00	3.35	0.95	0.22	0.005	19
MH21	3%Cr-Mo-V	0.38	0.009	0.024	0.27	0.63	0.00	3.25	1.04	0.23	0.003	33
MH22	3%Cr-Mo-V	0.38	0.010	0.011	0.29	0.61	0.00	3.30	1.02	0.23	0.004	21
MH23	3%Cr-Mo-V	0.37	0.010	0.020	0.33	0.67	0.00	3.35	0.98	0.24	0.006	23
MH24	3%Cr-Mo-V	0.37	0.010	0.003	0.30	0.65	0.00	3.20	1.00	0.24	0.006	17
MH25	1%Cr-Mo	0.31	0.012	0.014	0.30	0.50	0.17	1.00	0.20	0.00	0.006	19

Table 25. Composition and Trans-Varestraint Test Data for GBA Series Steels.
taken from JG Garland and N Bailey[60]

Series No	C	S	P	Si	Mn	Al	UCS
GBA1	0.11	0.007	0.006	0.04	0.50	0.004	20
GBA2	0.25	0.007	0.006	0.04	0.50	0.004	35
GBA3	0.11	0.046	0.005	0.04	0.49	0.005	34
GBA4	0.25	0.052	0.005	0.06	0.51	0.007	36
GBA5	0.11	0.007	0.046	0.04	0.51	0.007	22
GBA6	0.27	0.008	0.044	0.05	0.50	0.004	34
GBA7	0.12	0.050	0.046	0.05	0.50	0.007	29
GBA8	0.25	0.047	0.046	0.05	0.50	0.004	35
GBA9	0.12	0.006	0.005	0.06	1.50	0.008	10
GBA10	0.27	0.009	0.005	0.06	1.51	0.007	30
GBA11	0.13	0.044	0.005	0.06	1.48	0.006	28
GBA12	0.26	0.043	0.004	0.04	1.49	0.006	30
GBA13	0.12	0.010	0.051	0.05	1.52	0.007	28
GBA14	0.27	0.009	0.047	0.04	1.44	0.005	33
GBA15	0.12	0.047	0.046	0.05	1.47	0.005	29
GBA16	0.27	0.053	0.048	0.06	1.52	0.008	34
GBA17	0.21	0.032	0.028	0.06	1.00	0.010	31

Table 26. Composition and Trans-Varestraint Test Data for GBB Series Steels[66]

Series No	C	S	P	Si	Mn	Al	UCS
GBB1	0.11	0.006	0.005	0.03	0.46	0.004	18
GBB2	0.27	0.009	0.004	0.06	1.51	0.007	33
GBB3	0.12	0.006	0.004	0.65	0.52	0.044	1
GBB4	0.27	0.008	0.004	0.62	1.54	0.039	30
GBB5	0.11	0.007	0.046	0.06	1.53	0.041	20
GBB6	0.24	0.008	0.046	0.04	0.53	0.039	33
GBB7	0.11	0.008	0.048	0.65	1.50	0.006	12
GBB8	0.26	0.008	0.047	0.64	0.51	0.007	30
GBB9	0.13	0.044	0.005	0.06	1.48	0.007	27
GBB10	0.25	0.052	0.004	0.06	0.51	0.007	35
GBB11	0.12	0.045	0.004	0.64	1.48	0.040	2
GBB12	0.26	0.048	0.005	0.63	0.50	0.041	38
GBB13	0.11	0.047	0.046	0.04	0.51	0.045	19
GBB14	0.27	0.051	0.046	0.06	1.50	0.039	38
GBB15	0.12	0.048	0.045	0.64	0.52	0.006	26
GBB16	0.27	0.051	0.046	0.64	1.42	0.009	36
GBB17	0.11	0.009	0.004	0.05	0.51	0.040	12
GBB18	0.27	0.008	0.004	0.06	1.48	0.046	30
GBB19	0.11	0.007	0.004	0.64	0.51	0.006	16
GBB20	0.26	0.012	0.004	0.66	1.55	0.006	35
GBB21	0.11	0.008	0.046	0.05	1.46	0.007	14
GBB22	0.25	0.007	0.044	0.04	0.54	0.005	37
GBB23	0.11	0.008	0.046	0.64	1.50	0.033	12
GBB24	0.27	0.008	0.046	0.64	0.52	0.042	36
GBB25	0.12	0.049	0.005	0.06	1.51	0.041	21
GBB26	0.27	0.045	0.005	0.04	0.51	0.040	35
GBB27	0.11	0.049	0.004	0.67	1.50	0.006	14
GBB28	0.26	0.049	0.005	0.64	0.52	0.006	39
GBB29	0.11	0.051	0.044	0.03	0.49	0.006	21
GBB30	0.26	0.053	0.047	0.05	1.40	0.006	39
GBB31	0.13	0.052	0.047	0.64	0.53	0.039	26
GBB32	0.26	0.050	0.047	0.68	1.46	0.039	37

Table 27. The Statistics of Composition and Crack factor(CF) for 131
FW Series Steels.

Variable Name	Mean	Minimum	Maximum	Standard Deviation
CF	12	0	88	20
S	0.022	0.005	0.065	0.010
P	0.018	0.006	0.102	0.011
Si	0.25	0.00	0.54	0.10
Mn	0.59	0.00	1.40	0.24
Ni	0.00	0.00	0.00	0.00
Cr	0.88	0.00	1.22	0.37
Mo	0.26	0.00	0.46	0.11
Al	0.009	0.005	0.230	0.022
C x S	0.0061	0.0012	0.0195	0.0032
C x P	0.0049	0.0010	0.0275	0.0030

Table 28, The Statistics of Composition and CSF Values for MA+MB+MC+MD
Series(47 Steels).

Variable Name	Mean	Minimum	Maximum	Standard Deviation
CSF	33	0	70	26
C	0.21	0.02	0.50	0.13
S	0.040	0.007	0.180	0.046
P	0.014	0.005	0.058	0.013
Si	0.19	0.00	0.60	0.14
Mn	0.59	0.02	1.48	0.33
Ni	0.36	0.00	5.13	0.90
Cr	0.76	0.02	4.88	0.77
Mo	0.17	0.00	0.55	0.15
O	0.015	0.004	0.066	0.017

Variables at 10% Sig Level	Regression Coefficient	Standard Error	t Statistics
S	278	44	6.30
C x S	3602	439	8.20
C x P	2077	533	3.90
Regression Equation	$P(CSF, MA+MB+MC+MD) = 278S + 3602C.S + 2077C.P - 5$		

Table 29. Statistical Data for 3%Cr-Mo-V Steels(44 Specimens)

Variable Name	Mean	Minimum	Maximum	Standard Deviation
CSF	24	8	42	7
C	0.40	0.28	0.59	0.06
S	0.011	0.004	0.045	0.007
P	0.012	0.001	0.033	0.007
Si	0.33	0.03	1.02	0.10
Mn	0.67	0.27	0.86	0.10
Ni	0.08	0.00	0.28	0.008
Cr	3.16	2.88	3.35	0.15
Mo	1.03	0.84	2.10	0.23

Variables at 10% Sig Level	Regression Coefficient	Standard Error	t Statistics
S	175	95	1.83
P	523	89	5.90
Si	29	4	7.78
Ni	17	9	2.00
Mo	-17	3	6.48

Table 30. Statistical Data for all Huxley Cracking Test Results(217 Steels).

Variable Name	Mean	Minimum	Maximum	Standard Deviation
CSF	26	0	71	18
C	0.31	0.02	0.81	0.14
S	0.020	0.001	0.180	0.026
P	0.015	0.001	0.058	0.011
Si	0.41	0.00	2.12	0.46
Mn	0.65	0.02	1.80	0.28
Ni	0.29	0.00	5.13	0.65
Cr	1.62	0.00	11.70	1.88
Mo	0.57	0.00	5.06	0.59
C x S	0.0046	0.0018	0.0180	0.0032
C x P	0.0044	0.0001	0.0179	0.0031

Table 31. Statistics for the 272 Steels in the Mixed Series.

Variable Name	Mean	Minimum	Maximum	Standard Deviation
CF or CSF	52	0	88	50
C	0.31	0.02	0.81	0.11
S	0.019	0.001	0.180	0.023
P	0.015	0.001	0.102	0.011
Si	0.38	0.00	2.12	0.43
Mn	0.60	0.00	1.49	0.26
Cr	1.52	0.00	11.70	1.69
Mo	0.52	0.00	5.06	0.53

Table 32. Correlation between CSF and Crack Predictors based on 203 Observations in Huxley Cracking Test.

Compositional Factor or Crack Predictor	Reference	Correlation with CSF
Carbon		0.12
CE(Ostrovskaya, 1)	Equation 2.3	0.12
CE(Ostrovskaya, 2)	Equation 2.4	0.05
CE(Ostrovskaya, 3)	Equation 2.5	0.08
HCS(Wilkinson)	Equation 2.10	0.33
P(CSF, Cottrell)	Equation 2.11	0.51
P(CSF, MW, 1)	Equation 2.13	0.54
P(CSF, MW, 2)	Equation 2.14	0.52
C x S		0.58
C x P		0.32
C(S+0.5P)		0.63
Sulphur		0.42
Phosphorus		0.18
Silicon		-0.07
Manganese		-0.02
Chromium		0.12
Molybdenum		-0.22
Oxygen		0.04

Table 33. Comparison of CSF Values in Open Air and Closed Box (argon purged) Welding.

Series No	Steel Type	Observed CSF by Open Air Welding	Observed CSF by Closed Box Welding
MA1	SAE4130	17	16
MA2	SAE4130	12	8
MA3	SAE4130	62	59
MA4	SAE4130	57	54
MA5	SAE4130	1	0
MA6	SAE4130	0	0
MA7	SAE4130	62	60
MA8	SAE4130	60	63
MA9	SAE4130	43	37
MA10	SAE4130	53	50

Table 34. Comparison of CSF Values in Open Air and Closed Box(pre-evacuated and filled with argon) Welding.

Series No	Steel Type	Observed CSF by Open Air Welding	Observed CSF by Closed Box Welding
MC1	Fe-Mn-S-O	6	8
MC2	Fe-Mn-S-O	0	0
MC3	Fe-Mn-S-O	64	57
MC4	Fe-Mn-S-O	66	62
MC5	Fe-Mn-S-O	0	0
MC6	Fe-Mn-S-O	0	0
MC7	Fe-Mn-S-O	59	63
MC8	Fe-Mn-S-O	70	65
MC9	Fe-Mn-S-O	0	0
MC10	Fe-Mn-S-O	3	5
MC11	Fe-Mn-S-O	9	9
MC12	Fe-Mn-S-O	43	39
MD1	ASTM A387B	13	15
MD2	ASTM A387B	9	8
MD3	ASTM A387B	43	39
MD4	ASTM A387B	0	0
MD13	HY80	30	29
MD14	EN353	61	55
MD16	Hypress 23	21	17
MD17	Creusabro 32	20	11
MD18	EN5	68	65
MD19	EN19	53	60

Table 35. Huxley Cracking Test Results with Pure Argon, and 2% Oxygen-Argon Shielding Gas.

Steel No	CSF Value Test with Pure Argon Arc Current 95A Arc Voltage 11V	CSF Value Test with 2% O_2 + Argon Arc Current 85A Arc Voltage 12V
MA1	17	0
MA2	12	0
MA3	62	55
MA4	57	46
MA5	1	0
MA6	0	0
MA7	62	68
MA8	60	53
MA9	43	39
MA10	53	37
MD13 (HY80)	30	29
MD14 (EN353)	61	60

Table 36. Results of Oxygen Analysis for the Weld and Parent Metals.

Steel No	Type of Steel	Parent Metal Oxygen%	Weld Metal Oxygen % (Open Air Welding)	Weld Metal Oxygen % (Closed Box Welding)
MA1	SAE4130	0.010	0.012	0.009
MA2	SAE4130	0.004	0.009	0.004
MA3	SAE4130	0.006	0.008	0.005
MA4	SAE4130	0.007	0.011	0.007
MA5	SAE4130	0.008	0.010	0.006
MA6	SAE4130	0.016	0.018	0.013
MA7	SAE4130	0.011	0.015	0.010
MA8	SAE4130	0.013	0.017	0.014
MA9	SAE4130	0.010	0.011	0.009
MA10	SAE4130	0.010	0.012	0.007
MB1	SAE4130	0.006	0.014	0.006
MB2	SAE4130	0.006	0.013	0.007
MB3	SAE4130	0.006	0.008	0.007
MB4	SAE4130	0.007	0.023	0.011
MB5	SAE4130	0.010	0.014	0.007
MB6	SAE4130	0.005	0.012	0.005
MC1	Fe-Mn-S-O	0.011	0.022	0.006
MC2	Fe-Mn-S-O	0.005	0.011	0.005
MC3	Fe-Mn-S-O	0.005	0.015	0.005
MC4	Fe-Mn-S-O	0.017	0.026	0.015
MC5	Fe-Mn-S-O	0.063	0.064	0.062
MC6	Fe-Mn-S-O	0.064	0.064	0.057
MC7	Fe-Mn-S-O	0.066	0.064	0.061
MC8	Fe-Mn-S-O	0.064	0.064	0.062
MD1	ASTM A387B	0.015	0.025	0.010
MD2	ASTM A387B	0.014	0.022	0.009
MD3	ASTM A387B	0.009	0.010	0.006
MD4	ASTM A387B	0.012	0.013	0.010
MD5	EN24	0.005	0.008	0.007
MD6	EN24	0.005	0.008	0.005
MD7	EN24	0.007	0.011	0.008
MD8	EN24	0.006	0.012	0.005

Table 37. Results of Oxygen Analysis for Parent and Weld Metal Welded with Pure Argon and with 2% Oxygen-Argon Mixture.

Series No	Parent Metal Oxygen %	Weld Metal Oxygen % (Open Air Pure Argon)	Weld Metal Oxygen % (2% Oxygen-Argon Gas)
MA1	0.010	0.012	0.025
MA2	0.004	0.009	0.023
MA3	0.006	0.008	0.041
MA4	0.007	0.011	0.029
MA5	0.008	0.010	0.057
MA6	0.016	0.018	0.035
MA7	0.011	0.015	0.037
MA8	0.013	0.017	0.072
MA9	0.010	0.011	0.026
MA10	0.010	0.012	0.019
MD13	0.010	0.023	0.036
MD14	0.010	0.021	0.051

Table 38. Results of carbon analysis for the parent and weld metals.

Series No	Parent Metal Carbon %	Weld Metal Carbon% Welding with Pure Argon Shielding Gas	Weld Metal Carbon % Welding with 2% Oxygen-Argon Mixture
MA1	0.29	0.28	0.24
MA2	0.33	0.29	0.23
MA3	0.29	0.30	0.26
MA4	0.30	0.26	0.24
MA5	0.27	0.28	0.25
MA6	0.32	0.30	0.27
MA7	0.29	0.27	0.25
MA8	0.28	0.26	0.21
MA9	0.28	0.26	0.24
MA10	0.26	0.25	0.17
MD13	0.15	0.16	0.14
MD14	0.14	0.15	0.12

Table 39. The Inclusion Counts for the MA Series Steels(SAE4130).

Series No	Mn%	S%	O%	(S% + O%)	Mn/S	CSF	Inclusion Count per Unit Area
MA1	0.30	0.011	0.010	0.021	27.3	17	80
MA2	0.72	0.009	0.004	0.013	80.0	12	90
MA3	0.23	0.042	0.006	0.048	5.5	62	150
MA4	0.80	0.041	0.007	0.048	19.5	57	180
MA5	0.19	0.007	0.008	0.015	27.1	1	110
MA6	0.61	0.008	0.016	0.024	76.3	0	120
MA7	0.17	0.032	0.011	0.043	5.3	62	200
MA8	0.59	0.032	0.013	0.045	18.4	60	160
MA9	0.67	0.028	0.010	0.038	23.9	43	130
MA10	0.68	0.039	0.010	0.049	17.4	53	160

Table 40. The Influence of Carbon Content on Sulphur Coefficient for CSF.

Steel Series	Number of Samples	Mean of C%	Mean of S%	Coefficient of Sulphur
MA	10	0.30	0.025	1681
MB	6	0.33	0.023	1060
MC	12	0.04	0.086	431
MD	19	0.22	0.025	1035
MA+MB+MD	35	0.26	0.025	1320
MC+HD	44	0.13	0.052	453
MA+MB+MC+MD	47	0.21	0.040	756
C	55	0.36	0.010	1503
MW+MH	42	0.32	0.016	833
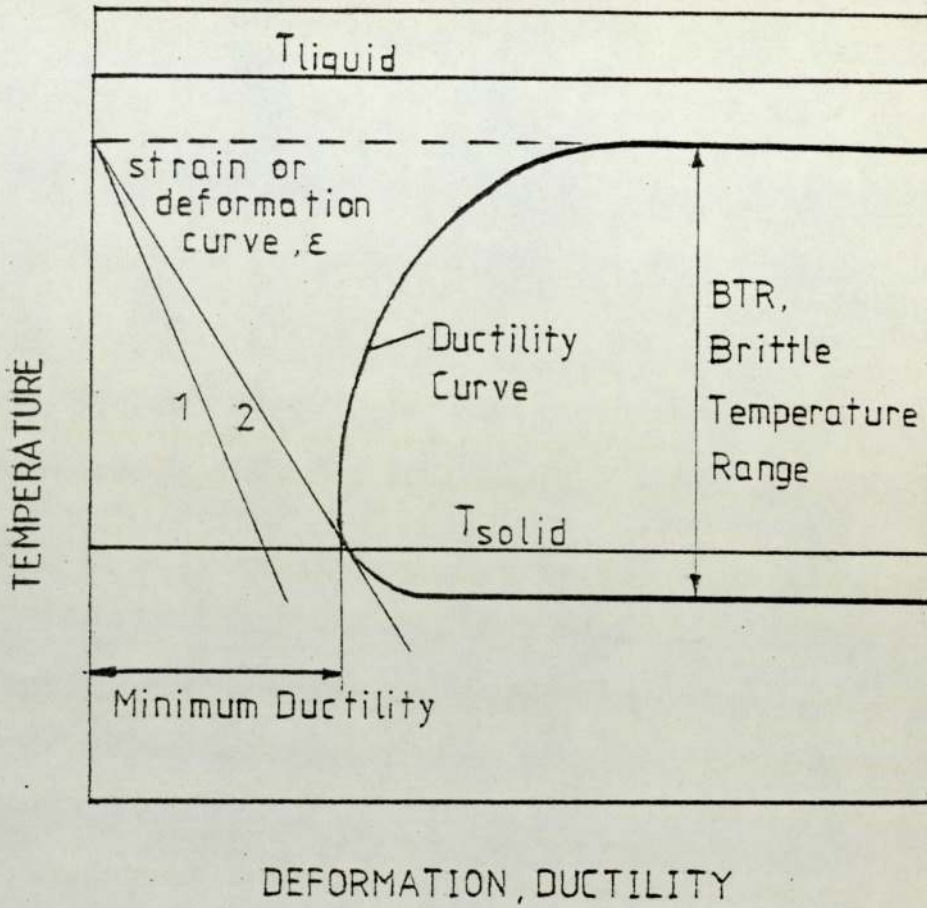
Fig 1. Schematic presentation of strain development and ductility curve of an alloy under cooling after welding (according to NN Prokhorov[14]).
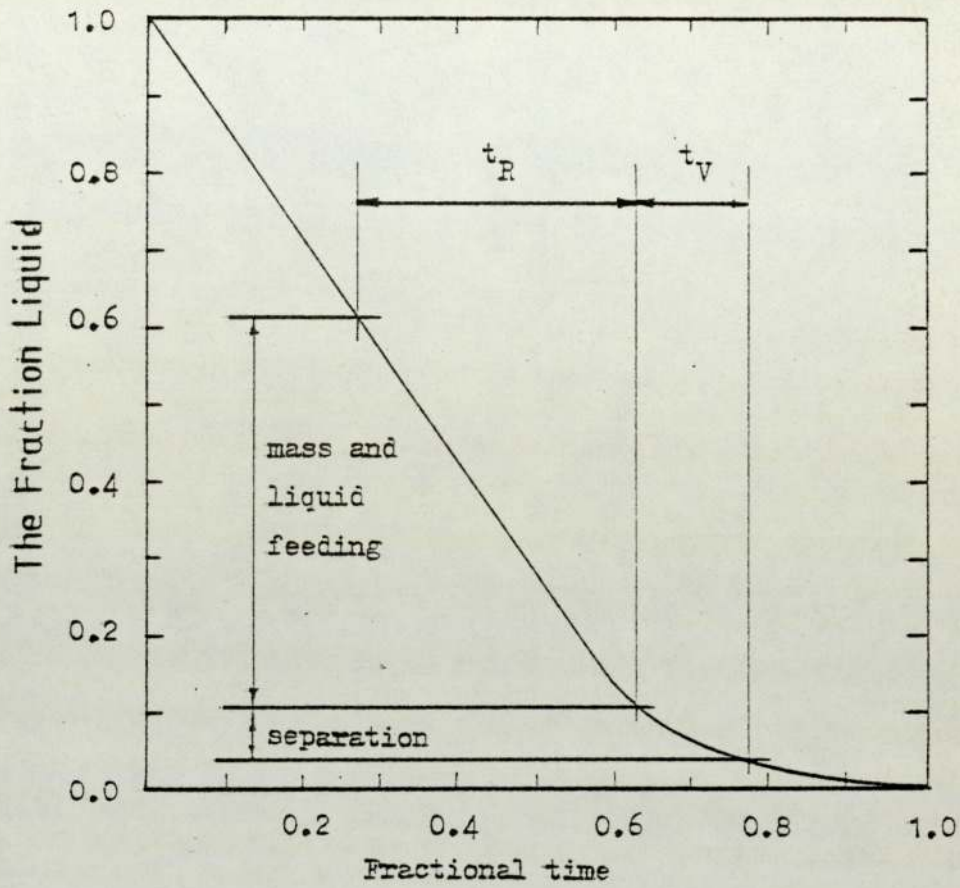
Fig 2. The method of determination of time of stress relaxation, t_R and the vulnerable time, t_V from a plot of the variation of liquid fraction with fractional time(according to TW Clyne[17]).
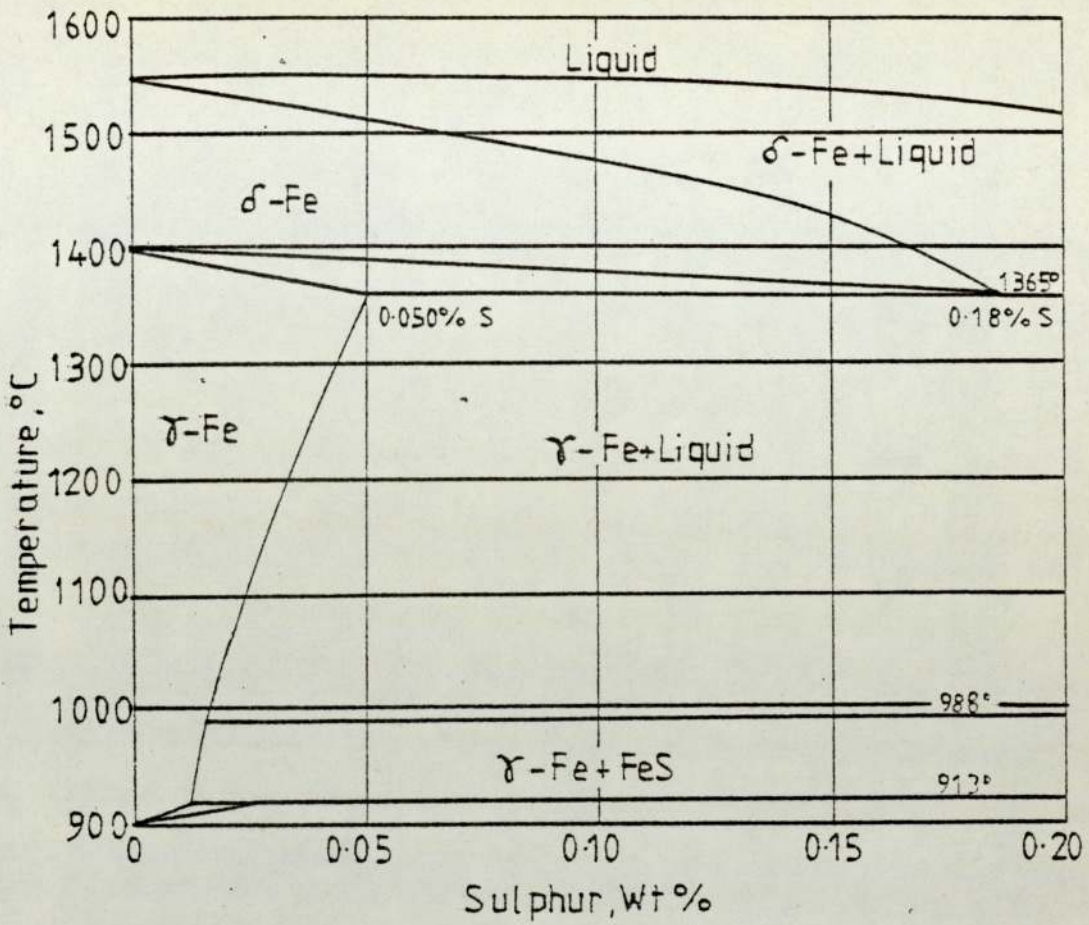
Fig 3. Iron-rich corner of the Fe-S binary phase diagram (according to ET Turkdogan et al[34]).
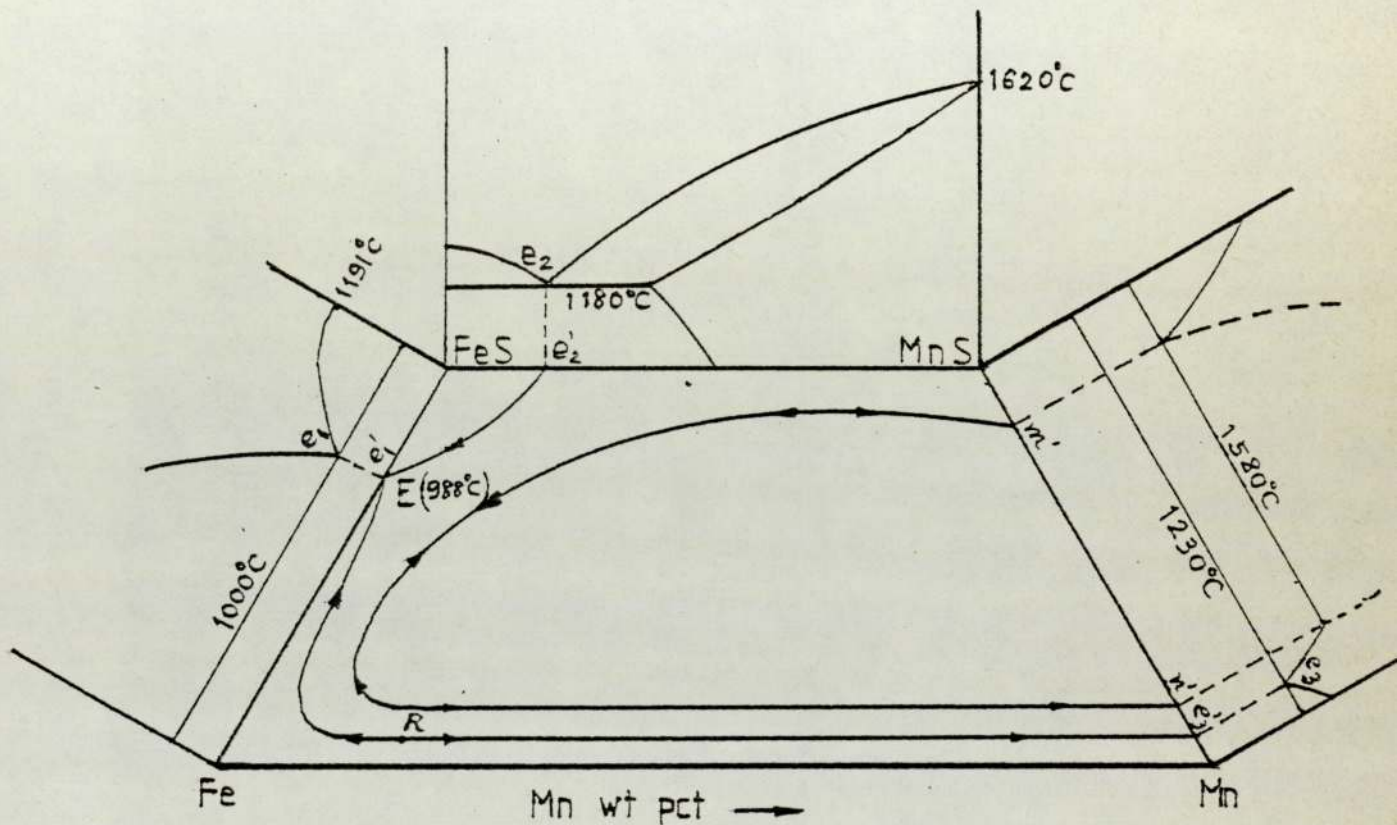
Fig 4. Qualitative representation of the Fe-Mn-S phase diagram according to R Vogel [36]. $e_1^!E$ is the Fe-FeS eutectic curve, $e_2^!E$ the FeS-(Mn,Fe)S eutectic curve and $e_3^!E$ the Fe-(Mn,Fe)S eutectic curve.
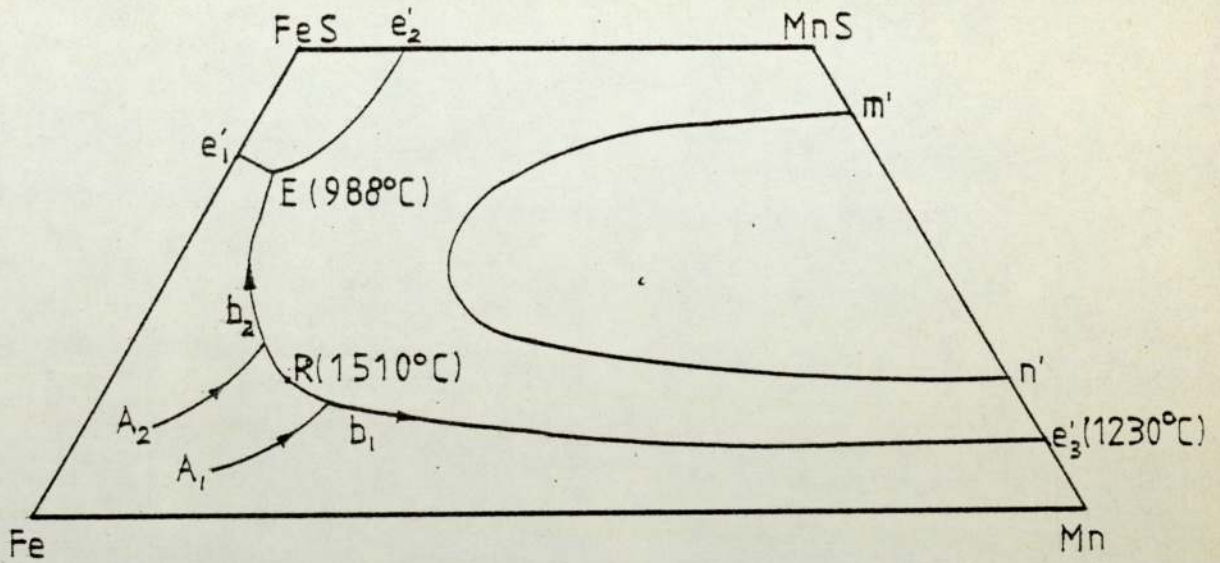
Fig 5. Two solidification paths in the qualitative Fe-Mn-S diagram.
First case: alloy A_1 solidifies following the path of $A_1 b_1 e_3'$; second
case: alloy A_2 solidifies following the path of $A_2 b_2 E$.
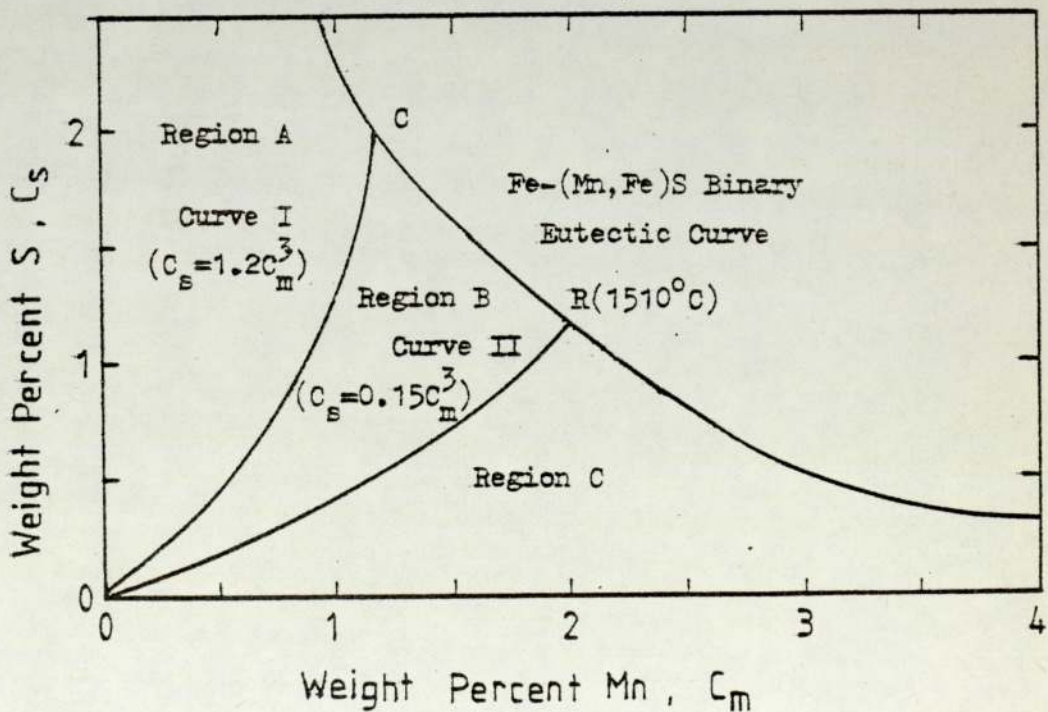
Fig 6. Illustration of three regions which correspond to the changes
in sulphide structure and solidification crack susceptibility.
(H Nakagawa et al [39]).
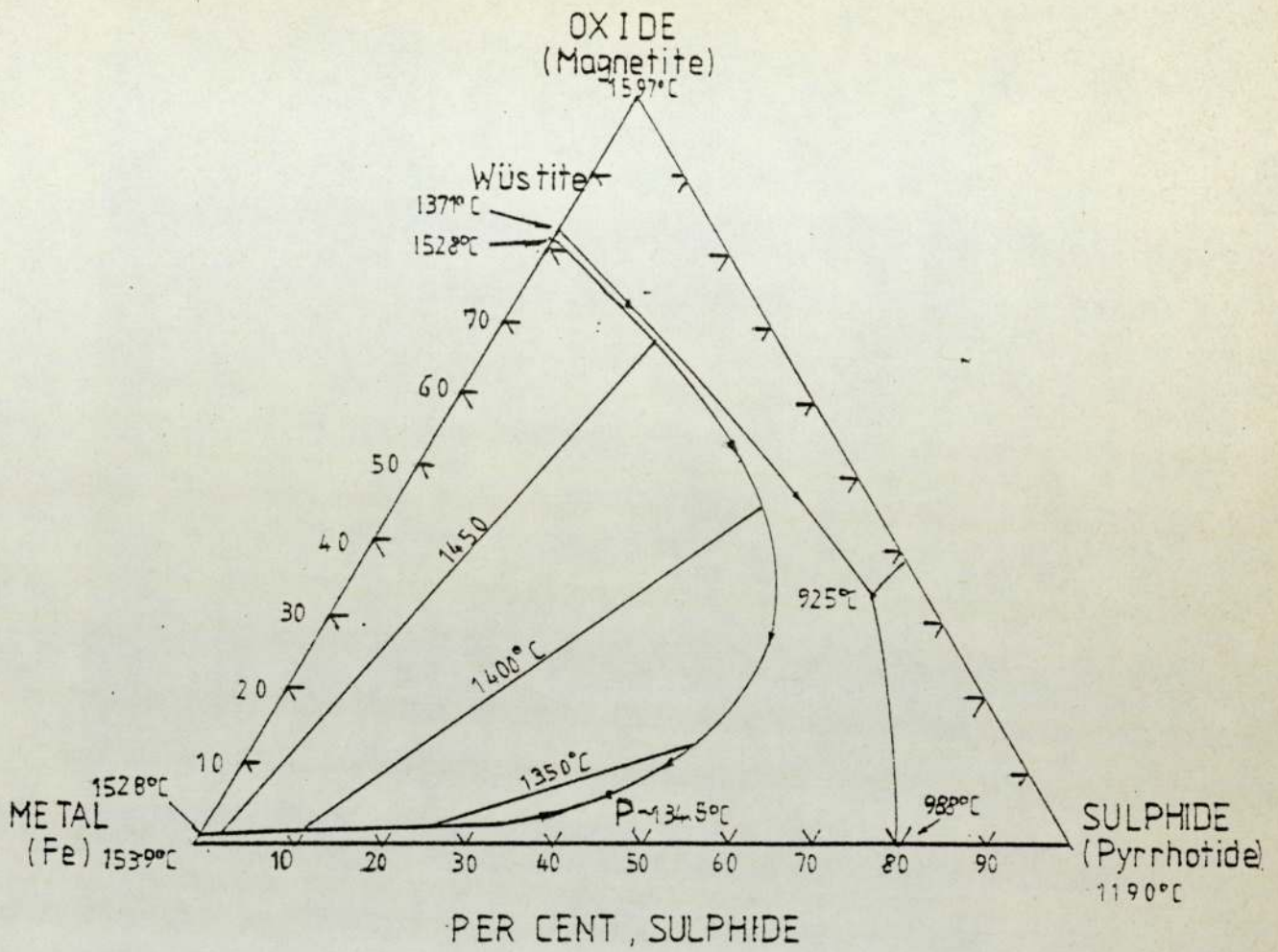
Fig 7. Fe-O-S phase diagram according to DC Hilty and W Crafts[40].

OXIDE

I

Oxide rich liquid phase
follows the path of dghE.

d

h

g

E

p

t

f

A

METAL

SULPHIDE
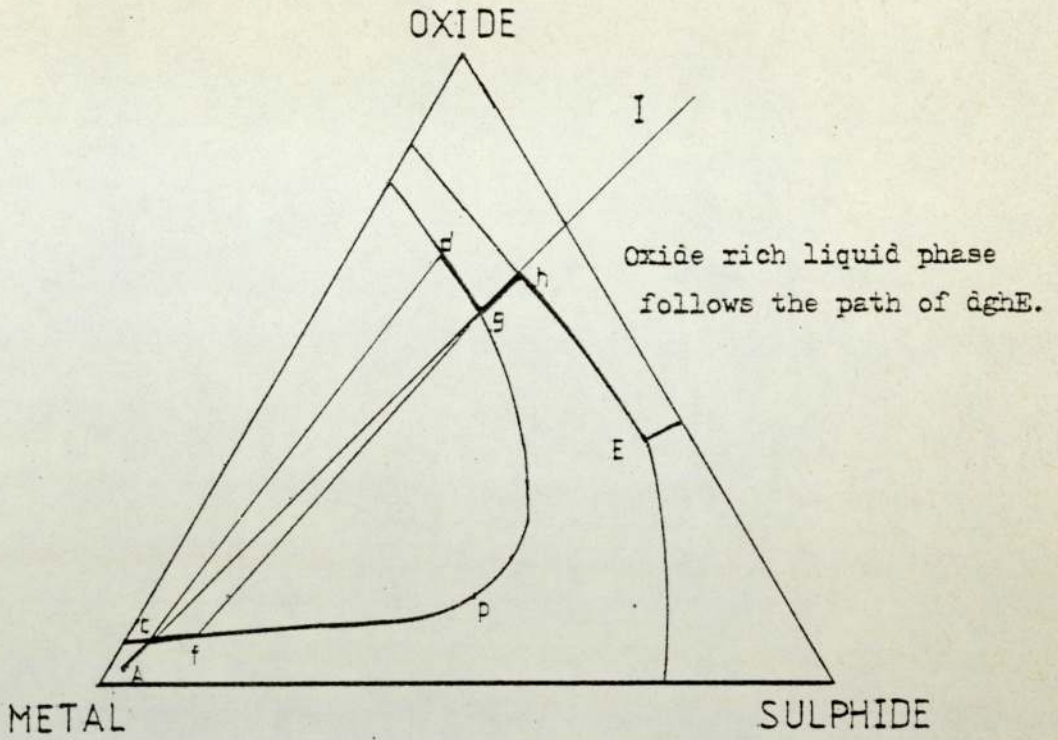
Fig 8. Solidification path of alloy A in Fe-O-S Diagram

OXIDE

II

j

E

m

Sulphide rich liquid
phase varies composi-
tion from j to l and
from l to m and E.

B

l

i

k

P

METAL

SULPHIDE
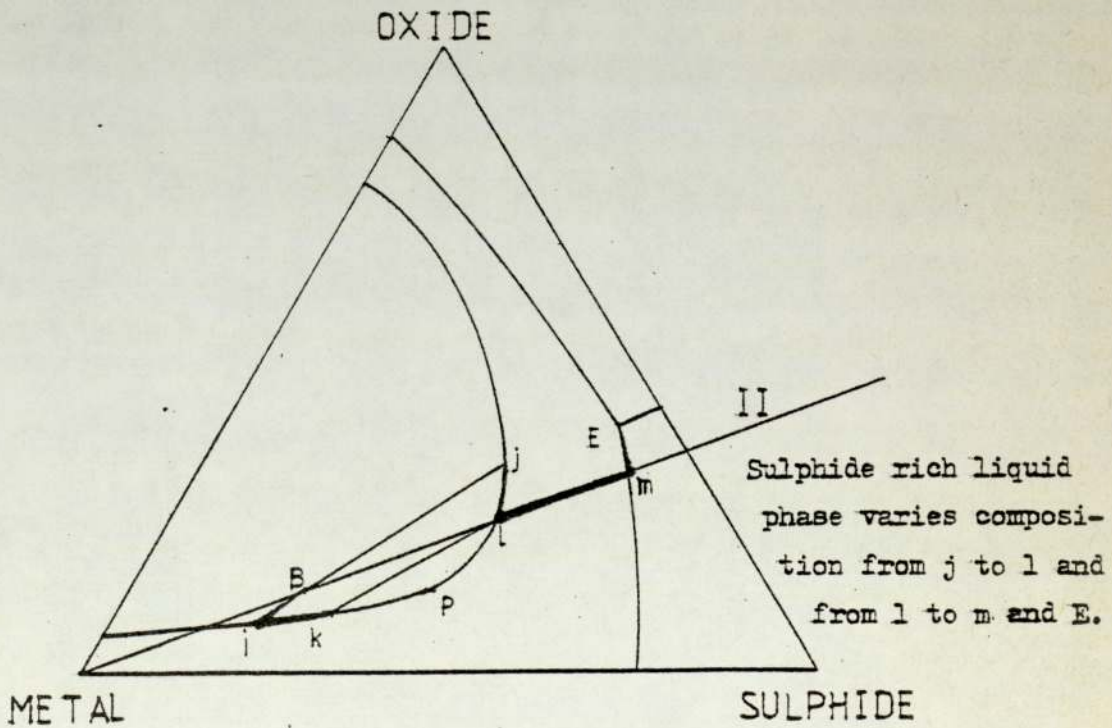
Fig 9. Solidification path of alloy B in Fe-O-S Diagram
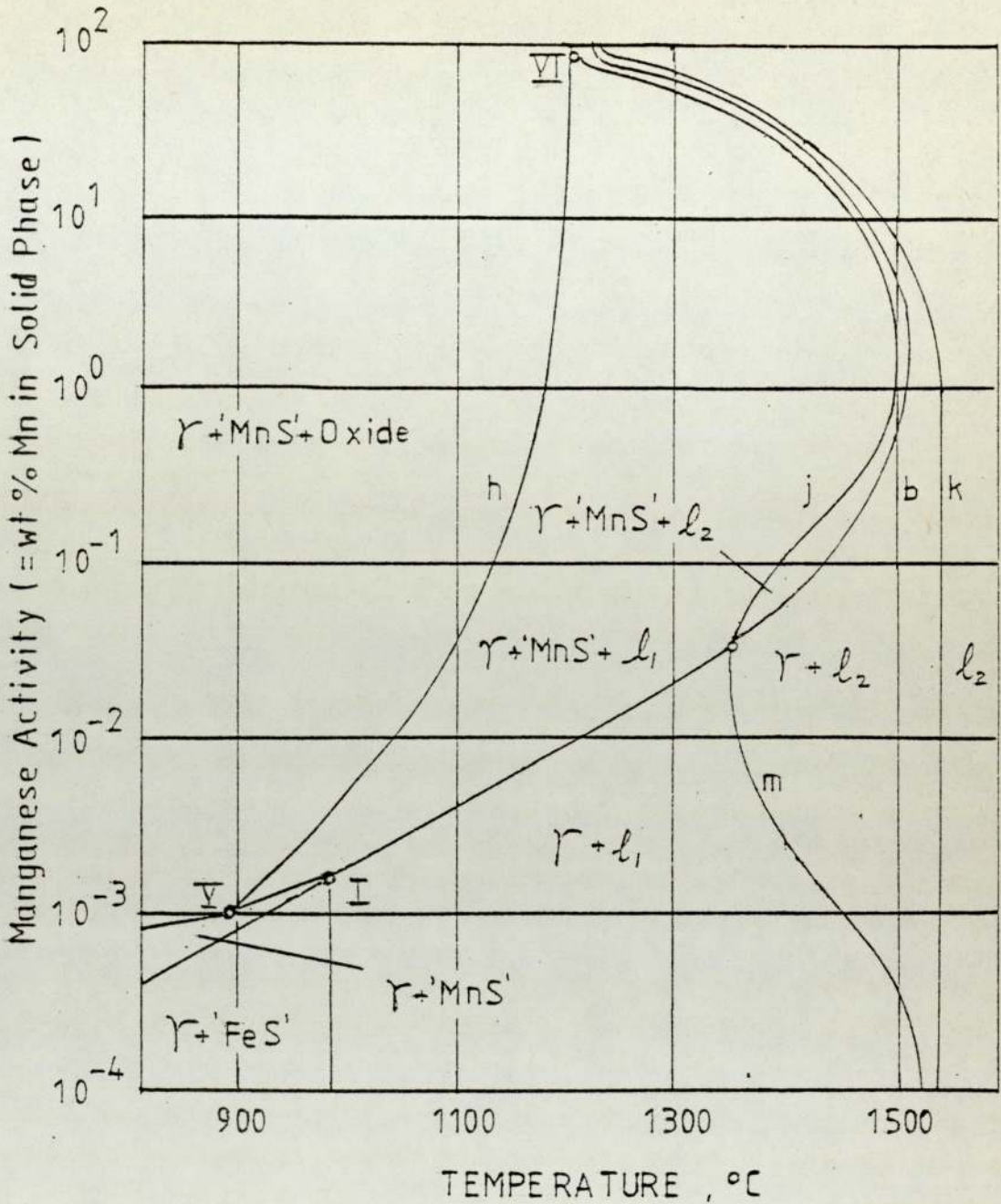
Fig 10. Univariant equilibria involving solid metal and 'MnS' in Fe-Mn-S-O system with ternary Fe-Mn-S and Fe-S-O and binary Fe-Mn terminal phase fields. (j) γ, 'MnS', l_1 , l_2 ; (m) γ, l_1, l_2 ; (k) γ, l_2 . According to ET Turkdogan and GJW Kor[42).
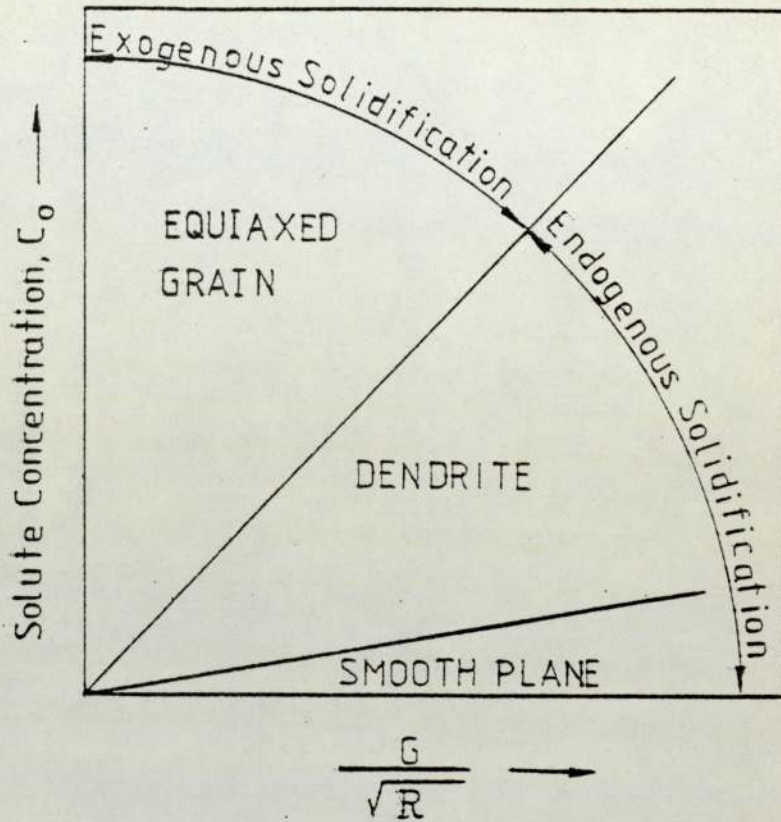
Fig 11. Influence of physical parameters on the solidification of a single phase alloy; G and R represent temperature gradient and growth rate respectively.
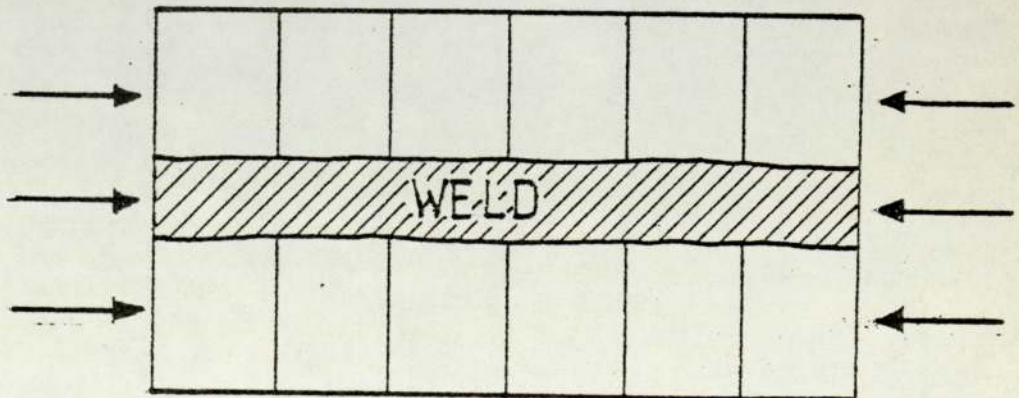
Fig 12. Assembly of strips for Pellini cracking test[55].
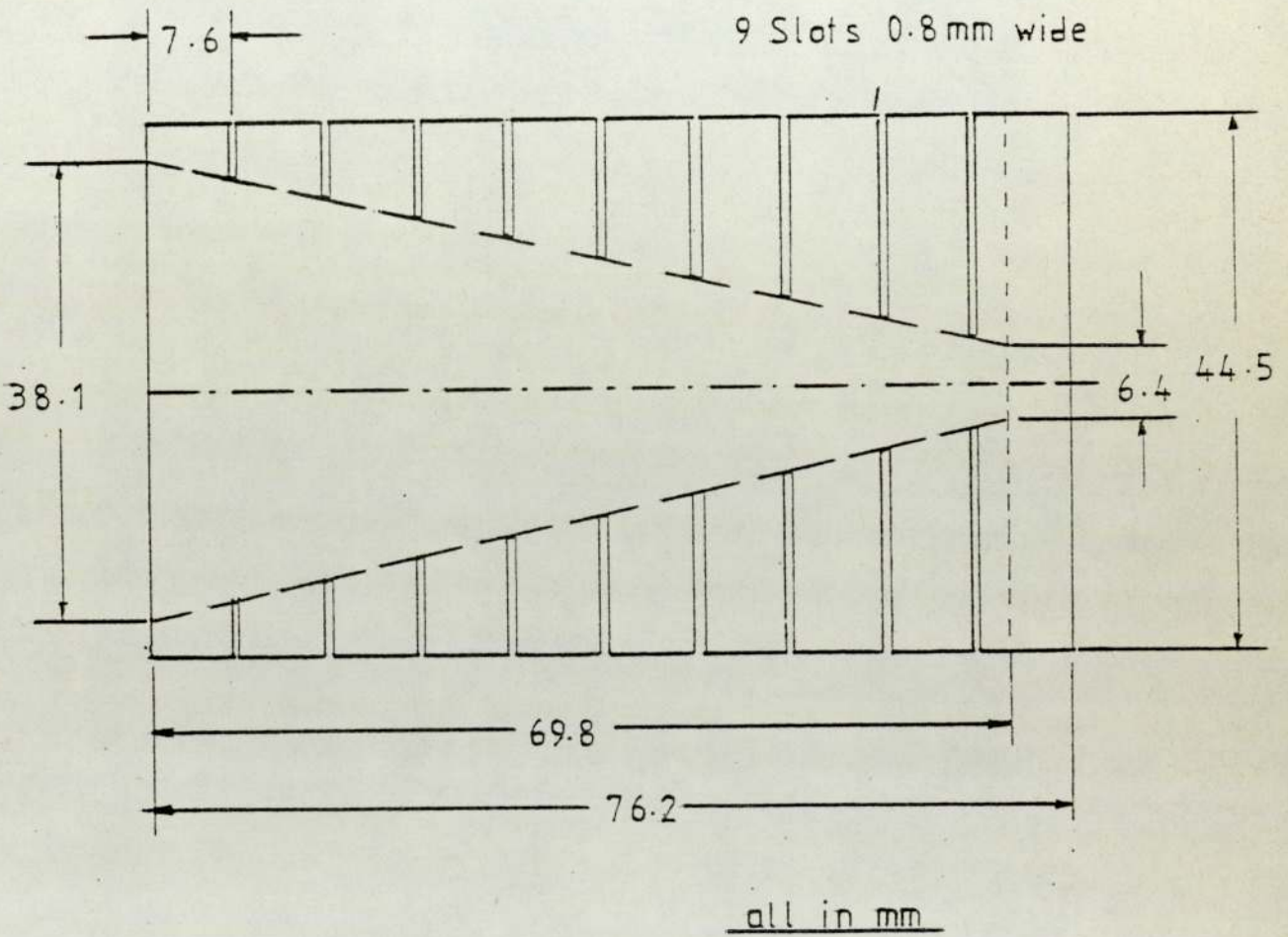
Fig 13. Specimen used for the Houldcroft cracking test[54].

38·1mm

50·8 mm run-in or run-out section

Slot approx 0·8mm wide 15mm deep

8 Test segments each 38·1mm Long

406·mm
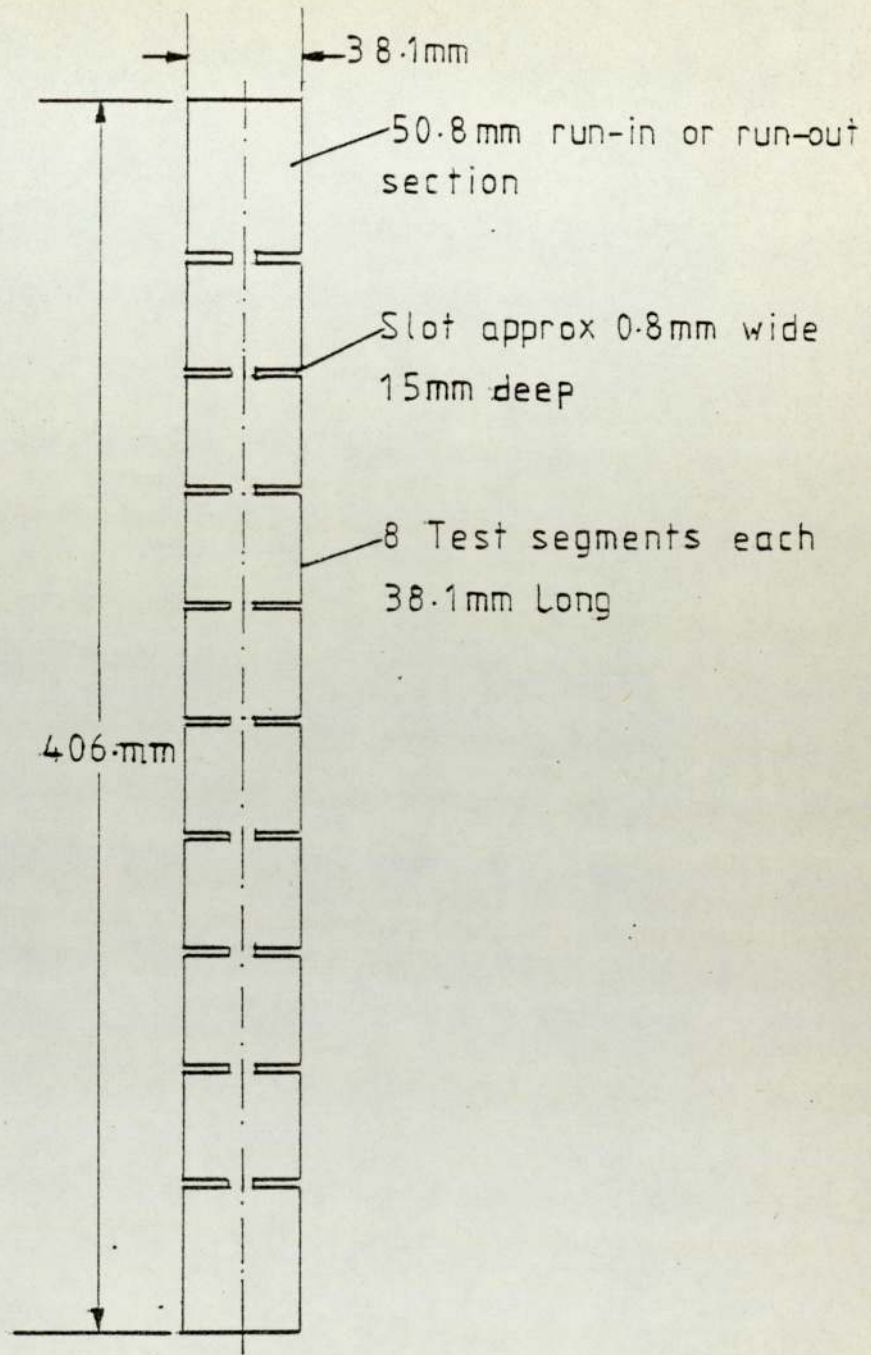
Fig 14. Huxley cracking test specimen[7].
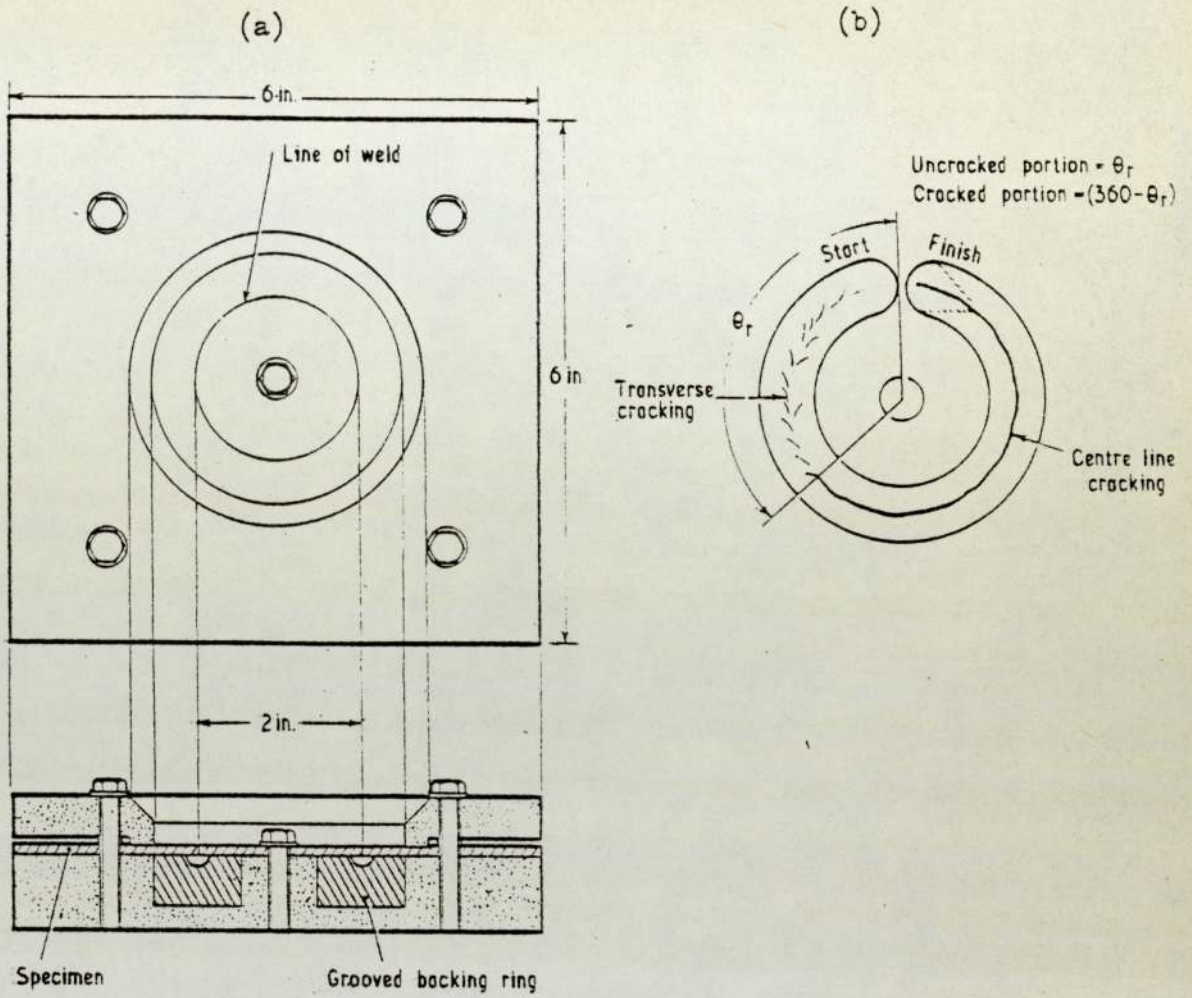
Fig 15. Illustration of Circular Patch Test. (a) Jig for the test;
(b) type, location and measurement of cracking[59].
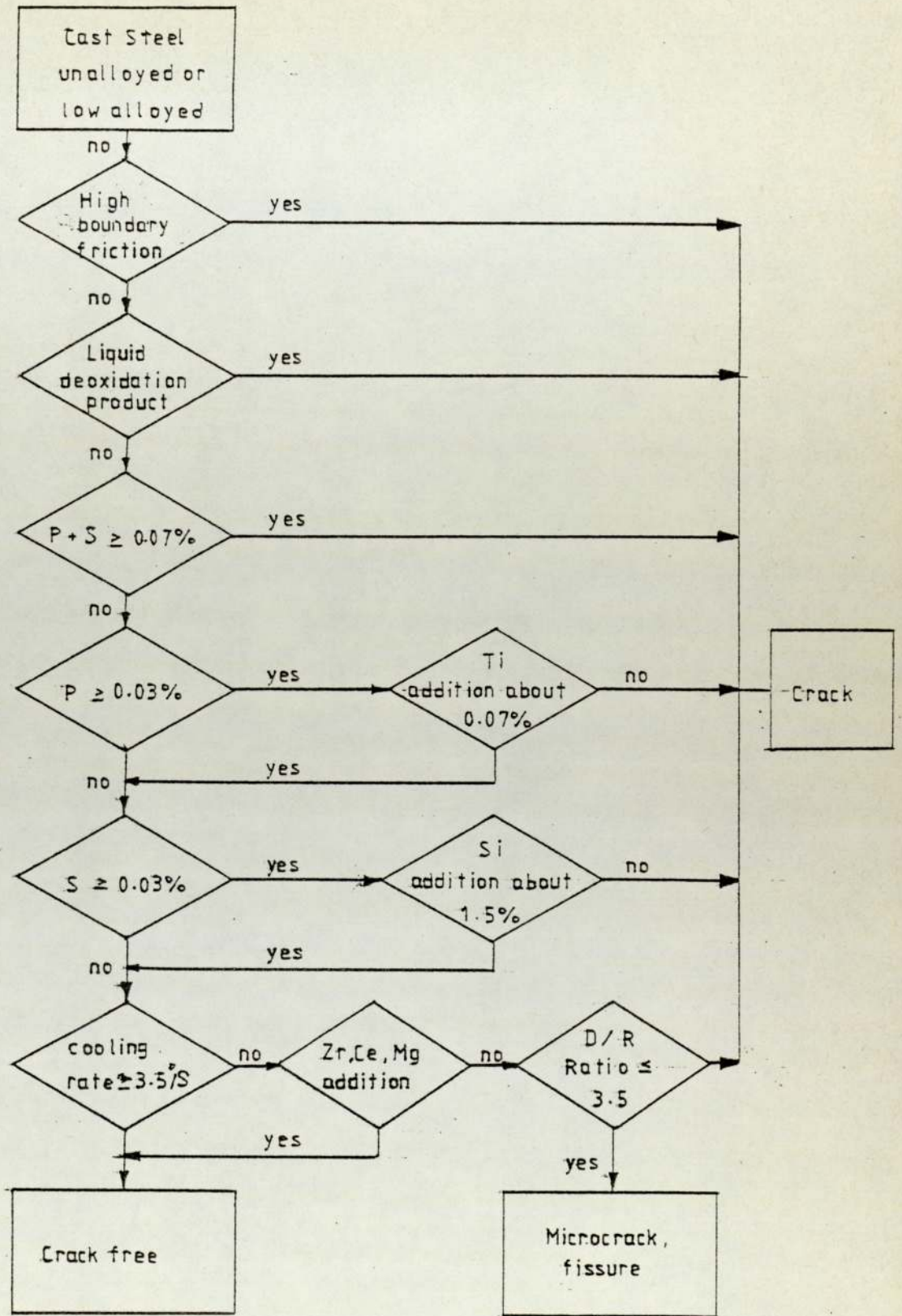
Fig 16. Decision chart of solidification cracking for alloyed and unalloyed cast steel (Orths and Kolorz)[67]
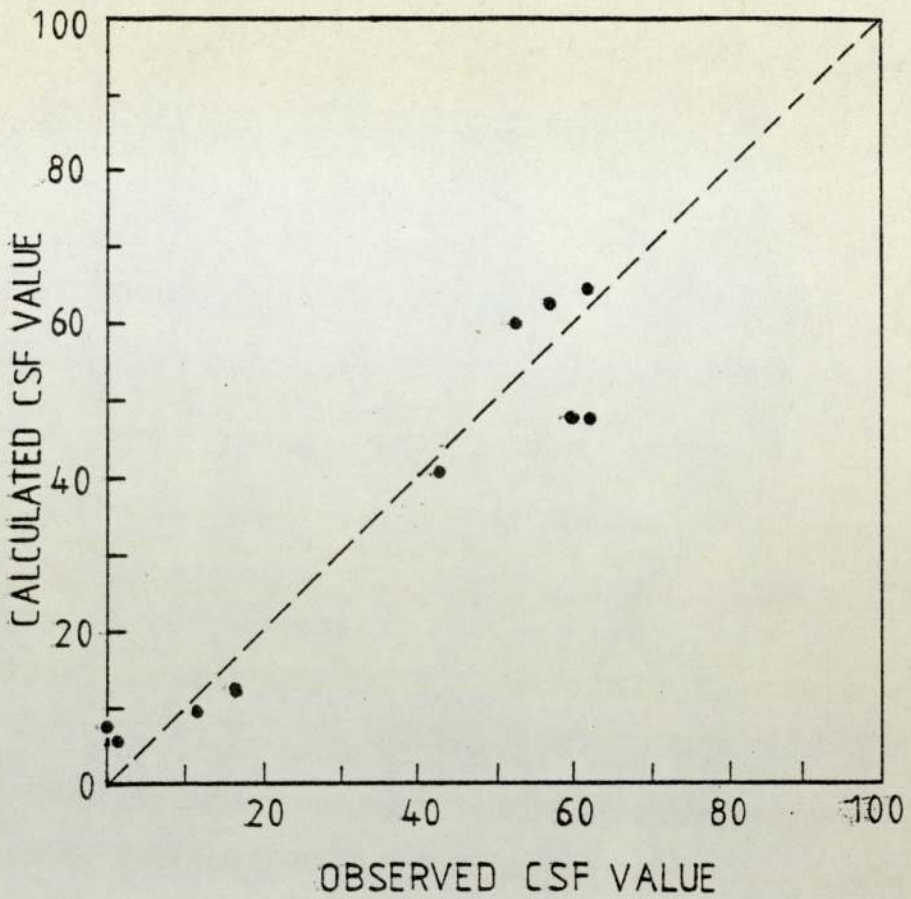
Fig 17. Comparison of calculated and observed CSF values for
MA series steels(SAE4130).
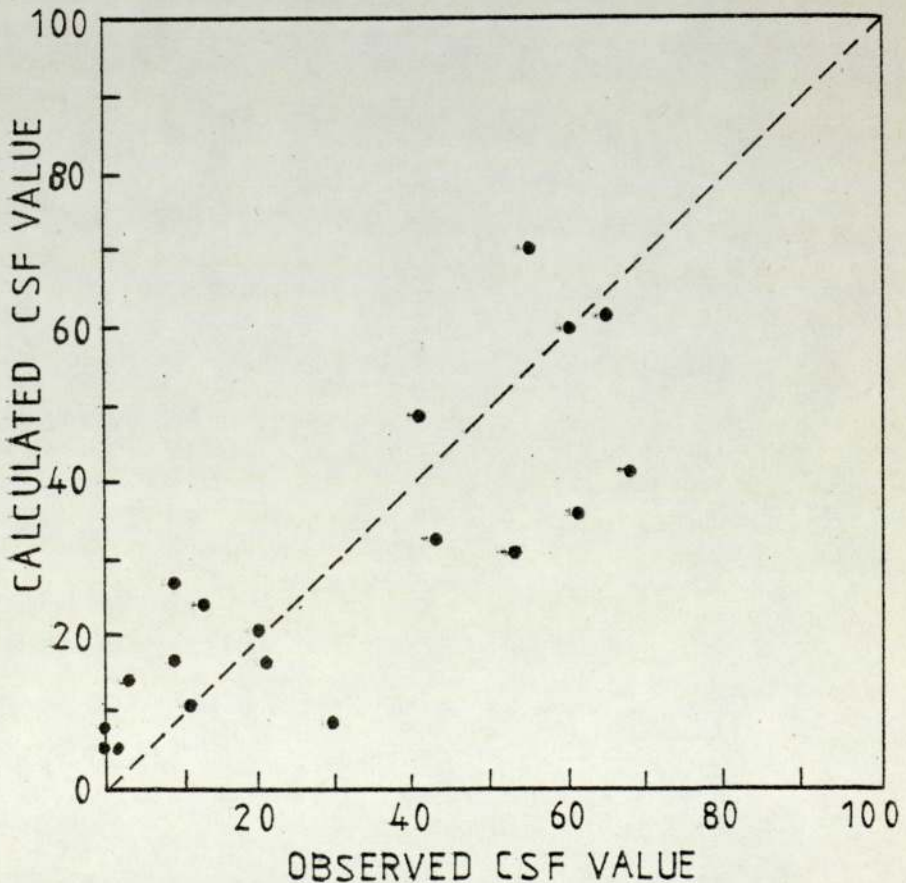
Fig 18. Comparison of calculated and observed CSF values for
steels in the MD series.
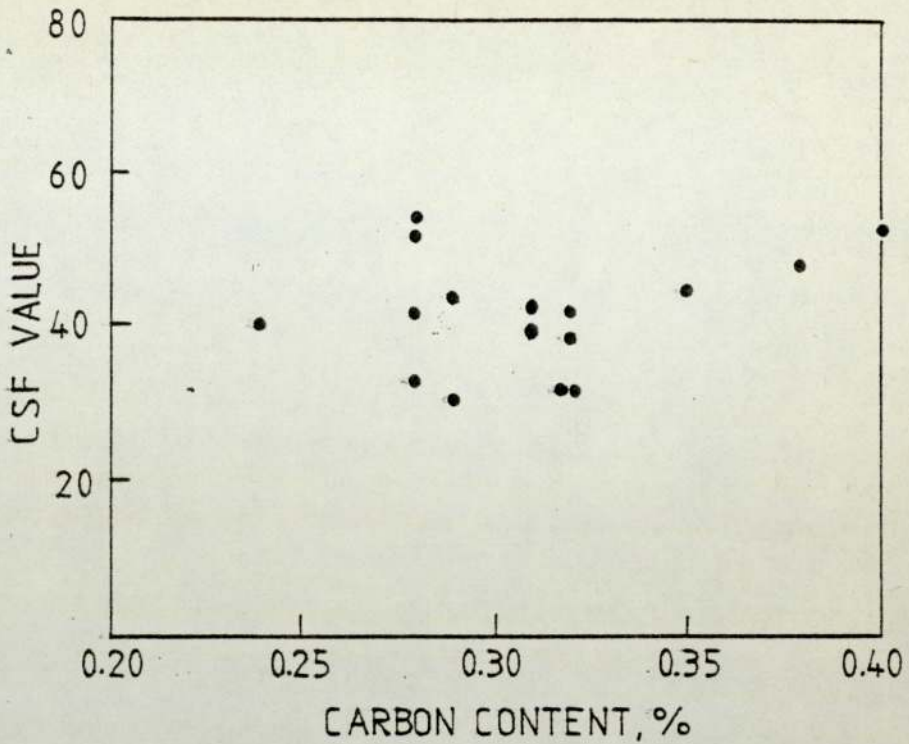
Fig 19. The effect of carbon content on the CSF value for the steels in the MA and MB series (all SAE4130).
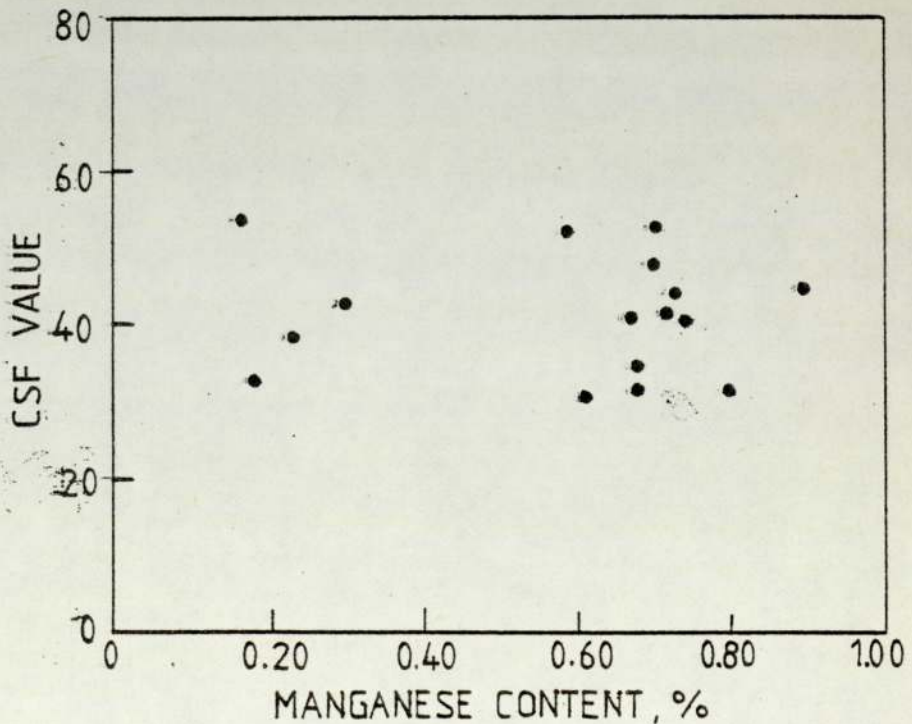
Fig 20. The Effect of manganese content on the CSF value for the steels in the MA and MB series (all SAE4130).
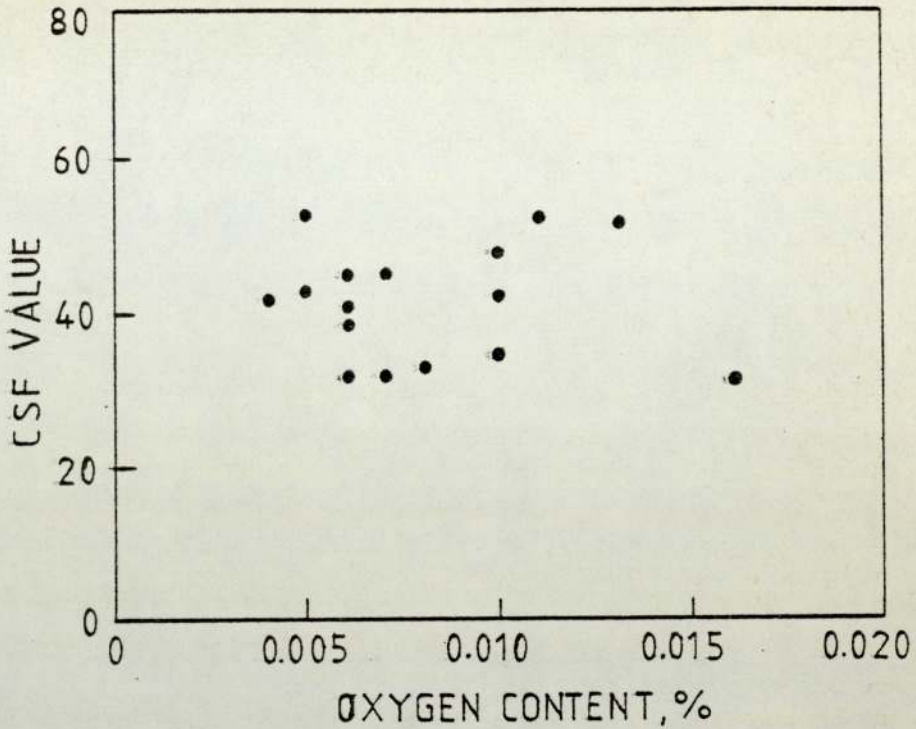
Fig 21. The effect of oxygen content on the CSF value for the steels in the MA and MB series (all SAE4130).
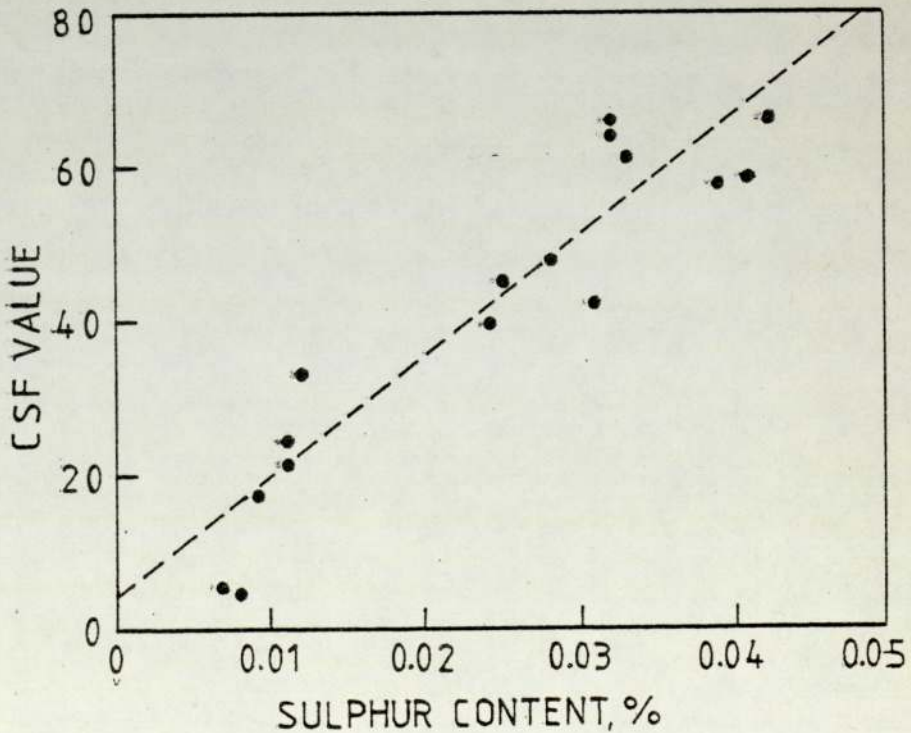
Fig 22. The effect of sulphur content on the CSF value for the steels in the MA and MB series (all SAE4130).
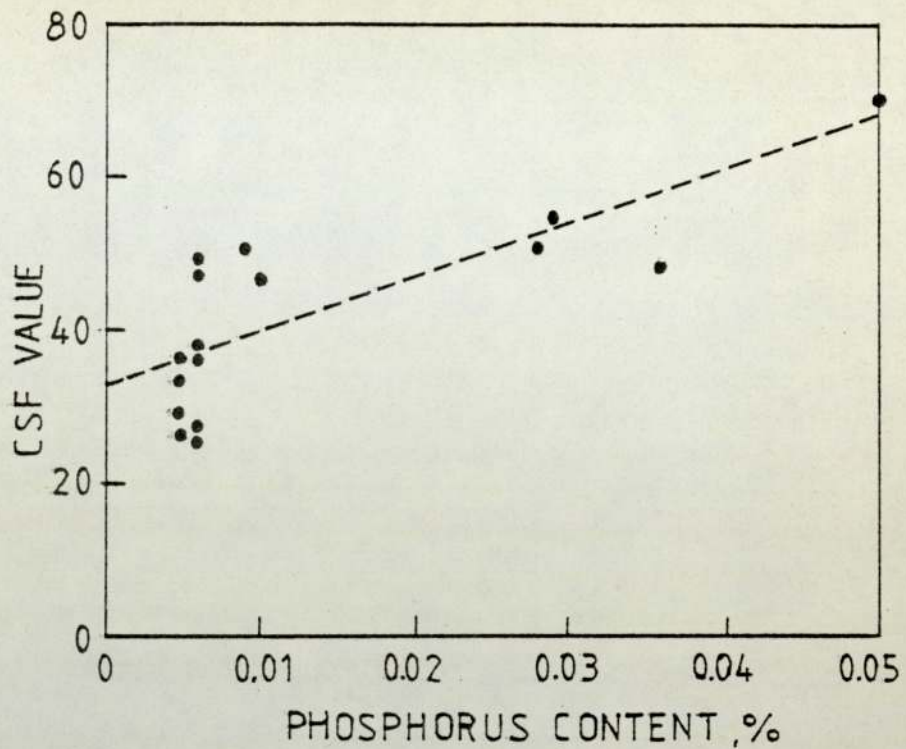
Fig 23. The effect of phosphorus content on the CSF value for
the steels in the MA and MB series (all SAE4130).
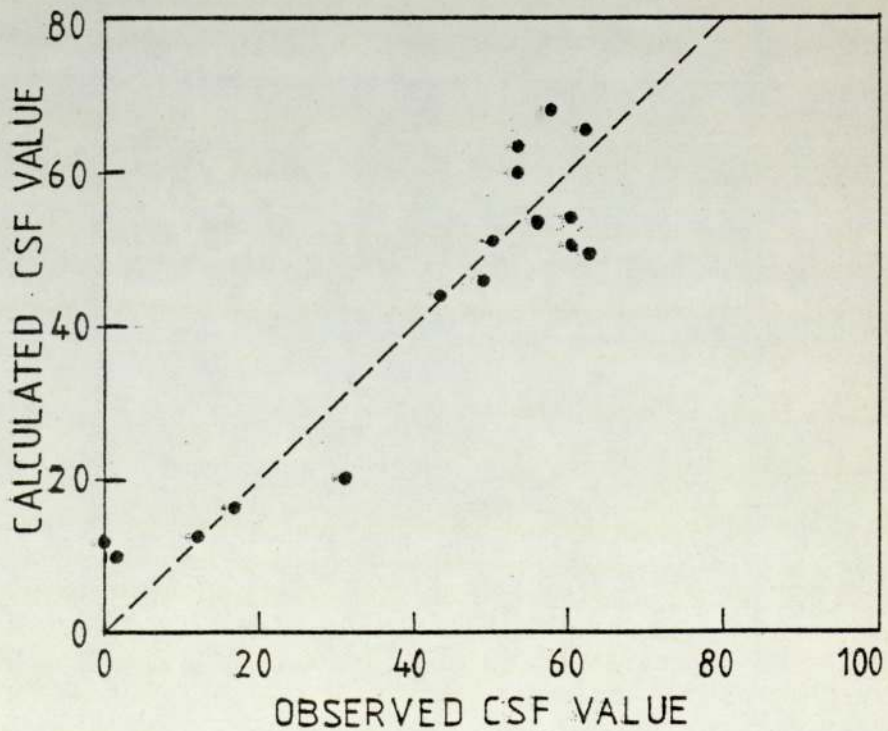
Fig 24. The comparison of observed and calculated CSF values
for the steels in the MA and MB series (all SAE4130).
Equation $P(CSF, MA+MB) = 1587S + 657P - 5$.

Fig 25. Flat section of the weld of MA3 (SAE4130, 0.042% S, 0.005% P, CSF = 62) showing the dendrites near a centreline crack boundary. Specimen etched in a solution of saturated picric acid with a wetting agent. X70.

Fig 26. Flat section of the weld of MA3 (SAE4130, 0.042% S, 0.005% P, CSF = 62) showing the dendrites near a centreline crack boundary. X70.

Fig 27. Flat section of the weld of MD19 (EN19, 0.015% S, 0.042% P, CSF = 53) showing the detachment and rupture of dendrites near the crack boundary. X70.
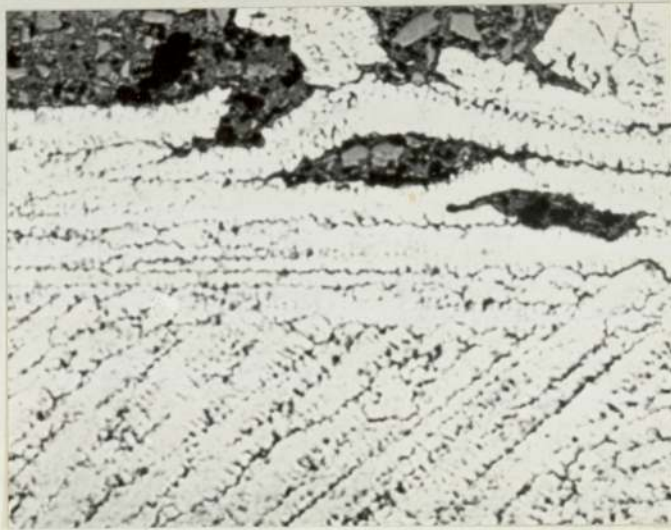
Fig 28. Flat section of the weld of MA8 (SAE4130, 0.032% S, 0.006% P, 0.59% Mn, CSF = 60) showing some dendrites growing in parallel with the welding direction being distorted and ruptured. X70.
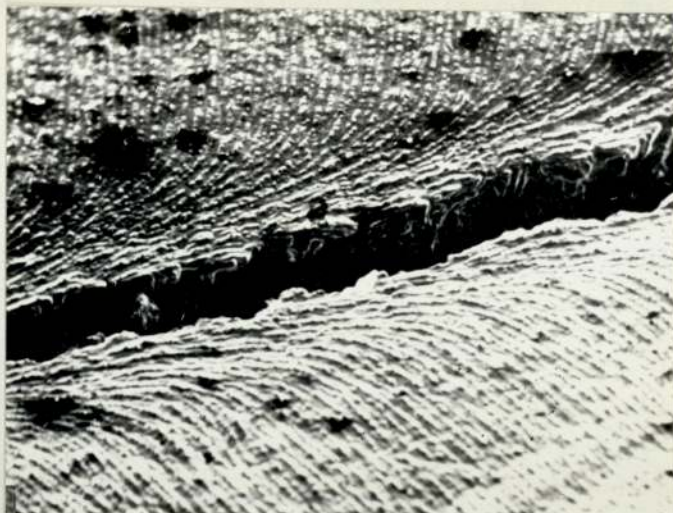
Fig 29. A typical weld surface with solidification crack.
MA8 (SAE4130, 0.032% S, 0.006% P, CSF = 60).   X50

Fig 30. A close-up view of the solidification of weld
surface with the growth markings. MA8 (SAE4130, 0.032% S,
0.006% P, CSF = 60).   X500

Fig 31. A atereomicrograph of a weld surface of MA3 (SAE4130, 0.042% S, 0.006% P, CSF = 62) with centre-line cracks, slightly etched.   X 20
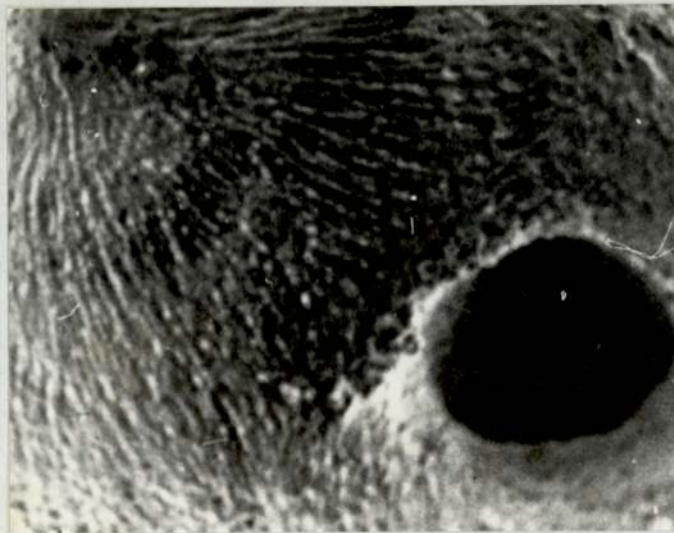
Fig 32. The interior of a gas pore with a leading channel in the specimen of MB4 (SAE4130, 0.011% S, weld metal oxygen content 0.023%, C x 0 = 0.008).   X 50
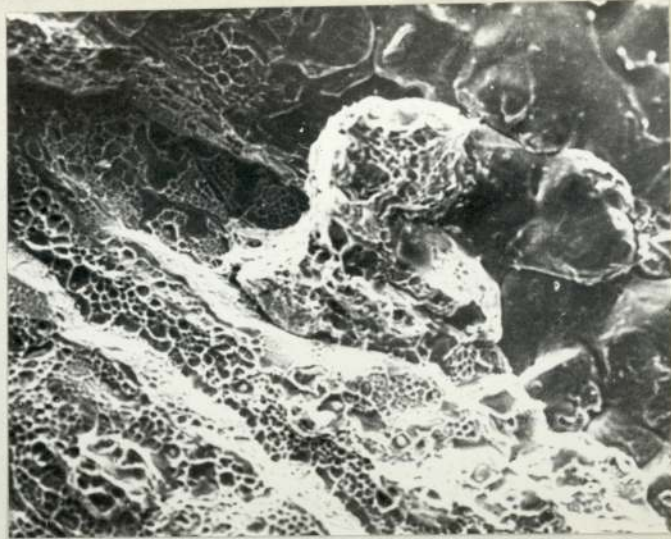
Fig 33. Extended fracture surface of solidification crack.
caused by mechanical rupturing at room temperature for MA4
(SAE4130, 0.041% S, 0.60% Mn, CSF = 57), the honeycomb-like
structure is believed to be the fractured FeS-MnS-Fe eutectic.

X 2000

Fig 34. Extended fracture surface of solidification crack
caused by mechanical rupturing at room temperature for a less
crack susceptible steel weld. MA5 (SAE4130, 0.007% S, CSF = 1).

X 2000

Fig 35. Oxidized solidification crack surface with bent dendritic columns, MD18 (EN5, 0.030% S, CSF = 68). X 200

Fig 36. Oxidized solidification crack surface, the true solidification structure being obscured by the presence of oxide skins. MD18 (EN5, 0.030% S, CSF = 68).   X 600

Fig 37. Oxidized crack surface with a general dendritic
pattern, MA 7 (SAE4130, 0.032% S, CSF = 62).   X 500
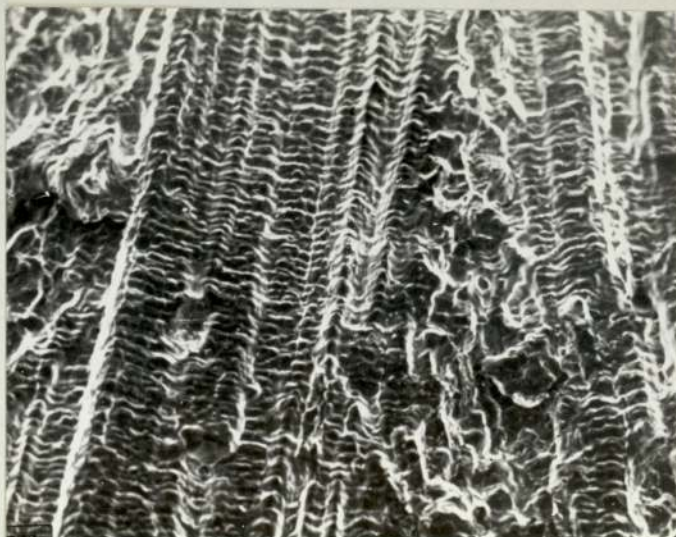
Fig 38. Fresh solidification crack surface showing a
typical columnar structure, MD15 (BS4360-50B, 0.17% C,
0.028% S, CSF = 1).   X 200

Fig 39. Gas pore interior with round dendritic tips or equiaxed grains, MA7 (SAE4130, 0.032% S, CSF = 62). X 1000
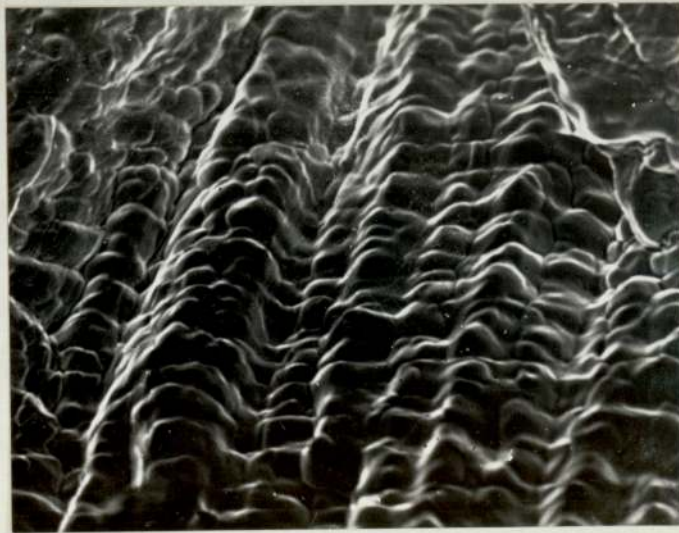
Fig 40. Stereomicrograph of distorted or ill-defined dendrites on the crack surface, MA2 (SAE4130, 0.009% S, CSF = 12), also seen in other less crack susceptible steels.   X 500
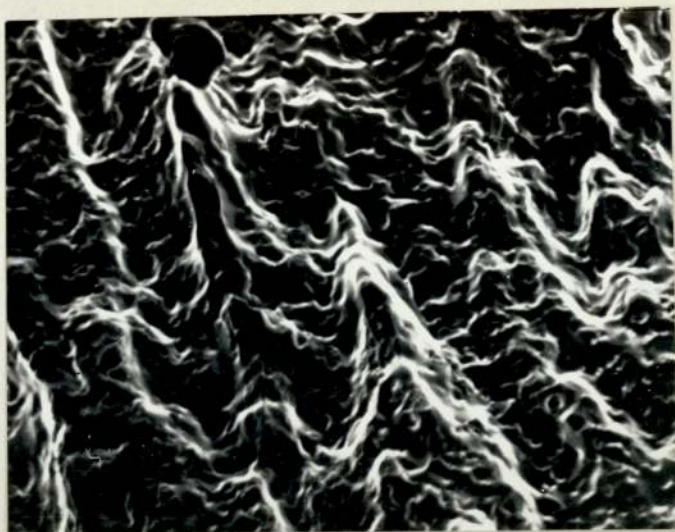
Fig 41. Distorted and ill-defined dendrites on the crack surface of the weld of MA9 (SAE4130, 0.028% S, CSF = 43).

X 500

Fig 42. Stereomicrograph of solidification crack surface with globules, MC12 (0.170% S, 0.016% O, CSF = 63).   X 1000
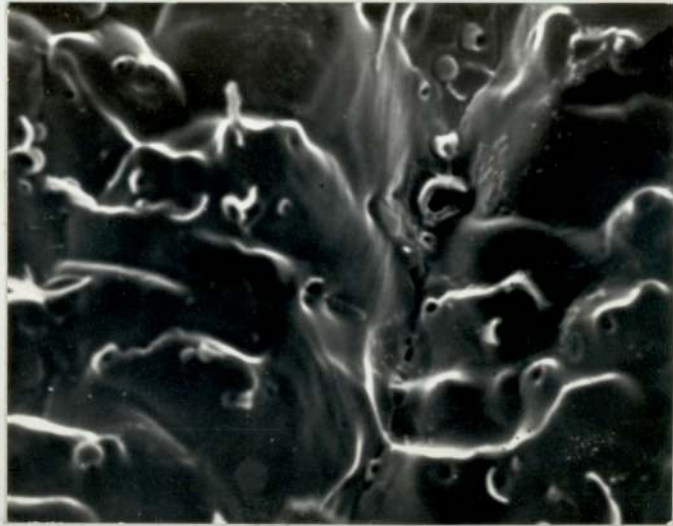
Fig 43. Stereomicrograph of solidification crack surface with globules and sunk cavities, MA4 (SAE4130, 0.042% S, CSF = 57).
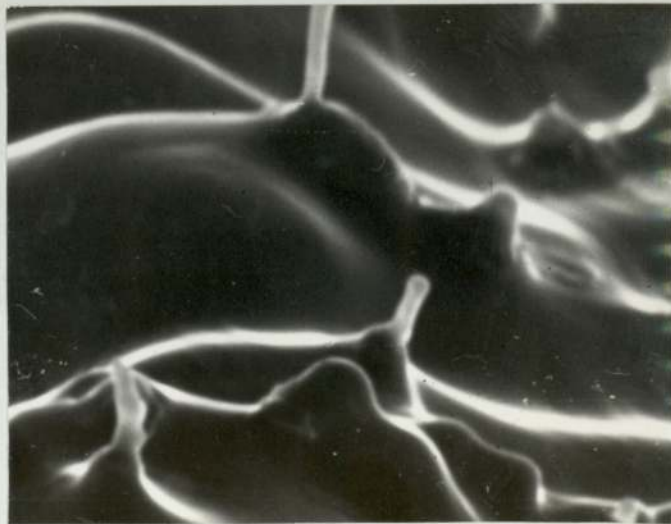
Fig 44. Rodlike non-metallic phase protruding out of the matrix of the solidification crack surface, weld of MA10 (SAE4130, 0.039% S, CSF = 53).

Fig 45. Crack surface showing extended tips of necked down bridges between grains, seen in the weld of MA7 (SAE4130, 0.032% S, 0.17% Mn, CSF = 62).   X 3000

Fig 46. Crack surface with a series of necked down bridges, seen in the weld of MC12 (Fe-Mn-S-O alloy, 0.17% S, 0.016% O, 0.03% Mn, CSF = 63).   X 2000

Fig 47. Crack surface showing dendrites with broken ends, MC11 (0.080% S, CSF = 9). X 500
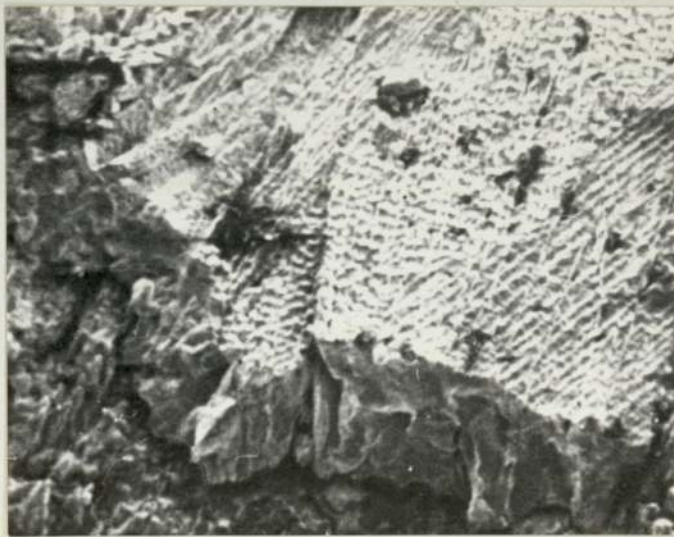
Fig 48. Crack surface showing brittle rupture of dendritic columns, MC4 (0.16% S, CSF = 66). X 50
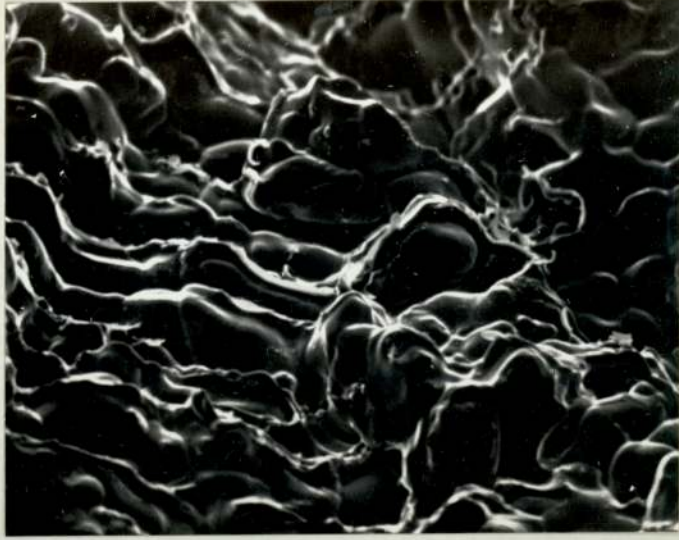
Fig 49. Crack surface of a steel weld showing liquid films or non-metallic inclusions, MA4 (0.041% S, SAE4130, CSF = 57).

X 1000
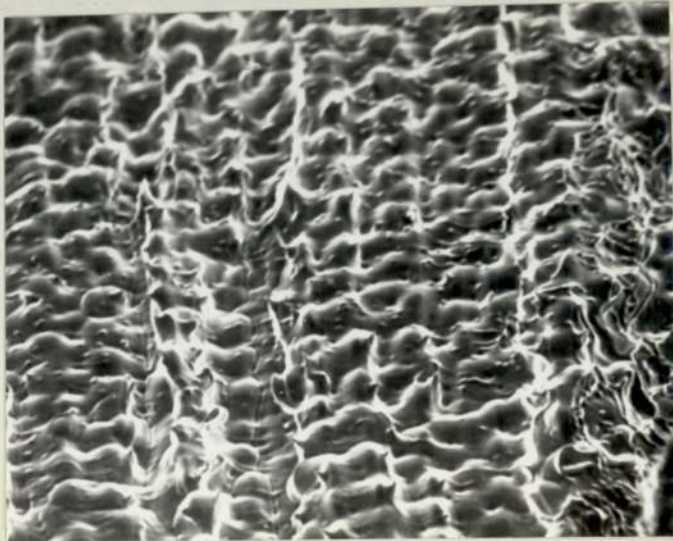
Fig 50. Crack surface showing liquated films or non-metallic inclusions, MC8 (Fe-Mn-S-0, 0.16% S, 0.064% 0, CSF = 70).

X 250

Fig 51. Crack surface showing some area being in a mushy
state during solidification cracking, MB6 (SAE4130, 0.40% C,
0.012% S, CSF = 31).   X 1000

Fig 52. Crack surface showing some area being in a mushy
state during solidification cracking, MB6 (SAE4130, 0.40% C,
0.012% S, CSF = 31).   X 1000

Fig 53. Crack surface with ridges seen in the specimen of a
less crack susceptible steel, MA2 (SAE4130, 0.009% S,
CSF = 12).   X 1000

Fig 54. Crack surface with ridges seen in the specimen of a
less crack susceptible steel. The ridges contain more sulphur
than the matrix does. Weld of MA2 (SAE4130, 0.009% S, CSF = 12).
                                                       X 800
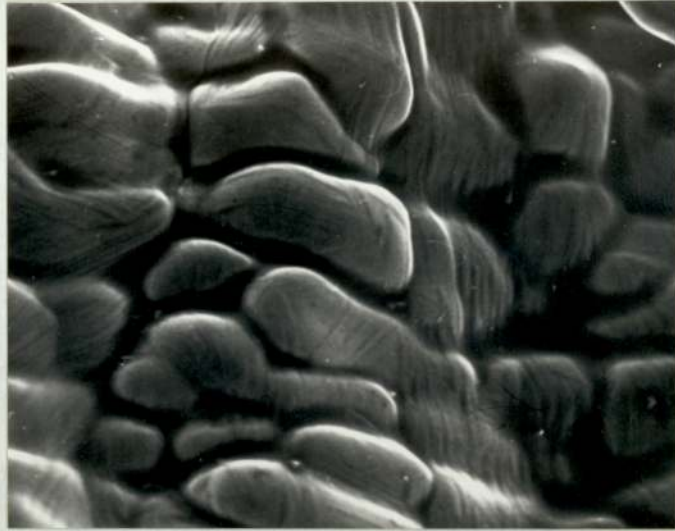
Fig 55a. Crack surface with a very clean appearance, in
which the striation can be seen, in the weld of MA5
(SAE4130, 0.006% S, CSF = 1).   X 500

Fig 55b. Freely solidified ball on the crack surface of
MA7 weld (SAE4130, 0.28% C, 0.032% S, CSF = 62).   The
ball diameter is about 20 μm.   X 5000
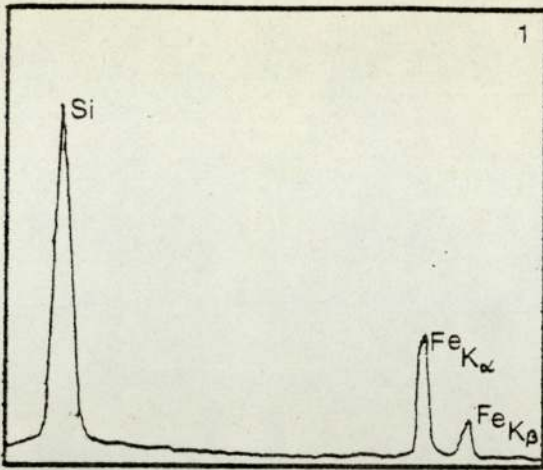
Fig 56. KEVEX chart of inclusion containing silicon, possibly SiO_2 or $SiO_2 \cdot FeO$, often observed.
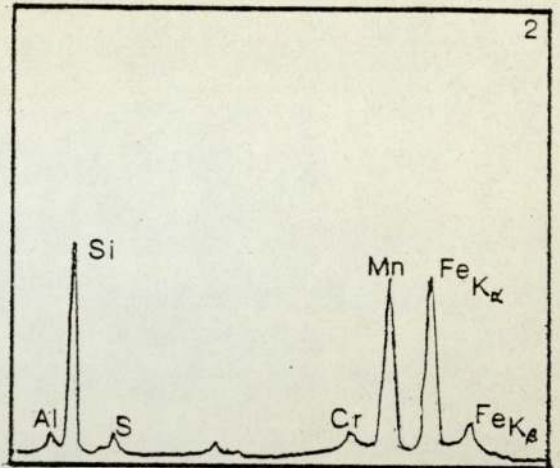
Fig 57. KEVEX chart of inclusion containing Si and Mn, possibly $SiO_2 \cdot MnO$ or $SiO_2 \cdot MnO \cdot FeO$, often observed.
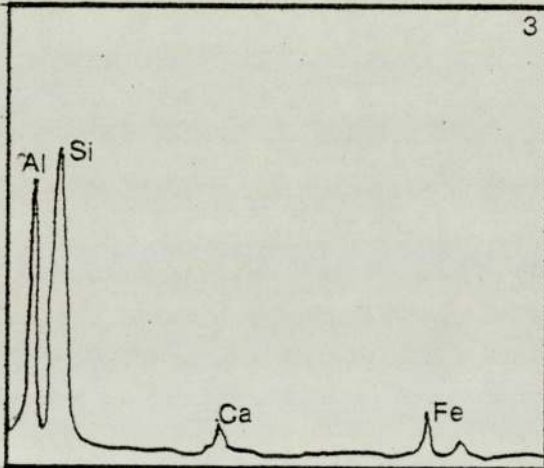
Fig 58. KEVEX chart of $Al_2O_3 \cdot SiO_2$ type inclusions, showing as a cluster, often found in the upper weld.
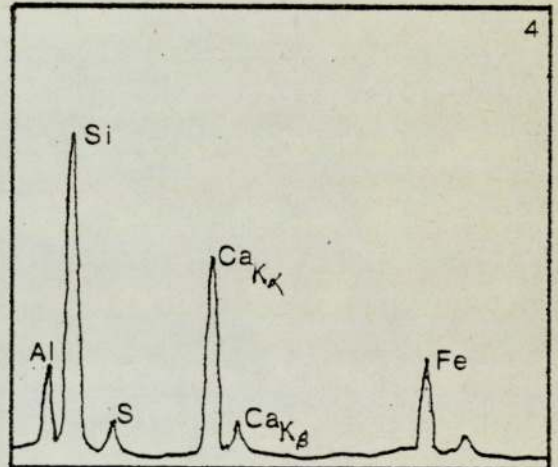
Fig 59. KEVEX chart of $Al_2O_3 \cdot SiO_2 \cdot CaO$ type inclusions, found near the surface of the weld.
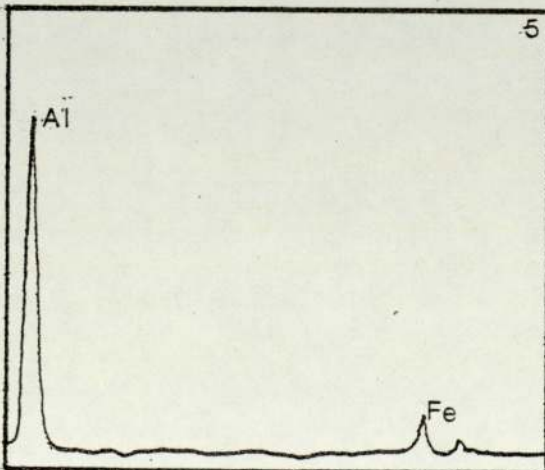
Fig 60. KEVEX chart of Al_2O_3 inclusion appearing as a lump, found in MB4 (0.110% Al).
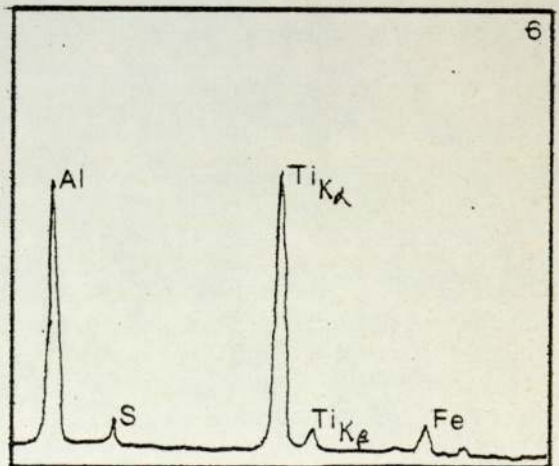
Fig 61. KEVEX chart of $Al_2O_3 \cdot TiO_2$ type inclusion, observed in MB4 (0.11% Al).
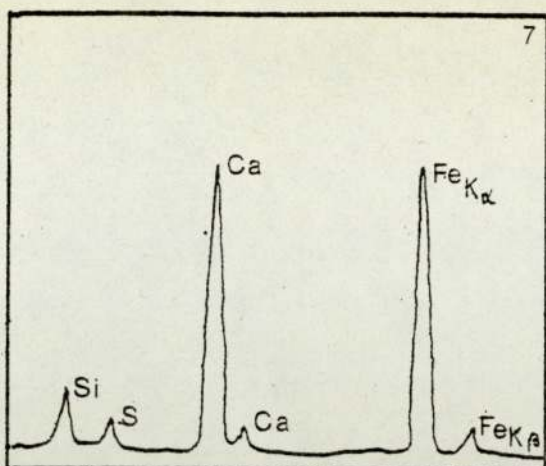
Fig 62. KEVEX chart of calcium-containing inclusion found in MB2, relatively seldom in occurrence.
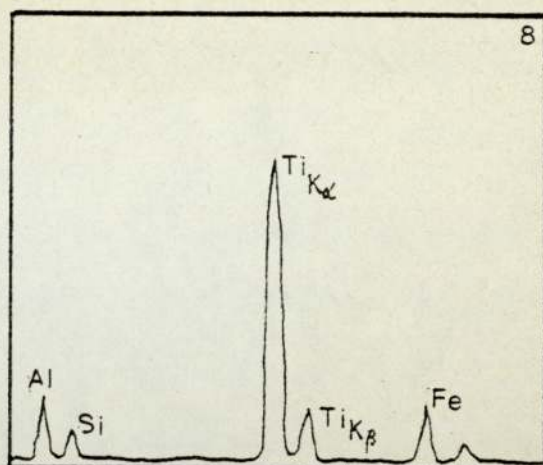
Fig 63. KEVEX chart of inclusion containing titanium found in MB4 and MB5.
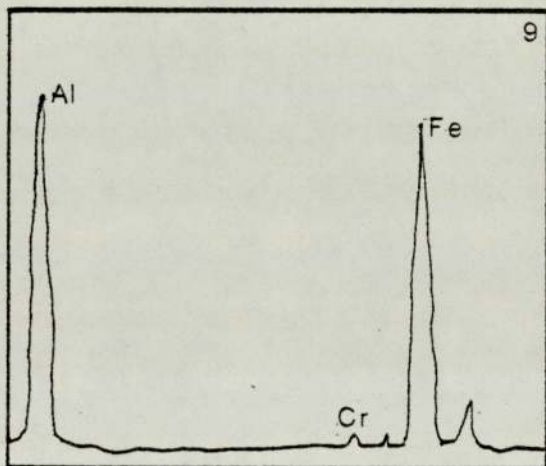
Fig 64. KEVEX chart, possibly representing $FeO \cdot Al_2O_3$ system inclusion (MB4).
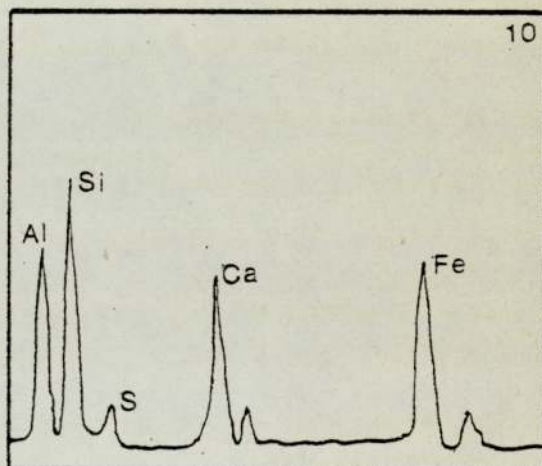
Fig 65. KEVEX chart similar to Fig 59, also found near the top surface of the weld.
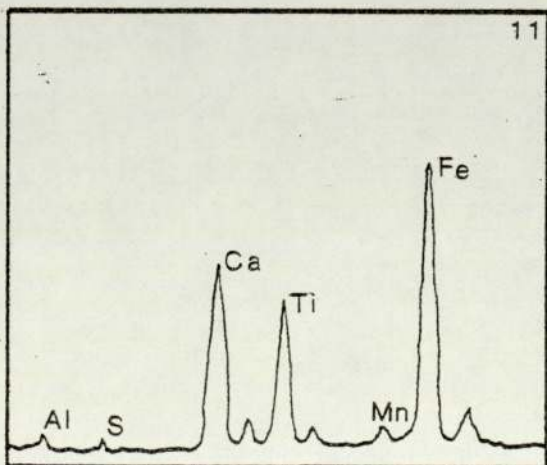
Fig 66. KEVEX chart of inclusion containing Ca and Ti, found in the MB series.
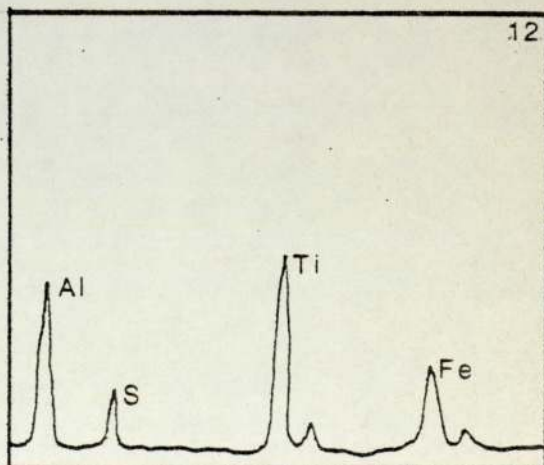
Fig 67. KEVEX chart of inclusion containing Al and Ti with absorption of sulphur, found in MB4.
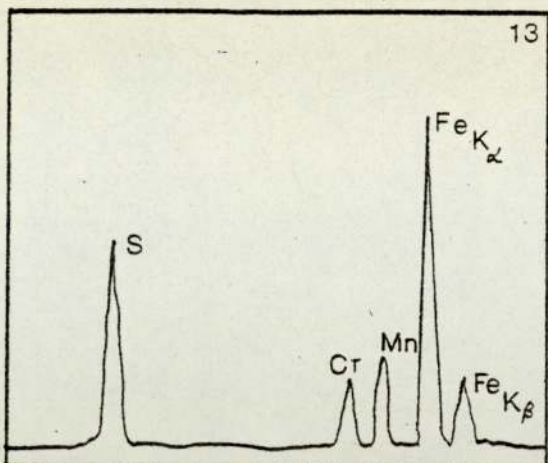
Fig 68. KEVEX chart of oxysulphide or sulphide inclusion. Observed in MA3, MA4, MA7 and MA8.
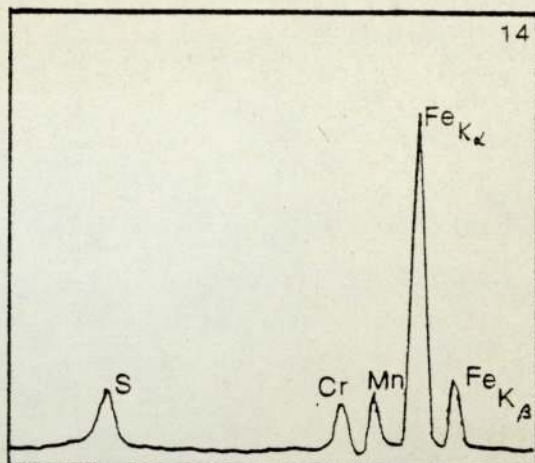
Fig 69. KEVEX chart for the weld crack surface of crack susceptible steels (MA3, MA4).
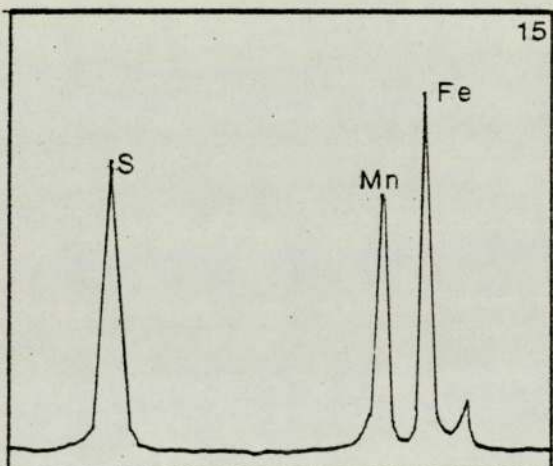
Fig 70. KEVEX chart for the liquated sulphide film found in the weld crack surface of MA4(CSF=57) or MC4(CSF=66).
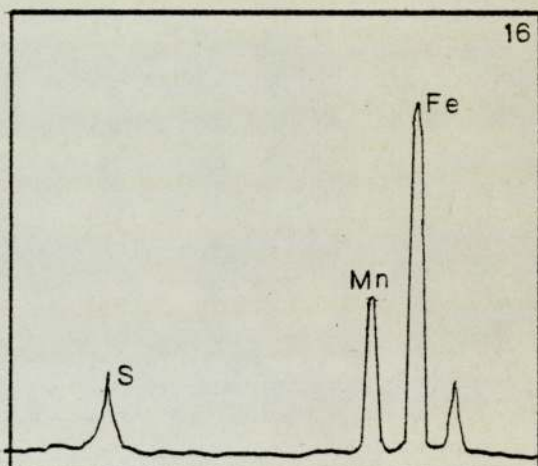
Fig 71. KEVEX chart for the weld crack surface of the MC series steels (MC8, 0.16%S, CSF=70).
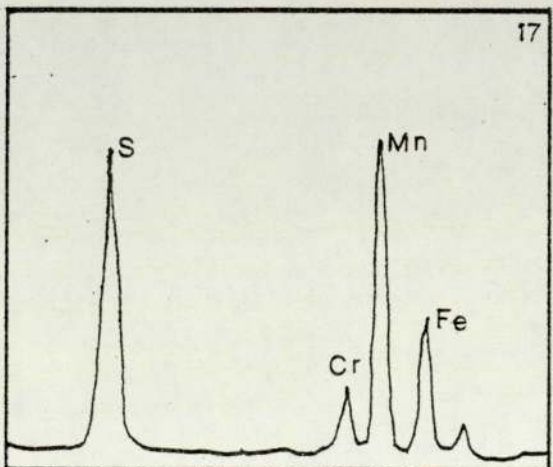
Fig 72. KEVEX chart for the inclusion shown in Fig 42 and Fig 43, MA8 (0.032%S, 0.59%Mn, CSF=60).
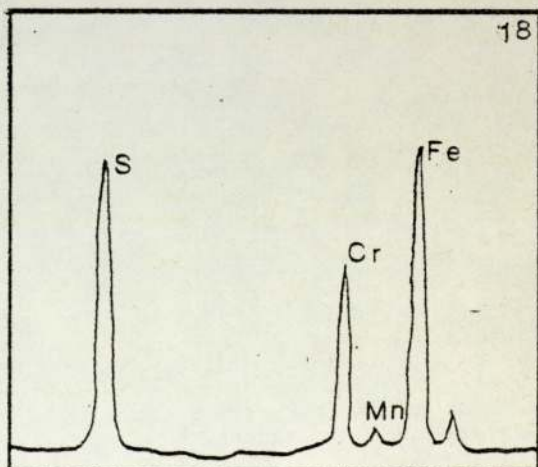
Fig 73. KEVEX chart for the inclusion found in the weld of MD14(EN 353, 0.040%S, 1.25%Cr, CSF=60).
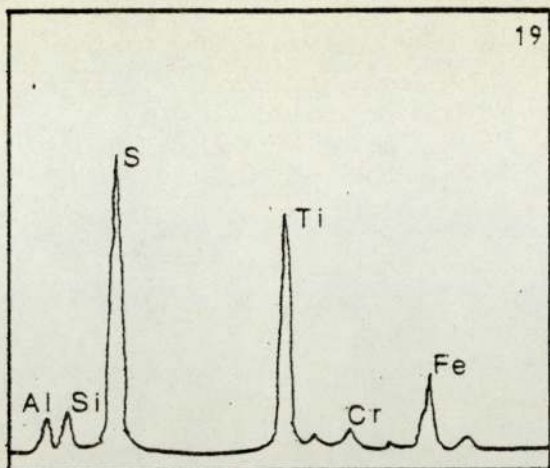
Fig 74. KEVEX chart of sulphide
inclusion containing Ti, found in
the weld of MB2(0.025%S, CSF=56).
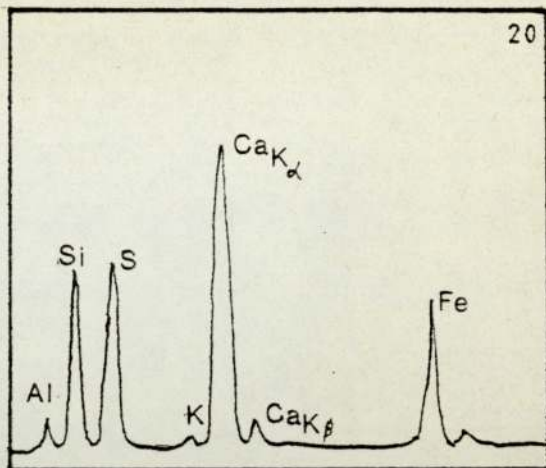
Fig 75. KEVEX chart for a complex
oxide and sulphide inclusion con-
taining Si and Ca, observed in MB2.
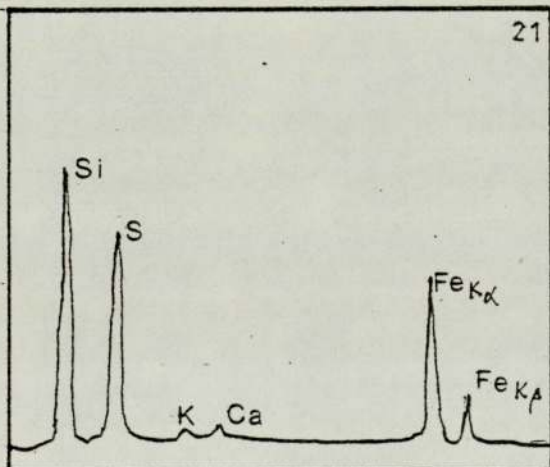
Fig 76. KEVEX chart for the inclu-
sion containing Si and S, observed
in the weld of MA3(0.29%Si, 0.042%S).
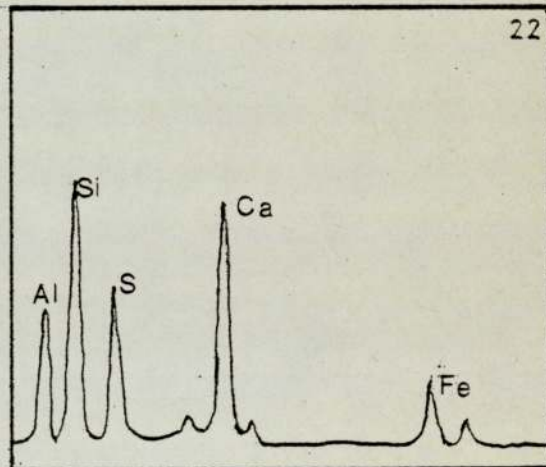
Fig 77. KEVEX chart for the inclu-
sion containing Al, Si, Ca and S,
in the weld of MB3(CSF=58).
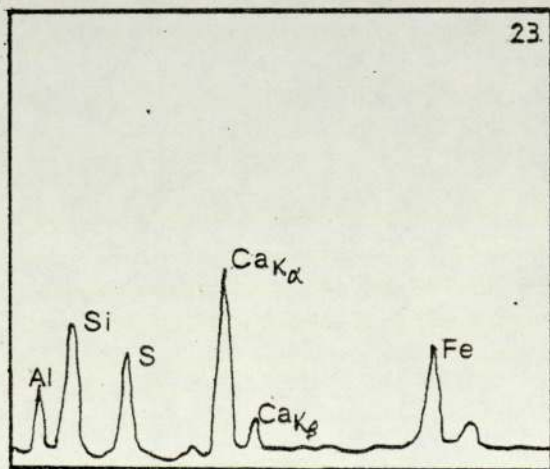
Fig 78. KEVEX chart for the inclu-
sion containing Al, Si, Ca and S,
observed in the weld of MB3.
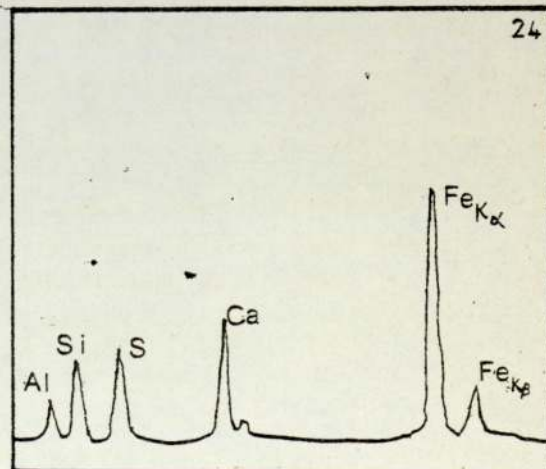
Fig 79. KEVEX chart for the inclu-
sion containing Al, Si, Ca, Fe and S,
observed in the weld of MB2(CSF=56).
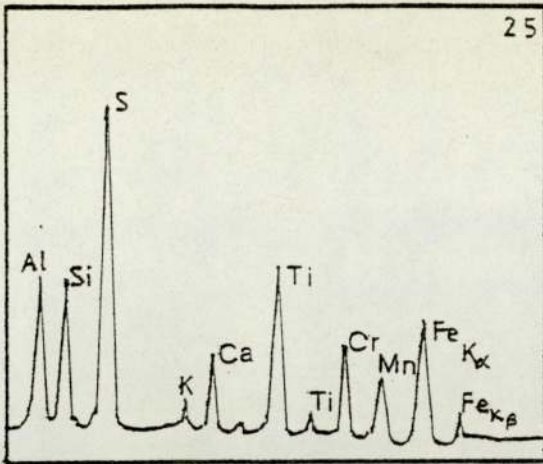
Fig 80. KEVEX chart for the inclusion containing Al,Si,S,Ca,Ti,Cr, Mn etc in the weld of MB1(CSF=50).
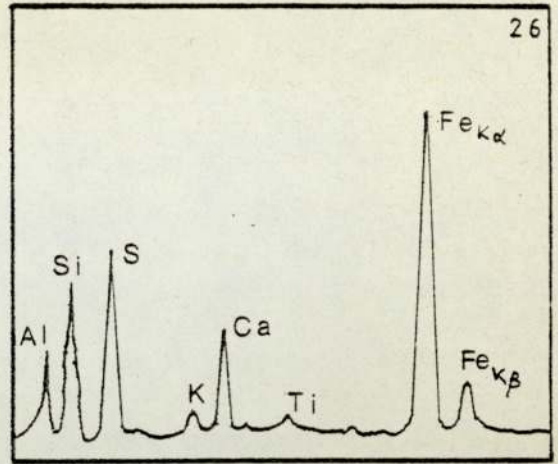
Fig 81. KEVEX chart for the inclusion containing Al,Si,Ca,S and Fe, in the weld of MA7(0.032%S,CSF=62).
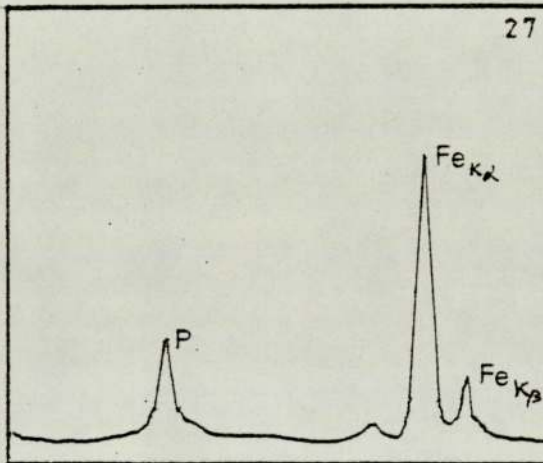
Fig 82. KEVEX chart for the crack surface of MD16(0.057%P,CSF=21). Not found in any other steels.
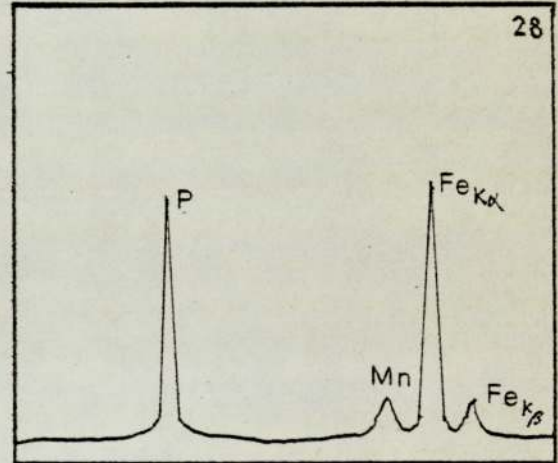
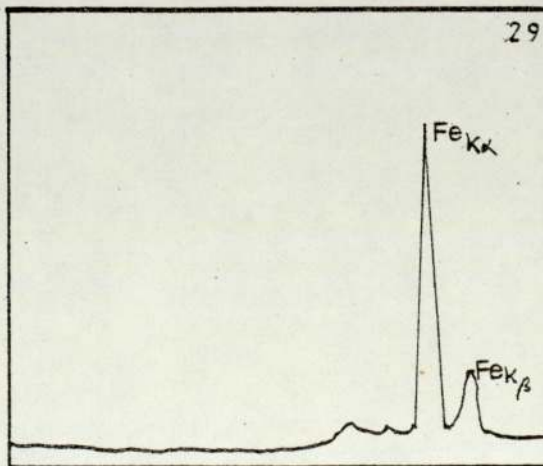Fig 83 KEVEX chart for the wormlike phosphide inclusion observed in the weld of MD16(CSF=21, 0.057%P).
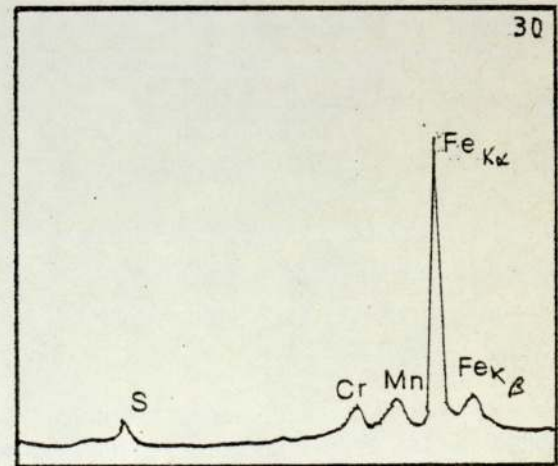
Fig 84. KEVEX chart for the crack surface of a less crack susceptible weld.

Fig 85. KEVEX chart for the crack surface of a more crack susceptible weld. S being detectable on the matrix.
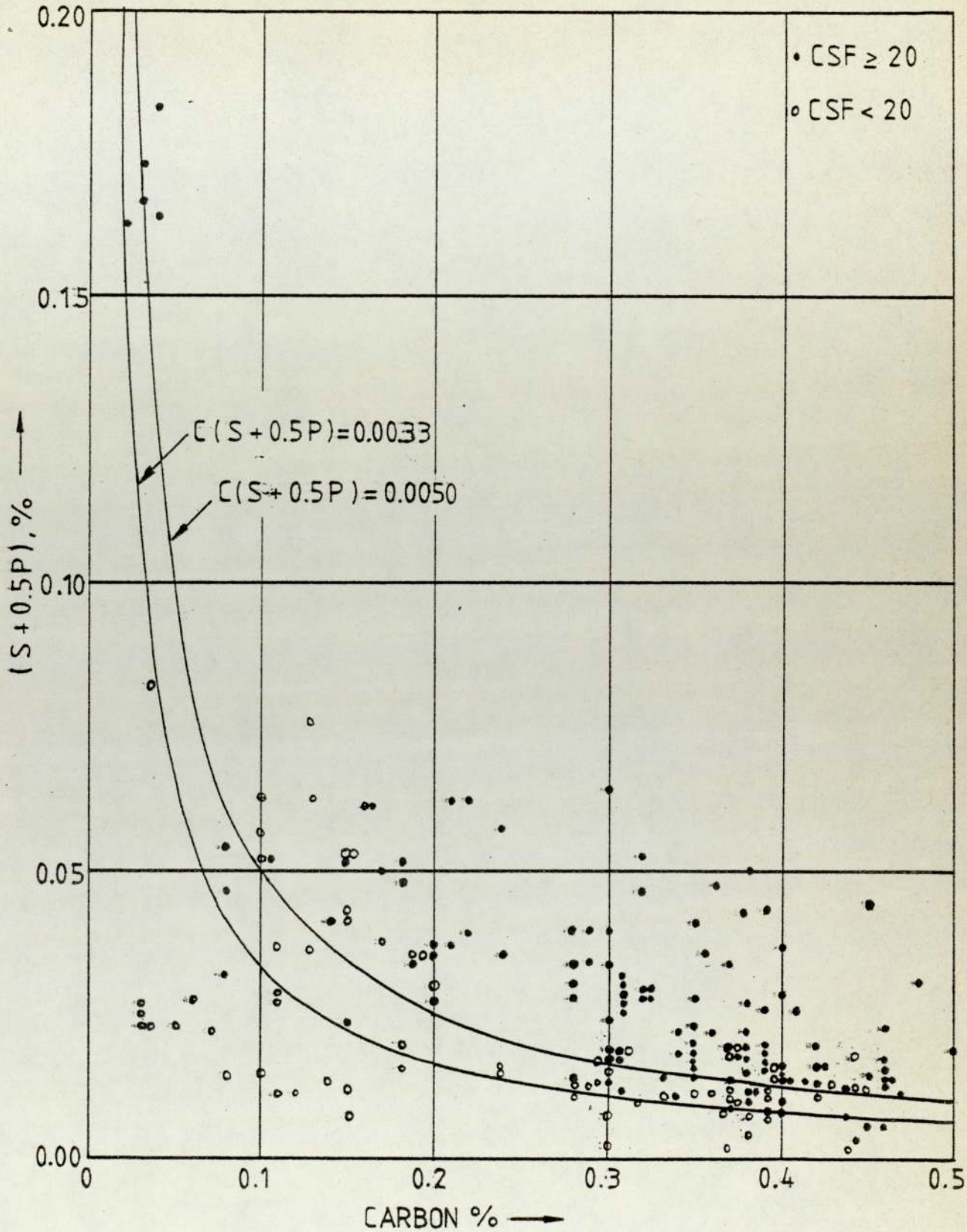
Fig 86. The influence of (S+0.5P) and C on the weld crack susceptibility according to 186 Huxley cracking test data. The steels with composition under the curve of C(S+0.5P) = 0.0033 are mostly crack resistant.
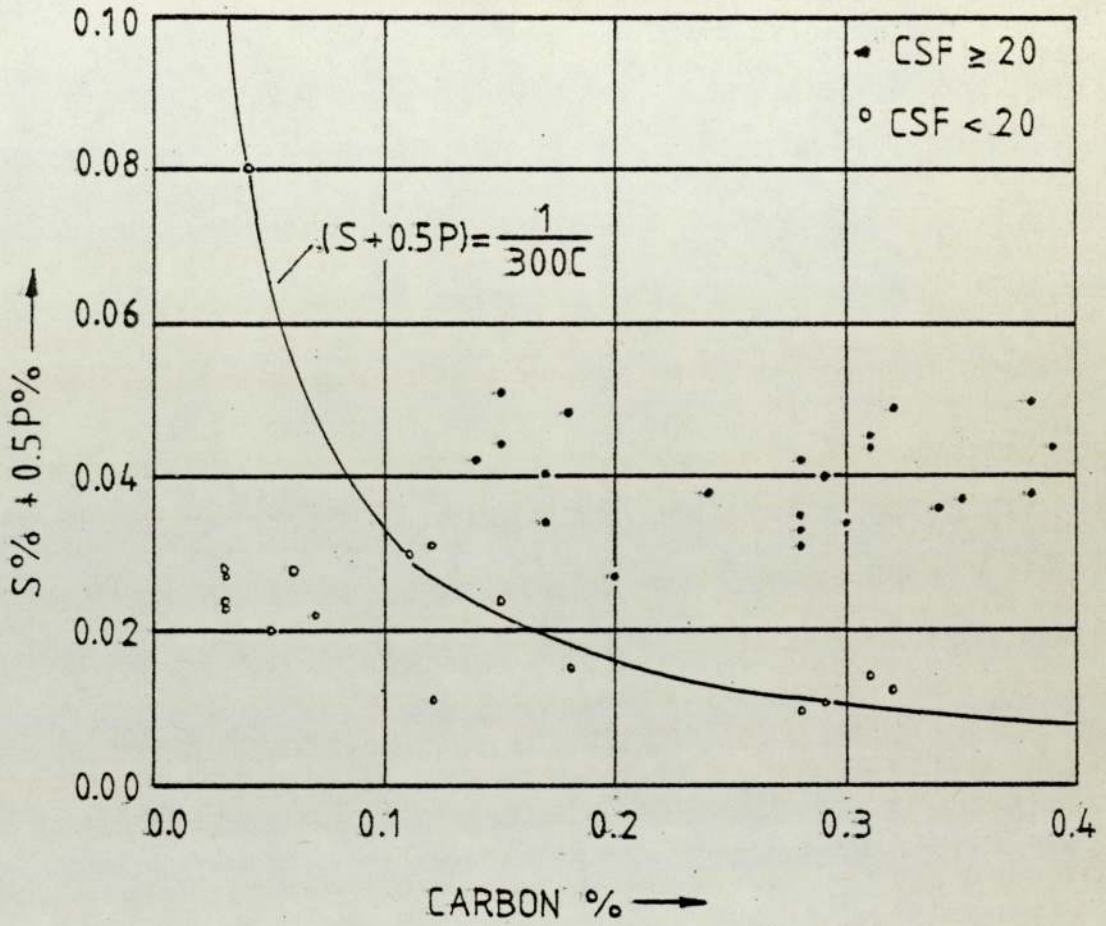
Fig 87. The influence of $(S + 0.5P)$ and C on the crack suscep-
tibility of steel weld metal according to the Huxley cracking
test data of the present research. Steels with $(S+0.5P) < \frac{1}{300C}$
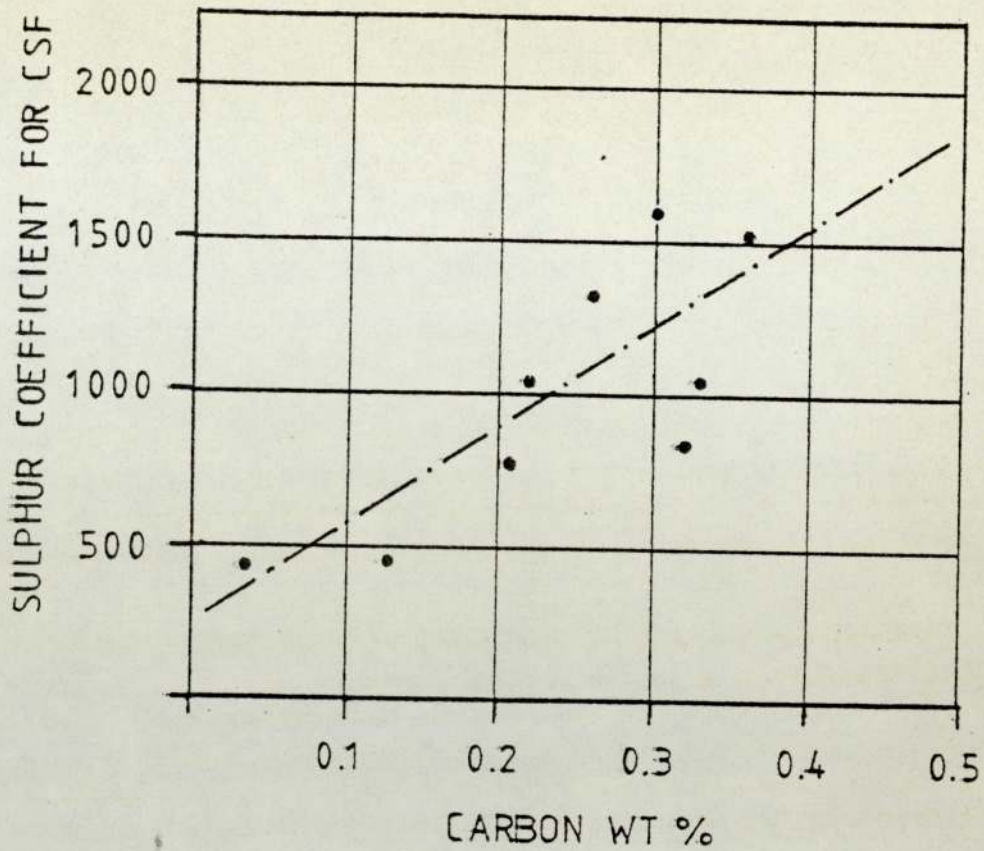were found not crack susceptible.

Fig 88. The effect of carbon in steel on the sulphur coefficient in the regression equations for the crack susceptible factor (CSF).